The Scientific World Journal

Critical Care and Perioperative Monitoring

Guest Editors: Dimitrios Karakitsos, Mahmoud El Barbary, Lawrence Marshall Gillman, Apostolos Papalois, and Ariel Shiloh

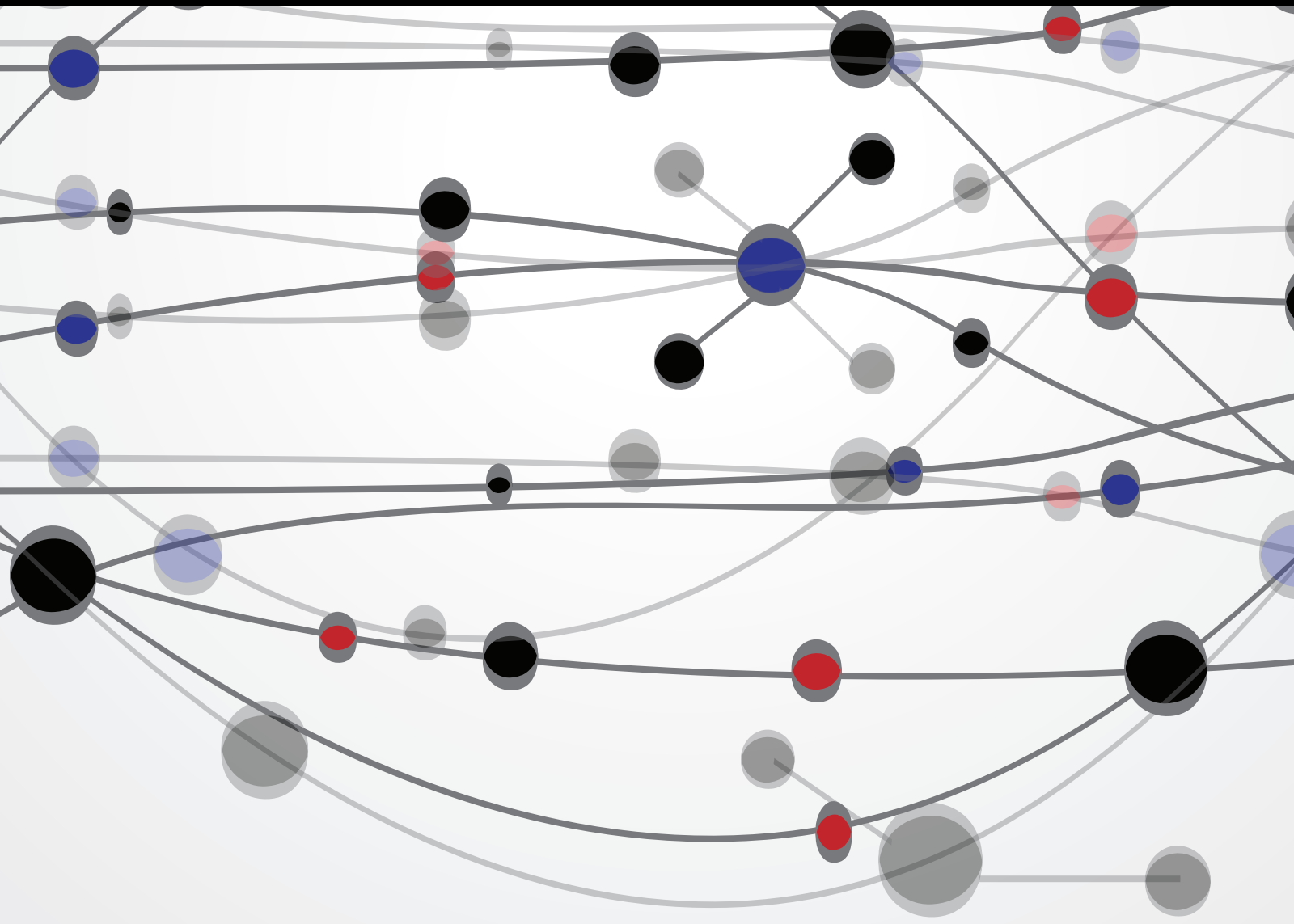

Critical Care and Perioperative Monitoring

The Scientific World Journal

Critical Care and Perioperative Monitoring

Guest Editors: Dimitrios Karakitsos, Mahmoud El Barbary, Lawrence Marshall Gillman, Apostolos Papalois, and Ariel Shiloh

Contents

Hindawi Publishing Corporation
The Scientific World Journal
Volume 2014, Article ID 737628, 3 pages
http://dx.doi.org/10.1155/2014/737628

Editorial

Critical Care and Perioperative Monitoring

Dimitrios Karakitsos,[1,2] Mahmoud El Barbary,[3] Lawrence Marshall Gillman,[4] Apostolos Papalois,[5] and Ariel Shiloh[6]

[1] *Department of Internal Medicine, University of South Carolina, School of Medicine, Columbia, SC, USA*
[2] *Department of Anesthesiology, Division of Critical Care Medicine, Keck School of Medicine, The University of Southern California, Los Angeles, CA, USA*
[3] *King Abdul-Aziz Cardiac Center, King Saud Bin Abdulaziz University for Health Sciences, Riyadh, Saudi Arabia*
[4] *Department of Surgery, University of Manitoba, Z3053-409 Tache Avenue, Winnipeg, MB, Canada R2H 2A6*
[5] *Critical Care Medicine Department, Athens University School of Nursing, 516 Mesogeion Avenue, Agia Paraskevi, 15342 Athens, Greece*
[6] *Division of Critical Care Medicine, Department of Medicine, Jay B. Langner Critical Care Service Montefiore Medical Center, Albert Einstein College of Medicine, NY, USA*

Correspondence should be addressed to Dimitrios Karakitsos; karakitsosdimitrios@gmail.com

Received 13 April 2014; Accepted 13 April 2014; Published 4 May 2014

Advances in perioperative and critical care monitoring have greatly improved the standard of care during the last decades. However, no monitoring tool, no matter how accurate, by itself has improved critical care patients outcome [1]. Moreover, aside from lung-protective mechanical ventilation there has really been no consistent intervention that has individually resulted in improved outcomes.

The purpose of a monitoring system is not to treat but to provide clinical information that may impact medical decision-making. Various techniques have been implemented in the pre-, intra-, and postoperative monitoring of surgical patients. Invasive and noninvasive methods facilitate the monitoring of nervous, cardiovascular, respiratory, renal, and hematologic systems as well as of metabolic status. While monitoring will not prevent all adverse incidents in the perioperative period, it reduces the risks of accidents by permitting the continuous recording of core data such as heart rate, blood pressure, and peripheral oxygen saturation. Monitoring facilitates the detection of the consequences of human errors, while alerting physicians that a patient's condition is deteriorating for other reasons [2–6].

The prevention of perioperative complications has obvious implications both to patients and to health care systems. With over 230 million surgical procedures performed annually around the globe, the successful management of perioperative complications either in the operating room or in the intensive care unit (ICU) is becoming a major concern for health care providers. Interestingly, up to 4% of noncardiac surgery patients may die and more will develop postoperative complications that will prolong the duration of ICU hospitalization and reduce long-term survival. In major surgery, even in groups with a low mortality rate, the rate of postoperative complications is rather high [7–10]. We still fail to answer many critical questions. Should we admit more postsurgical patients to the ICU? Is this a prudent strategy that could improve patients' outcome or would such a policy dramatically increase hospitalization costs without affecting their long-term survival? Although no definitive solution to the aforementioned dilemma exists, the application of multipurpose perioperative monitoring might prove to be a prudent and cost-efficient strategy. Hence, this issue of the journal is presenting several articles outlining the important role of perioperative monitoring in modern clinical settings.

In recent years, a rather important development has been the gradual introduction of ultrasound technology in perioperative and critical care monitoring. The important role of this noninvasive, by-the-bed, and relatively cheap technology in the practice of modern anesthesiology and

critical care is justified by the vast compendium of its applications in hemodynamic monitoring (echocardiography), neuromonitoring (transcranial color coded Doppler and ocular ultrasound), and guided procedures (vascular access and nerve blockade). Ultrasound has been introduced in medical school curriculums and resident training programs in several North American and European institutions. Our research group has recently presented the holistic approach (HOLA) concept of ultrasound imaging which defines critical care ultrasound as part of the patient examination by a clinician to visualize all or any parts of the body, tissues, organs, and systems in the patient's life, anatomically and functionally interconnected state, and the context of the whole patient's clinical circumstances. The application of ultrasound technology as an adjunct to physical examination may indeed change the face of perioperative and critical care monitoring in the upcoming years [11].

Physical examination remains a matter of particular concern to the ICU environment since the former is deprived of several of its physical elements. Apart from the physical examination and critical care ultrasound issues raised above, advances in the interpretation of arterial blood gases and in cardiorespiratory care became evident in recent years. The integration of the Stewart-Figge approach in the routine interpretation of arterial blood gases is becoming increasingly popular. This approach, amongst other things, aids in evaluating the anion gap value while taking into account its dependence on the concentrations of the nonvolatile weak acids, which in turn has improved our understanding regarding metabolic acidosis [12]. Another important development in respiratory monitoring has been the introduction of the new Berlin definition of acute respiratory distress syndrome (ARDS) as the pertinent task force has categorized ARDS as mild, moderate, and severe, without excluding the presence of heart failure [13]. This improvement of the ARDS definition corresponds to a simple clinical truth that there are indeed mixed types of pulmonary edema. Moreover, the imminent fusion of lung ultrasound and echocardiographic applications into general chest ultrasound cardiorespiratory monitoring protocols could further enhance our understanding of the aforementioned mixed types of pulmonary edema.

Conventional invasive and noninvasive ventilation have been the mainstay of ARDS therapy in critical care settings. Recently, the role of extracorporeal membrane oxygenation (ECMO) has been upgraded in the management of severe respiratory and circulatory failure. ECMO has been brought out of the operating room and to the bedside allowing clinicians to aid in the care of critically ill patients requiring cardiac or cardiopulmonary support, but it has also become remarkably portable and thus allowed for intra- and interhospital transport of otherwise unstable patients. Venoarterial ECMO provides both respiratory and hemodynamic support, in contrast to venovenous ECMO, which provides only respiratory support. VA ECMO is ideally placed in a patient with a reversible pathological process and is commonly placed in those with cardiogenic shock from any number of etiologies including myocardial infarction, postcardiac surgery with the inability to wean off bypass, early graft failure following heart transplantation, and myocarditis. Other conditions for which VA ECMO may be considered include pulmonary embolism, septic or peripartum cardiomyopathy, or trauma to the great vessels. In the case of myocardial infarction leading to cardiac arrest, peripheral VA ECMO can provide hemodynamic stabilization until the neurologic status of the patient is determined—a therapeutic strategy called bridge-to-decision [14]. Although the efficacy of ECMO in improving long-term survival remains questionable, it is extremely useful when used to replace some of the function of a failed cardiopulmonary system and to provide some rest to the myocardium. Apart from the upgraded role of ECMO in modern cardiorespiratory care, lung-protective ventilation with the use of low tidal volumes and positive end expiratory pressure remains the standard of care in the ICU. Interestingly, the use of a lung-protective ventilation strategy in intermediate- and high-risk patients undergoing major abdominal surgery has been suggested to be associated with improved clinical outcomes and reduced health care utilization by the IMPROVE group [15].

Another fundamental parameter of perioperative monitoring is the evaluation of hemodynamic status. Hemodynamic monitoring and thus management have greatly developed in recent years. Technologies have evolved from invasive to noninvasive, and the philosophy has shifted from a static approach to a dynamic one. Ultrasound technology has indeed contributed much to the aforementioned shift in current monitoring strategies. The application of several other noninvasive technologies have equally contributed towards that direction. However, a breach still exists between clinical research studies evaluating noninvasive hemodynamic monitors and clinical practice. There are not yet enough data, especially in the perioperative period, to suggest that hemodynamic monitoring systems coupled with goal directed therapies could improve patient outcome [1]. We have recently had suggestions that therapy guided by the tried and true method of invasive hemodynamic monitoring via the pulmonary artery catheter may not be as sound as we previously thought. Due to great technological advances we have witnessed the introduction of multiple new monitoring devices over the last decade. However, we must be careful to view these new devices with a combination of both cautious optimism and slight uncertainty until their clinical utility can be proven. In the same way we must question the utility of existing devices rather than accepting the status quo and continuing their use based solely on historic pretenses.

Surely, the prevention of perioperative complications is of vital importance for anyone caring for this group of patients. Developing systems that can avoid the complications occurring in the first place and thereafter identifying and treating complications when they arise represent the basic logistics of modern perioperative monitoring. The physiological derangement of patients in the operating room and/or in the ICU has led to the development of sophisticated continuous monitoring systems. The prudent evaluation and application of the latter could in turn enable the prioritization of all available health care resources to individual cases.

Notwithstanding, monitoring alerts physicians' senses and aids in guiding therapy but is not a therapy by itself.

Dimitrios Karakitsos
Mahmoud El Barbary
Lawrence Marshall Gillman
Apostolos Papalois
Ariel Shiloh

References

[1] M. R. Pinsky and D. Payen, "Functional hemodynamic monitoring," *Critical Care*, vol. 9, no. 6, pp. 566–572, 2005.

[2] J. H. Eichhorn, J. B. Cooper, D. J. Cullen, W. R. Maier, J. H. Philip, and R. G. Seeman, "Standards for patient monitoring during anesthesia at Harvard Medical School," *Journal of the American Medical Association*, vol. 256, no. 8, pp. 1017–1020, 1986.

[3] R. K. Webb, J. H. Van der Walt, W. B. Runciman et al., "Which monitor? An analysis of 2000 incident reports," *Anaesthesia and Intensive Care*, vol. 21, no. 5, pp. 529–542, 1993.

[4] W. P. S. McKay and W. H. Noble, "Critical incidents detected by pulse oximetry during anaesthesia," *Canadian Journal of Anaesthesia*, vol. 35, no. 3, pp. 265–269, 1988.

[5] D. J. Cullen, A. R. Nemeskal, J. B. Cooper, A. Zaslavsky, and M. J. Dwyer, "Effect of pulse oximetry, age, and ASA physical status on the frequency of patients admitted unexpectedly to a postoperative intensive care unit and the severity of their anesthesia-related complications," *Anesthesia and Analgesia*, vol. 74, no. 2, pp. 181–188, 1992.

[6] J. T. Moller, N. W. Johannessen, K. Espersen et al., "Randomized evaluation of pulse oximetry in 20,802 patients: II. Perioperative events and postoperative complications," *Anesthesiology*, vol. 78, no. 3, pp. 445–453, 1993.

[7] S. F. Khuri, W. G. Henderson, R. G. DePalma et al., "Determinants of long-term survival after major surgery and the adverse effect of postoperative complications," *Annals of Surgery*, vol. 242, no. 3, pp. 326–343, 2005.

[8] N. Lees, M. Hamilton, and A. Rhodes, "Clinical review: goal-directed therapy in high risk surgical patients," *Critical Care*, vol. 13, no. 5, article 231, 2009.

[9] A. Rhodes, R. P. Moreno, B. Metnitz, H. Hochrieser, P. Bauer, and P. Metnitz, "Epidemiology and outcome following post-surgical admission to critical care," *Intensive Care Medicine*, vol. 37, no. 9, pp. 1466–1472, 2011.

[10] R. M. Pearse, P. J. E. Holt, and M. P. W. Grocott, "Managing perioperative risk in patients undergoing elective non-cardiac surgery," *British Medical Journal*, vol. 343, Article ID d5759, 2011.

[11] A. Sargsyan, M. Blaivas, P. Lumb, and D. Karakitsos, "The holistic approach (HOLA) ultrasound concept," in *Critical Care Ultrasound*, P. D. Lumb and D. Karakitsos, Eds., pp. 12–14, Elsevier, 2014.

[12] P. A. Stewart, "How to understand acid base," in *Stewart's Textbook of Acid Base*, J. A. Kellum and P. W. G. Elbers, Eds., pp. 29–197, 2nd edition, 2009, http://www.lulu.com/.

[13] The ARDS definition task force, "Acute respiratory distress sybdrome. The Berlin definition," *Journal of the American Medical Association*, vol. 307, pp. 2526–2533, 2013.

[14] F. D. Pagani, K. D. Aaronson, F. Swaniker, and R. H. Bartlett, "The use of extracorporeal life support in adult patients with primary cardiac failure as a bridge to implantable left ventricular assist device," *Annals of Thoracic Surgery*, vol. 71, no. 3, pp. S77–S81, 2001.

[15] E. Futier, J. M. Constantin, C. Paugam-Burtz et al., "trial of intraoperative low-tidal-volume ventilation in abdominal surgery," *The New England Journal of Medicine*, vol. 369, no. 5, pp. 428–437, 2013.

Hindawi Publishing Corporation
The Scientific World Journal
Volume 2014, Article ID 393258, 10 pages
http://dx.doi.org/10.1155/2014/393258

Review Article

Monitoring of the Adult Patient on Venoarterial Extracorporeal Membrane Oxygenation

Mabel Chung,[1] Ariel L. Shiloh,[1] and Anthony Carlese[1,2]

[1] *Division of Critical Care Medicine—The Jay B. Langner Critical Care Service, Department of Medicine, Montefiore Medical Center, Albert Einstein College of Medicine, Bronx, NY 10467, USA*
[2] *Cardiothoracic Intensive Care Unit, Moses Campus, USA*

Correspondence should be addressed to Anthony Carlese; acarlese@montefiore.org

Received 11 October 2013; Accepted 27 November 2013; Published 3 April 2014

Academic Editors: W. W. Butt and H. Spapen

Venoarterial extracorporeal membrane oxygenation (VA ECMO) provides mechanical support to the patient with cardiac or cardiopulmonary failure. This paper reviews the physiology of VA ECMO including the determinants of ECMO flow and gas exchange. The efficacy of this therapy may be determined by assessing patient hemodynamics and device flow, overall gas exchange support, markers of adequate oxygen delivery, and pulsatility of the arterial blood pressure waveform.

1. Introduction

Cardiopulmonary bypass (CPB) was used successfully for the first time in 1953 when Dr. John H. Gibbon repaired an atrial septal defect in an 18-year-old woman. Since then, technological improvements in extracorporeal life support have allowed for the development of a type of partial cardiopulmonary bypass called extracorporeal membrane oxygenation (ECMO). Not only has the technology of ECMO been brought out of the operating room into the bedside allowing clinicians to aid in the care of critically ill patients requiring pulmonary or cardiopulmonary support, but EMCO has also become remarkably portable and has allowed for intra- and interhospital transport of otherwise unstable patients. While ECMO support can be venovenous (VV) or venoarterial (VA), this paper aims to focus on the functional mechanics and the monitoring considerations in a patient with VA ECMO.

2. Indications/Benefits

VA ECMO provides both respiratory and hemodynamic support, in contrast to VV ECMO, which provides only respiratory support. VA ECMO is ideally placed in a patient with a reversible pathological process and is commonly placed in those with cardiogenic shock as well as those with other causes of hemodynamic instability refractory to medical management (Table 1). In the case of a myocardial infarction leading to cardiac arrest, peripheral VA ECMO can be placed quickly and can provide hemodynamic stabilization until the neurologic status of the patient is determined— a therapeutic strategy called bridge to decision [1, 2]. If the patient recovers neurologic function, VA ECMO support can be continued, allowing clinicians time to determine the suitability of the patient for myocardial recovery or as a candidate for transplantation or placement of a durable ventricular assist device. A decision tree for utilization of VA ECMO in the setting of cardiac arrest and uncertain neurologic status is outlined in Figure 1.

3. Limitations/Contraindications

VA ECMO provides partial hemodynamic support and can provide ventricular decompression, augmentation of perfusion pressure, and oxygenation and removal of carbon dioxide in the blood; however, it also increases the afterload against which the left ventricle (LV) works. The balance of the beneficial effect of decompression against the detrimental effect of increased afterload depends on the level of support and the state of the myocardium. Those on VA ECMO must be anticoagulated, the requirement of which must

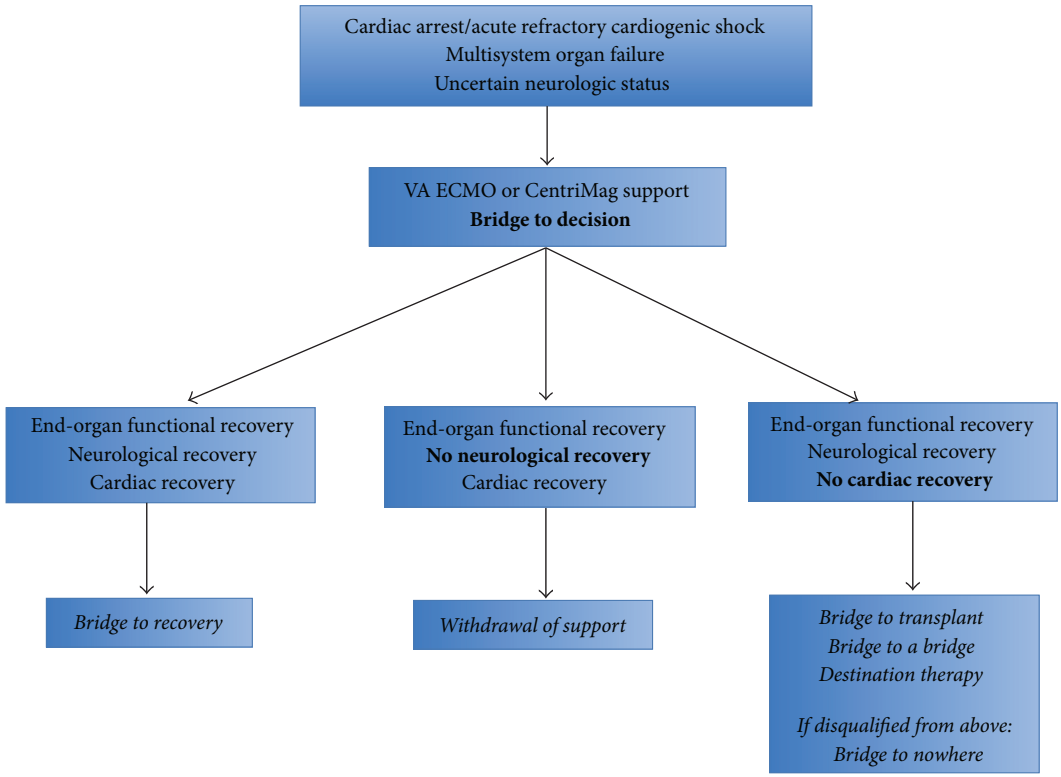

Figure 1: VA ECMO support after cardiac arrest provides hemodynamic stabilization, which allows time for therapeutic hypothermia and assessment of the neurologic status of the patient. If the patient achieves both neurologic and cardiac recovery, VA ECMO support will have functioned as a bridge to recovery and can subsequently be removed. If the patient does not recover neurologic function, VA ECMO support is typically withdrawn. If the patient awakens but does not have recoverable myocardial function, candidacy for heart transplant (bridge to transplant) and temporary (bridge to a bridge) or permanent (destination therapy) implantation of a ventricular assist device can be assessed. The neurologically intact patient that is disqualified from a heart transplant or ventricular assist device presents a dilemma that may be described as a bridge to nowhere. Figure adapted from [1].

be weighed against the risk of bleeding. In addition, VA ECMO cannot be maintained on a long-term basis. Although there is no set time frame for device therapy, correction of physiologic derangements should occur within the first 24–48 hours. Recent studies have published durations of support ranging from 1.4 days to 11.5 days [2, 5–12]. VA ECMO is contraindicated in a number of conditions (Table 2).

4. Types of Cannulations/Circuit

Cannulation for VA ECMO can be described as either peripheral or central (Figure 2) [3]. Peripheral cannulation can be accomplished either percutaneously or by cut-down, and typically utilizes the femoral or internal jugular vein for the venous (inflow) cannula and the femoral, axillary, or the carotid artery for the arterial (outflow) cannula. Peripheral cannulation, especially with the femoral vein and femoral artery, can be done quickly and on an emergency basis at the bedside. However, it often involves cannulas of smaller diameter than those used in central cannulation. Central cannulation, in contrast, requires a sternotomy or thoracotomy. It is frequently seen in the context of the inability to wean off CPB after cardiac surgery, as the cannulas used for bypass can be directly connected to the VA ECMO circuit. Central cannulation typically involves a venous cannula from the right atrium and an arterial cannula into the ascending aorta. The larger diameter cannulas allow for greater flow due to decreased resistance.

The fundamental components of a VA ECMO circuit include a venous inflow cannula, a pump, a membrane oxygenator/lung, and an arterial outflow cannula. The venous cannula withdraws blood at the level of the right atrium/vena cava. The blood is pumped through the membrane oxygenator allowing for oxygen uptake and carbon dioxide removal, and this arterialized blood is returned to the systemic circulation through an artery. Other components of the circuit may include a saturation sensor on the venous cannula to assess the mixed venous saturation (SvO_2), a flow probe that clips onto to the arterial cannula to directly assess flow in liters/minute, a pre- and postoxygenator pressure monitor, a console whereby the speed of the pump can be adjusted, various access ports through which medications can be infused and blood samples withdrawn, a heat exchanger by which temperature can be controlled, and a bridge between the venous and arterial lines. Such a bridge allows blood to continue to circulate through the circuit after proximal clamping, which can be performed to test the effects of temporarily suspending ECMO support.

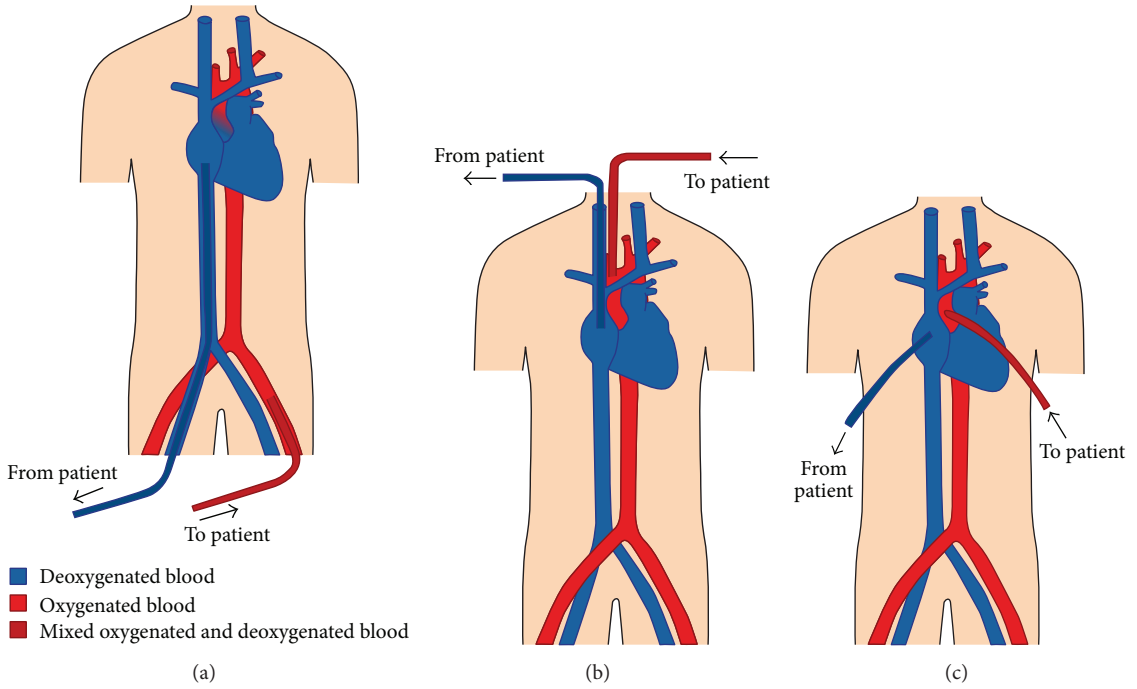

Figure 2: Illustrations of various VA ECMO cannulations. Diagram (a) depicts a femoral vein-femoral artery peripheral cannulation. Retrograde outflow from a femoral arterial cannula competes with anterograde cardiac output ejected from the left ventricle. In this situation, poor lung function results in the ejection of deoxygenated blood (blue) from the left ventricle, which mixes with oxygenated blood (red) from the ECMO circuit. The point of mixing (dark red) is located at the base of the aortic root, but will vary depending on the patient's heart function and ECMO flow. Poor lung function and good myocardial function in the context of a femoral-femoral ECMO cannulation may result in upper body hypoxemia (see text). Diagram (c) shows central cannulation with venous inflow drawn from the right atrium and arterial outflow pumped into the ascending aorta.

Table 1: Indications for VA ECMO.

Refractory cardiogenic shock
Myocardial infarction
Myocarditis
Primary graft failure following heart transplantation
Postcardiotomy (failure to wean from CPB after cardiac surgery)
Drug overdose resulting in profound myocardial depression
Septic cardiomyopathy
Peripartum cardiomyopathy
Pulmonary embolism
Recurrent dysrhythmias such as ventricular tachycardia/fibrillation
Severe pulmonary hypertension
Anaphylactic shock
Trauma to major vessels or myocardium
Massive hemoptysis or pulmonary hemorrhage
Pre- or postprocedure circulatory support for high risk interventional procedures

Table 2: Contraindications to VA ECMO.

Absolute contraindications
Uncontrolled, active bleeding or other contraindication to anticoagulation
End-stage, irreversible processes from which patient is not expected to recover (unless transplant candidate)
(i) Cardiac disease
(ii) Respiratory disease
(iii) Neurologic disease
Poor preexisting functional status or multisystem organ failure
Unwitnessed cardiac arrest or prolonged cardiopulmonary resuscitation (>60 min)
Aortic dissection
Severe aortic valve regurgitation
Other considerations
Advanced age
Renal or liver failure
Active malignancy
Morbid obesity
Significant peripheral vascular disease
Heparin-induced thrombocytopenia

The ability to circulate blood during clamping decreases the risk of stasis and thrombosis. An ECMO circuit may also include a venous reservoir or bladder located on the venous line prior to the pump to serve as an air bubble trap as

Table 3: Similarities and differences between VA ECMO oxygenation and ventilation.

Variable	Affects oxygenation	Affects CO_2 elimination
Diffusion gradient	Yes	Yes
Membrane surface area	Yes	Yes
F_DO_2	Yes	No
Blood flow	Yes	No
Fresh gas flow rate	No	Yes

well as a volume buffer. Centrifugal pumps (see following section) can generate substantial negative pressure at the venous inlet; thus, the presence of a reservoir can provide extra preload reserve to prevent cavitation of the cannulated vessel with resultant hemolysis. The bladder also allows for noninvasive monitoring of venous inlet pressure, although certain consoles may allow for pressure monitoring without the presence of a reservoir. Venous inlet pressures should not exceed negative 50 mm Hg.

5. Functional Mechanics: Flow and Gas Exchange

VA ECMO, as a form of partial cardiopulmonary bypass, provides 60–80% of the predicted resting cardiac output. The remaining 20–40% of venous return flows normally through the native pulmonary circulation. The cardiac output provided by the ECMO circuit (i.e., ECMO blood flow) is accomplished with one of two types of pumps—centrifugal or roller. This paper will focus on centrifugal pumps, which are more commonly used than roller pumps in the adult population. Centrifugal pumps like the CentriMag (Thoratec, Pleasanton, CA) propel blood forward with a magnetically levitated impeller that spins like a top.

The flow of blood through a VA ECMO circuit may be thought of as being governed by the modifiable variables of preload, afterload, and revolutions per minute (RPM) of the impeller as well as by the static variables of cannula length and diameter. Centrifugal pumps are preload dependent and afterload sensitive. The preload dependency of the centrifugal pump manifests as decreased flows with significant hypovolemia or with mechanical obstructive processes such as tamponade or tension pneumothorax. The centrifugal pump is also afterload sensitive. Decreased flows can occur with postpump obstructions such as thrombus in the oxygenator or kinks in the arterial cannula, as well as with excessive systemic vascular resistance (SVR) or mean arterial pressure (MAP). A decrease in the RPMs decreases flow through the circuit, while an increase in the RPMs, when not limited by preload, afterload, or circuit components, should cause an increase in the flow. Resistance to blood flow increases directly with cannula length and inversely with cannula diameter. Hence shorter and larger bore cannulas promote greater flow, while longer and smaller bore cannulas tend to limit flow. Circuit components are chosen to allow for at least 50–75 cc/kg/min of flow in adults (compared with 80 cc/kg/min for pediatric patients and 100 cc/kg/min for neonates). Larger patients may require additional inflow or outflow cannulas if adequate flows cannot be achieved with a given set of circuit components.

Gas exchange occurs in the membrane oxygenator (Figure 3) [4]. Extracorporeal venous blood is exposed to fresh gas (or sweep gas) that oxygenates and removes carbon dioxide. Both oxygen uptake and carbon dioxide removal depend on the presence of a diffusion gradient as well as on the available surface area of the semipermeable membrane. Oxygenation is affected by the fraction of delivered oxygen (F_DO_2) and the blood flow rate. A gas blender attached to the oxygenator mixes air and oxygen and allows for a range of F_DO_2. Increases in F_DO_2 will increase the partial pressure of oxygen in the blood (PaO_2). In addition, increases in blood flow will also increase oxygenation as a greater volume of blood is exposed to the surface of the membrane. Augmentation of oxygenation only occurs up to a certain point after which the time for oxygen transfer becomes too short. Oxygenation is independent of sweep gas flow rate. In contrast to oxygenation, carbon dioxide elimination is dependent on sweep gas flow rate and is independent of blood flow (Table 3). A flowmeter regulates gas flow to the membrane. An increase in the sweep gas flow rate results in a decreased concentration of carbon dioxide in the fresh gas. This increases the diffusion gradient, promotes greater carbon dioxide elimination, and causes a decrease in the partial pressure of carbon dioxide in the blood ($PaCO_2$). Carbon dioxide diffuses faster than oxygen because it is more soluble. As a result, it transfers approximately 10 times more efficiently than oxygen, sometimes necessitating the use of carbon dioxide enriched fresh gas in order to prevent hypocarbia. A comparison between pre- and postoxygenator blood samples should reveal an increase in PaO_2 and a decrease in $PaCO_2$. If such a change is not seen, membrane malfunction should be suspected.

Together, the blood flow and gas exchange of VA ECMO act as a surrogate heart and lung that supports end-organ function.

6. Monitoring

VA ECMO provides circulatory, oxygenation, and ventilatory support for the purpose of aiding with end-organ perfusion as well as to, potentially, provide myocardial rest. ECMO flows and the MAP should be monitored. The adequacy of gas exchange support must be verified by blood gases from an appropriately located arterial catheter. Markers of total body oxygenation—SvO_2 and lactate—should be tracked to ensure adequate perfusion and oxygen delivery to the end-organs. And finally, the hemodynamic effects of VA ECMO upon the myocardium—beneficial or detrimental—may be gauged by following the pulsatility of the arterial waveform (Table 5).

6.1. ECMO Flows and MAP. VA ECMO flows should be monitored for changes. In the setting of a stable RPM, a drop in flow in a circuit with a centrifugal pump may be caused by decreased preload or excessive afterload. Decreases

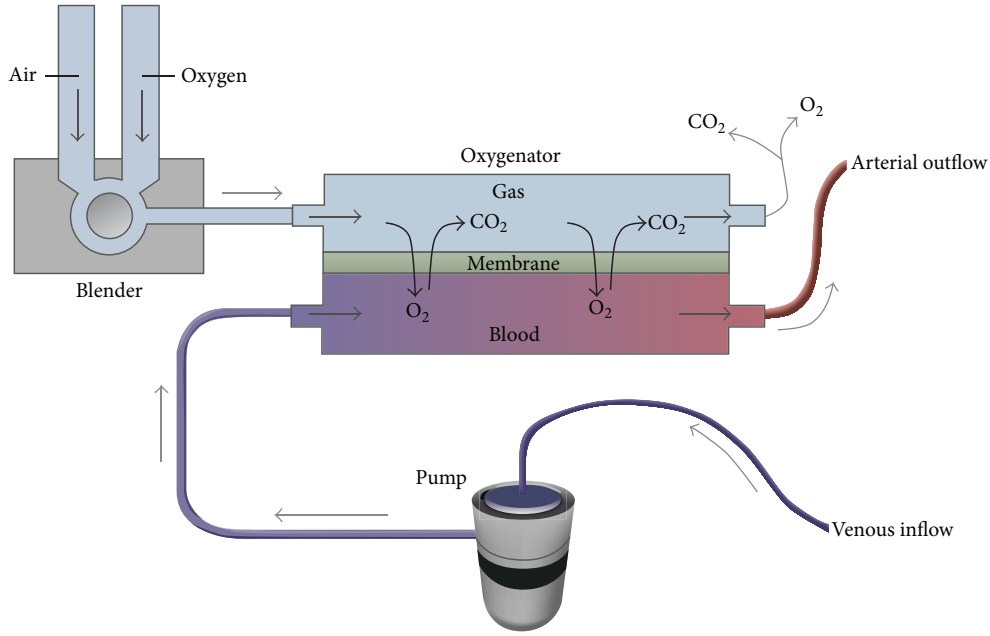

Figure 3: The oxygenator (also known as the membrane lung) is divided into a blood compartment and a gas compartment by a semipermeable membrane. The pump propels venous blood into the oxygenator and gas exchange occurs across the membrane as the blood interacts with fresh gas. After oxygenation and carbon dioxide removal, the arterialized blood is returned to the patient through an artery. A blender allows for adjustment of the fraction of delivered oxygen (F_DO_2). From [4]. Copyright © (2011) Massachusetts Medical Society. Reprinted with permission from Massachusetts Medical Society.

in preload may be secondary to hypovolemia or bleeding. The negative pressure generated by the pump in the hypovolemic state can cause hemolysis resulting in a rise in plasma free hemoglobin (significant if > 50 mg/dL) as well as a rise in lactate dehydrogenase (LDH). Spillage of free hemoglobin into the urine may result in a pink tinge to the urine. In addition, hypovolemia may also result in chattering— a low-frequency jerking or shaking movement of the cannulas due to a physical interaction between the inflow cannula and the vessel from decreased space. Hemolysis and chattering can occur independently of hypovolemia due to patient or cannula positioning or from excessive centrifugal pumps speeds (>3000 RPM) [13]. Inadequate preload may also be caused by mechanical obstructive processes such as tamponade, tension pneumothorax, and abdominal compartment syndrome. These processes decrease preload by restricting venous return and are typically associated with a rising central venous pressure (CVP). Drops in flow may also be caused by kinking of the venous cannula. Excessive afterload due to membrane oxygenator thrombus, a kink in the arterial cannula or a high SVR and MAP may also restrict flow through the VA ECMO circuit.

While maintenance of flows are crucial to the care of the patient on VA ECMO, attention must also be paid to the mean arterial pressure, as the end-organs require both a cardiac output as well as a perfusion pressure for optimal function. A goal MAP > 65 mm Hg may be used as a starting point but can be adjusted either lower or higher given individual circumstances. MAP should not exceed 90 mm Hg in order to limit afterload and to promote forward flow. Recall that

$$\text{MAP} = \text{CO} \times \text{SVR}, \tag{1}$$

where CO is cardiac output and SVR is systemic vascular resistance. In the hypotensive patient, MAP may be increased by manipulating either CO or SVR. The total cardiac output of the body is composed of native cardiac output and VA ECMO flows. Thus, hypotension may potentially be corrected by increasing VA ECMO flows and its contribution to total CO. Assuming a centrifugal pump, this may be achieved by administering volume or by increasing the RPMs of the pump. If the problem is related to SVR, such as with septic shock, a vasoconstrictor may be needed to increase MAP, although this must be weighed against the effect of increased afterload and the increase in pressure work of the left ventricle (described in "Pulsatility" below).

6.2. Gas Exchange Support. As a partial cardiopulmonary bypass circuit, VA ECMO creates a separate circulation system parallel to the native circulation by siphoning a certain portion of venous return and reinfusing it as a contribution to the overall cardiac output of the body. The body's net oxygenation and ventilation depends on the interaction between the body's own capacity to oxygenate, ventilate, and perfuse (native lung function and cardiac output) and the contribution from VA ECMO in doing the same (membrane lung function and flow). The accurate interrogation of net gas exchange support depends on where the two systems converge. The location of the arterial ECMO cannula determines the point of convergence and the suitability of a particular arterial site for blood sampling or monitoring of SpO_2.

Table 4 compares the different arterial cannulation sites with comments on the appropriate location of a peripheral arterial catheter for monitoring.

Cannulation of the right common carotid artery flushes well-oxygenated and ventilated blood down the right upper extremity. Thus, blood gases drawn from the right radial artery will not be reflective of net gas exchange support. Blood gases obtained distal to the location of mixing (e.g., the left radial artery) will be more accurate. Right radial arterial gases will not be accurate in right axillary artery cannulation, as well, due to its location relative to the ECMO cannulation site. Similarly, left radial arterial gases should be avoided in patients with left axillary artery cannulation. Direct aortic root cannulation allows for accurate blood gas analysis from any artery regardless of heart or lung function.

The preferred site of blood gas sampling with femoral artery cannulation is the right radial artery. When heart function is poor (with or without good lung function), retrograde ECMO flow should provide the vessels of the aortic arch with arterialized blood and allow good oxygen delivery to the coronary and cerebral circulations. Recovery of myocardial function pushes the mixing point of the two circulations more distally along the aorta causing native cardiac output to take over perfusion of the coronary and cerebral circulations. With good lung function, the coronary arteries, the innominate, and the right carotid artery will receive well-oxygenated blood. However, poor lung function in the setting of good myocardial function may cause these circulations to receive poorly oxygenated blood. In extreme cases, the patient's head may appear blue, while the lower extremities appear pink. Placement of a right radial arterial catheter, which interrogates oxygenation to the heart and brain, will allow for the detection of coronary and cerebral hypoxemia. This phenomenon is known by several descriptors including upper body hypoxemia, North-South Syndrome and Harlequin Syndrome.

Upper body hypoxemia may be addressed in several ways. The oxygen content of pulmonary venous blood may be augmented by adjusting ventilator settings, such as increasing the fraction of inspired oxygen (FIO_2) and/or positive end-expiratory pressure (PEEP). Depending on the etiology, inadequate lung function may be addressed by performing recruitment maneuvers to decrease atelectasis, diuresing to decrease pulmonary edema, instituting antibiotic therapy for pneumonia, or utilizing thoracentesis or bronchoscopy for significant pleural effusions or secretions and mucous plugging. Upper body hypoxemia may also be remedied by manipulating aspects of VA ECMO support. VA ECMO flows can be increased in an attempt to better perfuse the aortic root with retrograde arterialized blood. In addition, the arterial outflow cannulation site can be switched from the femoral artery to the axillary or carotid artery. As they are in closer proximity to the aortic arch, these cannulation sites may be more effective in washing the root with oxygenated blood. However, cannulation of these smaller vessels will require a smaller cannula, which will decrease the maximum achievable flows. A VA-V ECMO circuit can also be created where a portion of arterialized blood from the arterial outflow cannula is diverted via the right internal jugular artery to the right heart. This enriches the blood traveling through the pulmonary circulation and to the left ventricle to provide better oxygen delivery to the coronary and cerebral circulations. Finally, if cardiac function has recovered sufficiently, VA ECMO can be converted to VV ECMO to provide only gas exchange support until the lungs fully recover function.

6.3. SvO_2 and Lactate. SvO_2, a measure of total body oxygenation and the balance between oxygen consumption and delivery, should be routinely assessed in the patient on VA ECMO. The body responds to a decrease in oxygen delivery (DO_2) by increasing the extraction ratio (ER) of oxygen from the blood. Recall that

$$\mathrm{ER} = \frac{\mathrm{VO_2}}{\mathrm{DO_2}}, \tag{2}$$

where VO_2 is oxygen consumption. Simplification of this equation results in the following:

$$\mathrm{ER} = \frac{\left(\mathrm{SaO_2} - \mathrm{SvO_2}\right)}{\mathrm{SaO_2}}. \tag{3}$$

Given a constant arterial oxygen saturation (SaO_2), this equation reflects the inverse relationship of ER with SvO_2. Assuming a $SaO_2$of 100%, a normal extraction of 25–35% results in a normal SvO_2 of 65–75%. A state of high extraction will result in a low SvO_2 of <65–75%; once oxygen extraction reaches a maximum of 50–60% and the SvO_2 decreases to 40–50%, the body will begin to produce lactate due to the initiation of anaerobic metabolism.

A high ER or low SvO_2 due to inadequate oxygen delivery may be secondary to inadequate ECMO support. Recall that

$$\mathrm{DO_2} = \mathrm{CO} \times \mathrm{CaO_2}, \tag{4}$$

where CaO_2 is oxygen content. Given that the main components of CaO_2 are hemoglobin (Hb) and SaO_2 the equation may be simplified to

$$\mathrm{DO_2} = \mathrm{CO} \times \mathrm{Hb} \times \mathrm{SaO_2}. \tag{5}$$

Thus, increasing VA ECMO flows (via increases in volume or RPM) to increase total CO will increase DO_2 and may improve a suboptimal SvO_2. Oxygen delivery can also be increased by red cell transfusion as well as by ensuring adequate arterial saturation. Because the anemic patient requires higher ECMO flows to achieve the same oxygen delivery, optimization of Hb prior to manipulation of flows may be desirable. A high ER or low SvO_2 may also be caused by an increase in oxygen consumption; thus, interventions to decrease VO_2 (antipyretics, cooling, antishivering agents, increasing sedation, etc.) can also be made concomitantly. A more complete description of oxygen delivery on VA ECMO may be delineated with this equation:

$$\begin{aligned}\mathrm{DO_2} = {} & \left(\text{native cardiac output} \times \mathrm{CaO_2} \text{ of native lung}\right) \\ & + \left(\text{ECMO Flow} \times \mathrm{CaO_2} \text{ of membrane lung}\right).\end{aligned} \tag{6}$$

A true SvO_2 cannot be measured because venous return is split between the native and ECMO circulations. However,

Table 4: Different sites of VA ECMO arterial cannulation and arterial catheter placement.

Arterial Cannula	Location of mixing	Arterial catheter site	Comments
Right common carotid artery	Aortic arch	Avoid right radial	Right radial blood gases inaccurate due to sampling of immediate downstream arterialized blood
Right axillary artery	Aortic arch	Avoid right radial	Right radial blood gases not reflective of blood to which rest of body is exposed
Left axillary artery	Aortic arch	Avoid left radial	Left radial blood gases not reflective of blood to which rest of body is exposed
Femoral artery	Between aortic root and descending aorta—exact location depends on native cardiac output and magnitude of retrograde flow	Preferred site right radial Avoid dorsalis pedis of cannulated limb	Right radial cannulation detects upper body hypoxemia (see text)
Aorta	Aortic root	Any	

because the majority of blood flows through the VA ECMO circuit, it can be reasonably estimated by interrogating the venous cannula leading towards the membrane oxygenator either by blood gas analysis or a saturation probe to obtain a premembrane saturation. The minority of blood flows through the native pulmonary circulation. Hence, measurement of SvO_2 from a pulmonary artery catheter may not be accurate.

Rearrangement of the equation for VO_2 renders another equation for the variables that affect SvO_2:

$$SvO_2 = SaO_2 - \frac{VO_2}{CO \times Hb}. \quad (7)$$

6.4. Pulsatility. VA ECMO provides rest to the myocardium by decreasing venous return and subsequently the volume work and wall tension of the heart. In addition, the decrease in preload decreases left ventricular end-diastolic volume (LVEDV) and pressure (LVEDP), thus promoting better coronary perfusion pressure due to a greater pressure gradient (coronary perfusion pressure = diastolic pressure – left ventricular end diastolic pressure). However, the return of blood into the arterial system increases afterload and the pressure work of the myocardium. The overall effect of the decrease in volume work and the increase in pressure work depends on the level of ECMO support as well as myocardial function and its response to these phenomena.

The ejection of blood flow out of the left ventricle generates a stroke volume and its arterial correlate, a pulse pressure. The absence of pulsatility in the arterial waveform in the setting of an appropriate level of support (60–80% of the predicted cardiac output allowing for the remaining 20–40% to pass through the lungs and heart) may be a sign of poor contractility and the heart's inability to overcome the increase in afterload despite the decrease in preload and volume work. Without pulsatility, blood within the left ventricle and at the aortic root may stagnate. In this situation, the risk of thrombus formation and subsequent embolic complications is increased. In addition, without the adequate ejection of blood, persistent venous return from thebesian and bronchial veins into the left atrium (LA) and ventricle will result in overdistension of the LV. This increase in LVEDV will cause an increase in LVEDP, which can compromise coronary perfusion pressure and cause additional ischemic damage to the myocardium. Finally, an increase in afterload in the setting of severe mitral regurgitation may result in left atrial hypertension and the transmission of pressures to the pulmonary system resulting in pulmonary edema and hemorrhage. Such a complication may occur even without preexisting valvular pathology, as the stasis of blood may cause left ventricular dilation and a functional mitral insufficiency due to dilation of the annulus. In this scenario, a pulmonary artery catheter may demonstrate an increase in the pulmonary capillary occlusion pressure. While assessment of the heart in a partially bypassed state can be challenging, transesophageal echocardiography may aid in confirming aortic valve opening as well as by providing an assessment of the left ventricular end-diastolic dimension.

VA ECMO flows can be reduced in an attempt to reduce afterload. However, this maneuver may not be possible if it compromises oxygen delivery and end-organ perfusion due to the inability of the heart to produce a compensatory increase in native cardiac output. Inotropic support can be instituted or escalated to increase contractility of the myocardium. In addition, afterload reduction with a vasodilator or intra-aortic balloon pump (IABP) may be implemented. An IABP brings the added benefit of improving coronary perfusion with balloon inflation during diastole. If these maneuvers fail to promote left ventricular ejection, decompression of the left ventricle may be necessary. Decompression may be accomplished by a percutaneous left atrial septostomy, which allows blood from the LA to drain down its pressure gradient into the right atrium (RA) to then be drained via the venous cannula. A catheter may also be placed into the LA through a transseptal puncture to facilitate drainage [14]. In addition, the left atrium or left ventricle can be directly cannulated allowing blood to be vented into the venous arm of the ECMO circuit. Finally, use of a left

Table 5: Summary of monitoring in VA ECMO.

	Monitor for	Treatment
Rhythm	Dysrhythmias such as ventricular fibrillation that may prevent ventricular ejection	Antiarrhythmics Cardioversion Pacing Ablation
MAP	Hypotension (MAP = CO × SVR) (i) Inadequate VA ECMO flow (ii) Inadequate SVR	(i) See "Flow" below (ii) Start vasoconstrictor
Pulsatility	Lack of pulsatility on arterial waveform caused by (i) poor myocardial function (ii) excessive VA ECMO support (iii) Inadequate preload (iv) RV failure May result in (i) thrombus (ii) myocardial ischemia (iii) pulmonary edema (assess CXR, wedge)	If poor myocardial function, consider: decreasing VA ECMO flow starting or increasing inotrope starting or increasing vasodilator IABP myocardial decompression
Flow (liters/min)	Low flows (assuming centrifugal pump) (i) Inadequate preload (a) Hypovolemia (may see hemolysis, chattering) (b) Mechanical obstructive (ii) Excessive afterload (thrombus, kink, SVR) (iii) Inadequate RPM	(i) Volume: crystalloid/colloid/transfusion Release of mechanical obstruction (ii) Exchange oxygenator, relieve cannula kink, vasodilator to decrease SVR (iii) Increase RPM
Gas exchange	Inadequate PaO_2 inadequate or excessive CO_2 elimination (i) VA ECMO settings (a) F_DO_2 (b) VA ECMO flow (c) Sweep gas flow rate (ii) Oxygenator function (a) Pre- and postmembrane pressures (b) Pre- and postoxygenator gases (iii) Upper body hypoxemia (femoral-femoral cannulation)	(i) If hypoxemia, increase F_DO_2 or flow. If hypercarbia, increase sweep. If hypocarbia, decrease sweep or add CO_2. (ii) Increased ΔP and inadequate arterialization of postoxygenator gases suggest oxygenator malfunction (iii) Increase pulmonary venous O_2 content Adjust ventilator settings Treat etiology of pulmonary dysfunction Increase VA ECMO flow Change to axillary/carotid cannulation VA-V ECMO VV ECMO
Oxygen delivery: SvO_2 and lactate	Decreased SvO_2 and increasing lactate suggest inadequate oxygen delivery ($DO_2 = CO \times CaO_2$) (i) VA ECMO flow (ii) Hemoglobin (iii) SaO_2 Excessive oxygen consumption ($ER = VO_2/DO_2$) (i) Febrile (ii) Shivering	(i) Increase VA ECMO flow (ii) Transfuse (iii) Ensure adequate gas exchange (i) Antipyretics (ii) Consider agents such as meperidine or dexmedetomidine
Distal limb ischemia	Loss of pulses Cyanosis and coolness of limb	Femoral-femoral cannulation: DP or PT anterograde perfusion catheter
Anticoagulation	Adequate heparinization by PTT	
Temperature	Normothermia unless therapeutic hypothermia	

ventricular assist device such as the Impella 2.5 (Abiomed, Danvers, MA) to provide left ventricular decompression as well as forward flow has been described [15, 16].

Pulsatility is a dynamic property. Loss of pulsatility may signal worsening myocardial function, while the appearance of pulsatility or an improvement in pulse pressure may signal recovery. The differential diagnosis for loss of pulsatility also includes:

VA ECMO Flows That Are Too High. The greater the ECMO flows, the more blood that drains into the circuit causing a greater decrease in LV preload, stroke volume, and pulse pressure. Total bypass, where the ECMO circuit takes over 100% of the cardiac output, creates a flat, nonpulsatile arterial tracing and signifies the lack of ejection of blood from the left ventricle.

Hypovolemia/Mechanical Obstruction. A decrease in intravascular volume or a mechanical cause of decreased venous return may result in a decrease in LV preload that leads to a decreased stroke volume and pulse pressure.

RV Failure. VA ECMO decreases RV preload and the volume work of the ventricle. However, pulmonary edema, lung collapse, or other parenchymal disease may cause hypoxic pulmonary vasoconstriction and may result in clinically significant pulmonary hypertension and an increase in RV pressure work. If this occurs to a significant extent, the right ventricle may be unable to deliver volume to the left side of the heart, resulting in a decrease in stroke volume and in pulsatility. In this scenario, pulmonary afterload reduction with nitric oxide or with inodilators such as milrinone and dobutamine (which will also provide inotropic assistance) may be beneficial. If systemic pressures allow, nitroglycerin or nitroprusside may also be utilized.

6.5. Rhythm. While it may be possible to maintain adequate hemodynamic and gas exchange support with VA ECMO during dysrhythmias that would otherwise be fatal, nonsinus rhythms such as ventricular fibrillation should be rectified due to the ineffective ejection of blood flow from the LV. Such arrhythmias should be addressed with direct current cardioversion, antiarrhythmics, pacing, or ablation.

6.6. Other Considerations

Pre- and Postmembrane Oxygenator Pressures. Exposure of blood to nonbiologic surfaces results in contact activation of the coagulation system resulting in a propensity to develop clot in the VA ECMO circuit. Premembrane pressures should be followed to assess for increases greater than 300–400 mm Hg. The postmembrane pressure can give useful context to the pre-membrane pressure. An elevated premembrane pressure in the setting of a normal post-membrane pressure suggests that the source of the increased resistance lies within the oxygenator. This scenario produces an increase in the difference between pre- and post-membrane pressures (i.e., an increase in ΔP, significant if >40 mm Hg) and may be indicative of thrombus on the membrane lung. If thrombus is suspected and is accompanied by a deterioration in gas exchange, the oxygenator may need to be replaced. An elevated pre-membrane pressure in the setting of an elevated post-membrane pressure suggests that the source of increased resistance is located downstream to the oxygenator, perhaps as a clot or kink in the cannula.

Partial Thromboplastin Time/Activated Clotting Time. Heparinization is used to decrease the risk of developing clot. Adequate anticoagulation is monitored by partial thromboplastin time (PTT) and/or the activated clotting time (ACT). Heparin levels and antithrombin III levels may also be followed.

Distal Ischemia. Ipsilateral distal pulses as well as limb color and warmth should be assessed routinely with peripheral cannulations such as the axillary artery (arm ischemia) and the femoral artery (leg ischemia). In the case of femoral cannulations, a dorsalis pedis (DP) or posterior tibial (PT) distal perfusion cannula can be placed to promote perfusion to the lower extremity. Ischemic brain injury may occur as a consequence of carotid cannulation.

Central Venous Pressure. The CVP is altered by venous drainage during VA ECMO support; however, a rise in CVP in the setting of stable settings may be indicative of a mechanical obstructive process.

7. Recovery

Myocardial recovery on VA ECMO support is suggested by an increase in pulse pressure and by improved contractility on echocardiography. The ultimate test of myocardial recovery, however, is accomplished by assessing hemodynamic stability on minimal or no support. The RPMs can be decreased to achieve ~1 liter/min of flow or the VA ECMO cannulas can be briefly clamped. The native ventricle must be able to handle the full load of native cardiac output. If the myocardium has recovered, a decrease in or the temporary withdrawal of VA ECMO support should result in acceptable contractility on echocardiography and a stable MAP and CVP. Hypotension, a rising CVP, and a poorly contractile myocardium on echocardiography suggest inadequate recovery.

8. Conclusion

VA ECMO, a form of mechanical circulatory support, had its origins in the operating room as cardiopulmonary bypass and has evolved for use in the intensive care unit and beyond. Its purpose is simple—to replace some of the function of a failed cardiopulmonary system and to provide some rest to the myocardium. The successful achievement of such an aim, however, requires a thorough understanding of basic physiologic principles so that the weaknesses inherent to this therapy can be identified and rectified. As this technology continues to improve and becomes more accessible, knowledge of the principles underlying VA ECMO will only grow in importance to those involved in the care of the critically ill.

Conflict of Interests

The authors declare that there is no conflict of interests regarding the publication of this paper.

References

[1] R. John, K. Liao, K. Lietz et al., "Experience with the Levitronix CentriMag circulatory support system as a bridge to decision in patients with refractory acute cardiogenic shock and multisystem organ failure," *The Journal of Thoracic and Cardiovascular Surgery*, vol. 134, no. 2, pp. 351–358, 2007.

[2] C. F. Russo, A. Cannata, M. Lanfranconi et al., "Veno-arterial extracorporeal membrane oxygenation using Levitronix centrifugal pump as bridge to decision for refractory cardiogenic shock," *The Journal of Thoracic and Cardiovascular Surgery*, vol. 140, no. 6, pp. 1416–1421, 2010.

[3] A. M. Gaffney, S. M. Wildhirt, M. J. Griffin, G. M. Annich, and M. W. Radomski, "Extracorporeal life support," *British Medical Journal*, vol. 341, Article ID c5317, 2010.

[4] D. Brodie and M. Bacchetta, "Extracorporeal membrane oxygenation for ARDS in adults," *The New England Journal of Medicine*, vol. 365, no. 20, pp. 1905–1914, 2011.

[5] S. Schopka, A. Philipp, D. Lunz et al., "Single-center experience with extracorporeal life support in 103 nonpostcardiotomy patients," *Artificial Organs*, vol. 37, no. 2, pp. 150–156, 2013.

[6] E. Mikus, A. Tripodi, S. Calvi et al., "CentriMag venoarterial extracorporeal membrane oxygenation support as treatment for patients with refractory postcardiotomy cardiogenic shock," *ASAIO Journal*, vol. 59, no. 1, pp. 18–23, 2013.

[7] I. Slottosch, O. Liakopoulos, E. Kuhn et al., "Outcomes after peripheral extracorporeal membrane oxygenation therapy for postcardiotomy cardiogenic shock: a single-center experience," *Journal of Surgical Research*, vol. 181, no. 2, pp. e47–e55, 2013.

[8] H. Kim, S.-H. Lim, J. Hong et al., "Efficacy of veno-arterial extracorporeal membrane oxygenation in acute myocardial infarction with cardiogenic shock," *Resuscitation*, vol. 83, no. 8, pp. 971–975, 2012.

[9] E. Barth, M. Durand, C. Heylbroeck et al., "Extracorporeal life support as a bridge to high-urgency heart transplantation," *Clinical Transplantation*, vol. 26, no. 3, pp. 484–488, 2012.

[10] F. Formica, L. Avalli, L. Colagrande et al., "Extracorporeal membrane oxygenation to support adult patients with cardiac failure: predictive factors of 30-day mortality," *Interactive Cardiovascular and Thoracic Surgery*, vol. 10, no. 5, pp. 721–726, 2010.

[11] X.-J. Luo, W. Wang, S.-S. Hu et al., "Extracorporeal membrane oxygenation for treatment of cardiac failure in adult patients," *Interactive Cardiovascular and Thoracic Surgery*, vol. 9, no. 2, pp. 296–300, 2009.

[12] N. Doll, B. Kiaii, and M. Borger, "Five-year results of 219 consecutive patients treated with extracorporeal membrane oxygenation for refractory postoperative cardiogenic shock," *The Annals of Thoracic Surgery*, vol. 77, no. 1, pp. 157–157, 2004.

[13] J. M. Toomasian and R. H. Bartlett, "Hemolysis and ECMO pumps in the 21st century," *Perfusion*, vol. 26, no. 1, pp. 5–6, 2011.

[14] R. M. Aiyagari, A. P. Rocchini, R. T. Remenapp, and J. N. Graziano, "Decompression of the left atrium during extracorporeal membrane oxygenation using a transseptal cannula incorporated into the circuit," *Critical Care Medicine*, vol. 34, no. 10, pp. 2603–2606, 2006.

[15] M. S. Koeckert, U. P. Jorde, Y. Naka, J. W. Moses, and H. Takayama, "Impella LP 2.5 for left ventricular unloading during venoarterial extracorporeal membrane oxygenation support," *Journal of Cardiac Surgery*, vol. 26, no. 6, pp. 666–668, 2011.

[16] D. Vlasselaers, M. Desmet, L. Desmet, B. Meyns, and J. Dens, "Ventricular unloading with a miniature axial flow pump in combination with extracorporeal membrane oxygenation," *Intensive Care Medicine*, vol. 32, no. 2, pp. 329–333, 2006.

Hindawi Publishing Corporation
The Scientific World Journal
Volume 2014, Article ID 468269, 8 pages
http://dx.doi.org/10.1155/2014/468269

Research Article

Quasi-Stationarity of EEG for Intraoperative Monitoring during Spinal Surgeries

Krishnatej Vedala,[1] S. M. Amin Motahari,[1] Mohammed Goryawala,[1] Mercedes Cabrerizo,[1] Ilker Yaylali,[2] and Malek Adjouadi[1]

[1] *Center for Advanced Technology and Education, FIU College of Engineering and Computing, Room Number EC2672, 10555 West Flagler Street, Miami, FL 33174, USA*
[2] *Department of Clinical Neurophysiology, Oregon Health and Science University, Portland, OR 97239-3098, USA*

Correspondence should be addressed to Malek Adjouadi; adjouadi@fiu.edu

Received 30 August 2013; Accepted 2 January 2014; Published 17 February 2014

Academic Editors: L. M. Gillman, D. Karakitsos, and A. E. Papalois

We present a study and application of quasi-stationarity of electroencephalogram for intraoperative neurophysiological monitoring (IONM) and an application of Chebyshev time windowing for preconditioning SSEP trials to retain the morphological characteristics of somatosensory evoked potentials (SSEP). This preconditioning was followed by the application of a principal component analysis (PCA)-based algorithm utilizing quasi-stationarity of EEG on 12 preconditioned trials. This method is shown empirically to be more clinically viable than present day approaches. In all twelve cases, the algorithm takes 4 sec to extract an SSEP signal, as compared to conventional methods, which take several minutes. The monitoring process using the algorithm was successful and proved conclusive under the clinical constraints throughout the different surgical procedures with an accuracy of 91.5%. Higher accuracy and faster execution time, observed in the present study, in determining the SSEP signals provide a much improved and effective neurophysiological monitoring process.

1. Introduction

Sensory evoked potentials (SEP) are the signals that are observed in the brain due to an applied stimulus. When the stimulus is applied to the somatic sensory neuron, it is termed as somatosensory evoked potential (SSEP) [1, 2]. The value of these SSEP is important during neurosurgeries wherein the SSEP travels from the sensory neuron through the spinal cord to the brain. The SSEP is recorded and noted prior to the surgical procedure and are expected to remain consistent throughout the procedure [3]. Hence, a discrepancy in the SSEP is a cause of alarm for the concerned neurosurgeons informing a possible dysfunction along the nervous pathway. This fact is utilized for the early detection of potential changes leading to spinal cord dysfunction. The surgeons can then adopt the necessary protocols to prevent potential neuro physiological defects. Coupled with the fact that this is a non-invasive technique, the SSEP monitoring has become an inherent part of intraoperative neurophysiological monitoring (IONM). The SSEP recordings from cortical electrodes are buried deep within the ongoing EEG signals and surrounding equipment noise. The fact that SSEP remains consistent was used to implement a signal averaging method to extract the SSEP [4, 5]. This method, however, has the major disadvantage of requiring a large number of trials to be averaged, typically of the order of 200–5000, which need few minutes to process.

The primary objective of the present study was in providing the ability to extract the SSEP signal using a minimal number of trials. Earlier workers have proposed methods like parametric modeling [6–8], adaptive filtering [9–11], and time frequency analysis to obtain SSEP with minimum trials [6, 10, 12, 13]. Nonetheless, these methods still pose different constraints and contend with different limitations in extracting the SSEP accurately, consistently, and with the appropriate morphology. For example, in an earlier study [14],

we proposed the use of the AMUSE algorithm followed by an infinite impulse response (IIR) filter and a unique application of the Walsh transform to automate the SSEP detection. Although the accuracy and time consistency were achieved with a high degree, the method did not reveal the true nature of the morphological characteristics of the SSEP. This limitation is due to the fact that with a minimal number of unfiltered trials that were fed to the algorithm, it was very difficult to recover the true morphology of the SSEP signal, although accurately detected by the Walsh transform.

For these reasons, the proposed study presents a comprehensive and fast approach to overcome such limitations, with an initial first step of preprocessing the raw signals using a Chebyshev time window. This method, its validation, implementation results, and the improvement achieved therein are reported in the present communication.

2. Methods

2.1. Ethics Statement. The experimental work of this study was approved by the Office of Research Integrity, Florida International University, Miami; the approval numbers are 052708-03 and 100410-00. The data was collected as a routine part of a spine surgery and deidentified at the source, thus protecting the human subjects. A written consent was not obtained from the patients and waived by IRB number 104100-00 since no information that identifies the individuals was stored.

2.2. Data Acquisition. The programming applications Matlab (The Mathworks Inc., Natick, Massachusetts, USA) and GNU Octave (http://www.octave.org/) were used to implement the algorithm explained below.

(a) Stimulus of intensity 45 mV was applied to the posterior tibial nerve at a rate of 3.1 Hz.

(b) The corresponding cortical response was recorded simultaneously via C_3-C_4 and C_Z-F_Z bipolar channels for a duration of 100 ms. The sampling rate of the recordings was 6400 Hz and thus, the recordings had 640 time samples.

(c) In the clinical settings, it is common for the electrodes to get disturbed and the recordings become fraught with noise levels that are nonsensical or seem at time as if they are disconnected. Such trials can be identified and eliminated if (i) the amplitude is zero or (ii) the amplitude is higher than 25 V. This restriction criterion is in accordance with the established SSEP clinical guidelines and is routinely adopted [2]. Hence, in this study, the same criterion was adopted for bad trial rejection as illustrated in Figure 1.

For analysis, data was collected from 12 surgical procedures and analysed remotely as presented in Table 1. The surgeries were performed by trained neurosurgeons at Oregon Health and Science University, Portland, OR, USA. The IONM recording equipment used was Cascade Intraoperative Monitoring System (Cadwell, Kennetwick, MA). The data was collected as a routine part of a spine surgery and were deidentified at the source, thus protecting the human subjects. A written consent was not obtained from the patients and waived by IRB number 104100-00 since no information that identifies the individuals was stored.

2.3. Window-Based Signal Preconditioning. Each of the signals, as they are acquired, was first zero padded to move the SSEP to the middle of the window function where the tapering effect of filtering in frequency domain was minimal. We chose Chebyshev window as an improvement to our previously presented Gaussian template [15]. A Chebyshev window of the same length was applied to this signal. This has the effect of minimizing the Chebyshev norm of the side lobes while increasing the main lobe width on every FFT component that is to be calculated. This implies that the SSEP signal is concentrated in the main lobe ensuring the SSEP morphology is maintained in further processing. The signal is converted to frequency domain by FFT. In this domain, we applied rectangular passband window from 50 Hz to 120 Hz. The 60 Hz component was completely removed.

The inverse FFT of this signal is what is termed as the preconditioned signal when the zero padding is removed. Given the 640 time samples, the nth preconditioned signal can then be represented as follows:

$$\mathbf{x}_n = x_n(t) = \left[x_n(t_0) \;\; x_n(t_1) \;\; \cdots \;\; x_n(t_{639})\right], \tag{1}$$

where the time samples are uniformly distributed between 0 ms and 100 ms.

Once 12 such uncorrupted and preconditioned trials were obtained, they were ordered to form a 12×640 matrix $\mathbf{X}$:

$$\mathbf{X} = \begin{bmatrix} \mathbf{x}_1 \\ \mathbf{x}_2 \\ \vdots \\ \mathbf{x}_{12} \end{bmatrix} = \begin{bmatrix} x_1(t_0) & x_1(t_1) & \cdots & x_1(t_{639}) \\ x_2(t_0) & x_2(t_1) & \cdots & x_2(t_{639}) \\ \vdots & \vdots & \ddots & \vdots \\ x_{12}(t_0) & x_{12}(t_1) & \cdots & x_{12}(t_{639}) \end{bmatrix}. \tag{2}$$

The window-based preconditioning, along with its specific steps, is illustrated in Figure 2.

2.4. Eigenspace Filtering. Algorithm for multiple signal extraction (AMUSE) is a principal component analysis (PCA) based algorithm intended for blind source separation [16]. It is equivalent to cascading two PCA systems with the following assumptions:

(a) signals in the data set are zero-mean wide sense ergodic processes, the components of which are mutually independent;

(b) noise in the data is zero-mean white Gaussian noise.

The two assumptions were found to be valid for their application here because (i) the SSEP is a very small component of the recording and (ii) the major component is the background brain activity. This brain activity is what we need to eliminate in order to obtain the buried SSEP. The brain activity possesses the characteristic of of being zero-mean Gaussian process under anesthesia [17] and thus it satisfies the above condition (ii). For this, the assembly matrix $\mathbf{X}$ was used and implemented as follows (Figure 3).

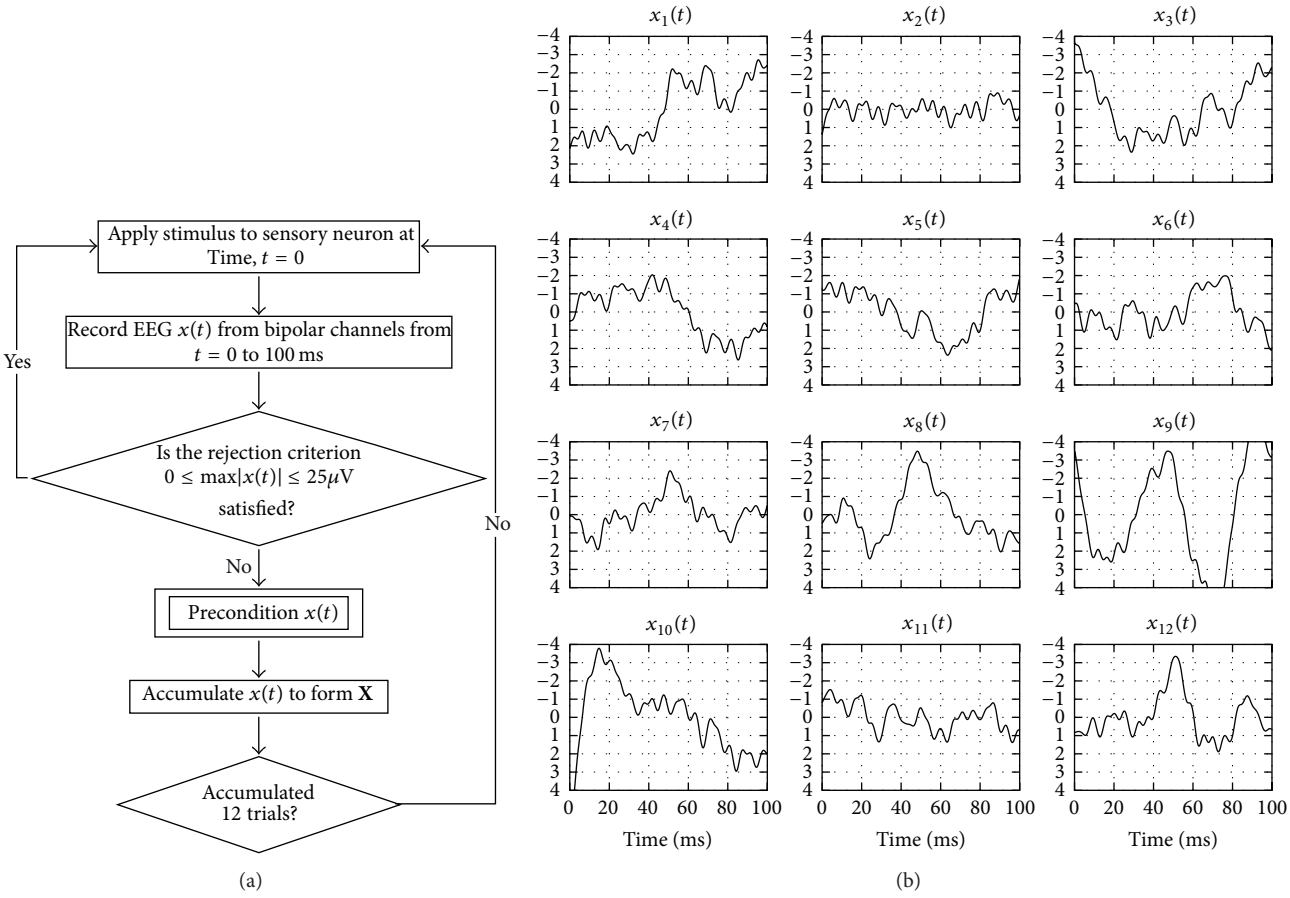

FIGURE 1: Diagram for "data acquisition" inclusive of the rejection criterion: (a) algorithm flowchart for data acquisition; (b) one such resulting matrix consisting of 12 satisfactory trials for patient 8 from Table 1.

2.4.1. Covariance Matrix. The covariance matrix of $\mathbf{X}$ was obtained as

$$\mathbf{R}_{\mathbf{X}} = \mathbf{X} \cdot \mathbf{X}^T. \tag{3}$$

Thus, the covariance matrix had the dimension 12×12.

2.4.2. Singular Value Decomposition (SVD). The covariance matrix $\mathbf{R}_{\mathbf{X}}$ was then decomposed into singular values using the SVD algorithm [18]:

$$\mathbf{R}_{\mathbf{X}} = \mathbf{V} \cdot \mathbf{\Phi} \cdot \mathbf{U}, \tag{4}$$

where $\mathbf{V}$ is the matrix whose columns are left-singular vectors, $\mathbf{\Phi}$ is the diagonal matrix whose elements are singular values or eigenvalues, and $\mathbf{U}$ is the matrix whose rows are right-singular vectors.

2.4.3. Gaussian Brain Activity Removal. The variance of the Gaussian noise component, due to the brain activity surrounding the electrodes during the 12 recordings, was estimated from this decomposition:

$$\sigma^2 = \text{mean}\left(\mathbf{\Phi}^{-1/2} \cdot \mathbf{V} \cdot \mathbf{X}\right). \tag{5}$$

Hence, elimination of this noise minimized the spatial source spread and ensured the components to be independent:

$$\mathbf{X}_b = \mathbf{X} - \sigma^2. \tag{6}$$

2.4.4. Intertrial Brain Activity Removal. The independent components of the remaining background brain activity were obtained by further decomposition following Sections 2.4.1 and 2.4.2 above.

(i) Transform the data using the singular matrix $\mathbf{\Phi}$:

$$\mathbf{W} = \mathbf{\Phi}^{-1} \cdot \mathbf{X}_b. \tag{7}$$

(ii) Estimate the covariance matrix for $\mathbf{W}_b$:

$$\mathbf{R}_W = \mathbf{W} \cdot \mathbf{W}^T. \tag{8}$$

(iii) Consider singular value decomposition of $\mathbf{R}_W$ and obtained $\mathbf{\Lambda}$ as its eigenvectors.

(iv) The possible sources (components) of the data were obtained by

$$\mathbf{H} = \mathbf{\Lambda}^T \cdot \mathbf{\Phi}^{-1}, \qquad \mathbf{Y} = \mathbf{H} \cdot \mathbf{X}_b. \tag{9}$$

Table 1: Algorithm implementation and results. Description of the 12 surgical procedures including the procedure they underwent and the time for which the patients were monitored using SSEP and the algorithm implementation results including the accuracy and the number of false alarms detected per hour.

Number	Surgical procedure	Duration (hrs)	Accuracy (%)	False alarms per hour
1	Cerebral aneurysm clipping	2	92.7	4
2	T10-S1 posterior spinal fusion	2	88.1	3
3	Cerebral aneurysm clipping	2	95.9	4
4	T10-S1 posterior spinal fusion	6	94.4	5
5	Anterior and posterior lumbar fusion	4	94.7	4
6	T4-S1 posterior spinal fusion	1.5	91.2	2
7	Posterior spinal fusion for scoliosis	2	89.4	2
8	L5-S1 TLIF	2	96.3	5
9	T10-S1 posterior spinal fusion	2.5	87.2	4
10	T2-T12 post spinal fusion	3.5	95.4	3
11	Carotid endarterectomy	1.4	94.3	3
12	AV fistula	1.2	78.6	2
		Average:	91.5	1.6

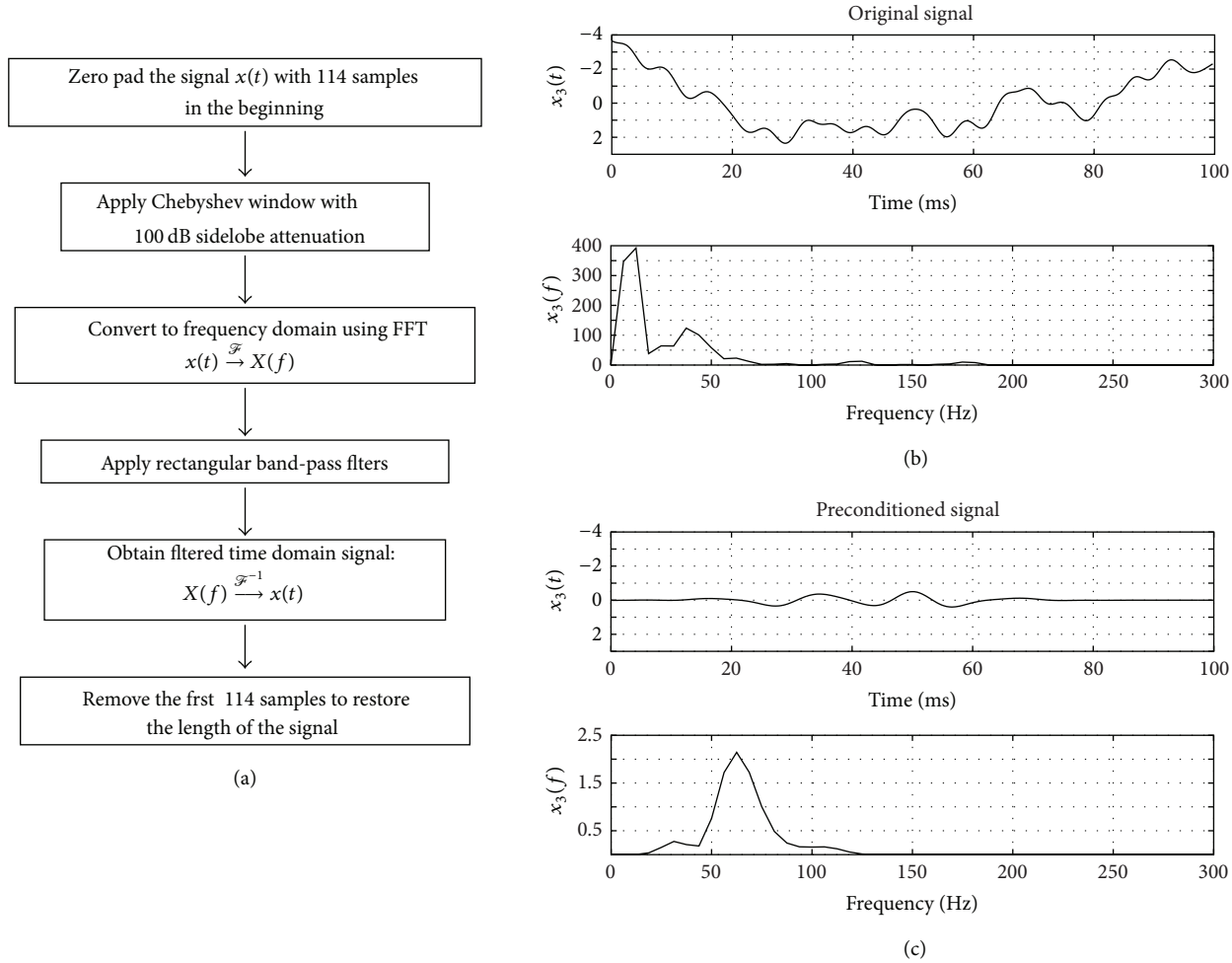

Figure 2: Diagram for "window based preconditioning." (a) Algorithm flowchart for signal preconditioning. (b) The signal $x_3(t)$ before preconditioning from Figure 1(b) along with its power spectrum. (c) The result of preconditioning the signal in (b) and its corresponding power spectrum.

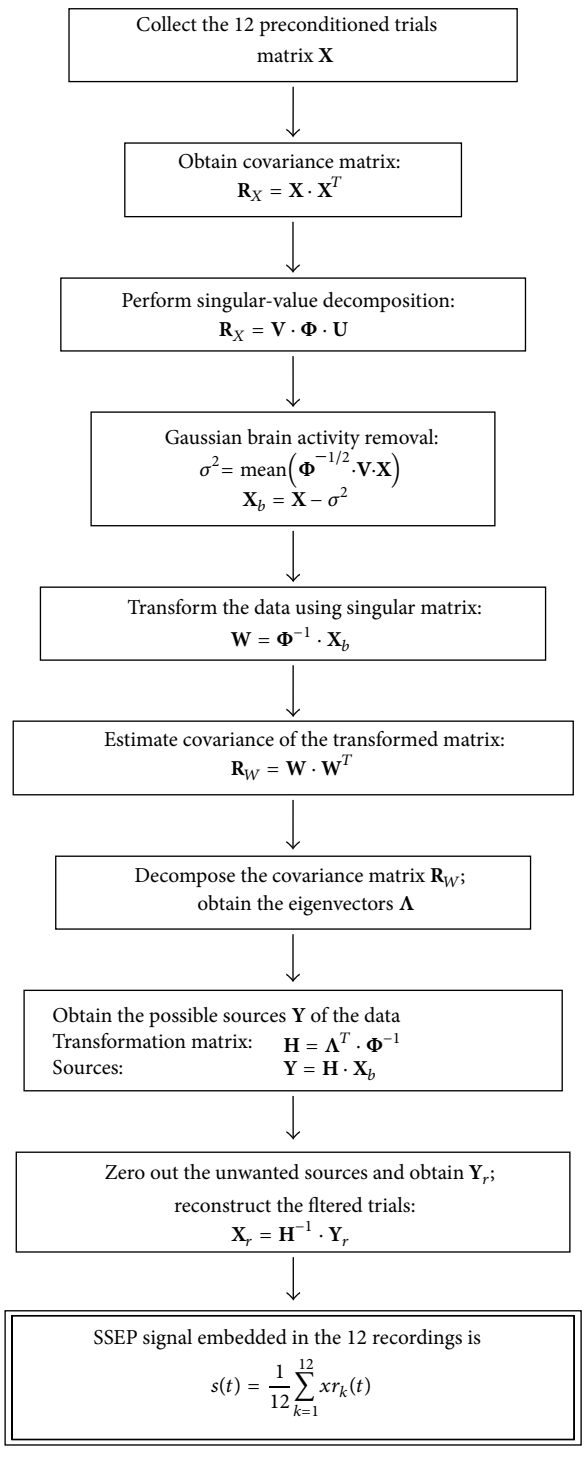

(a)

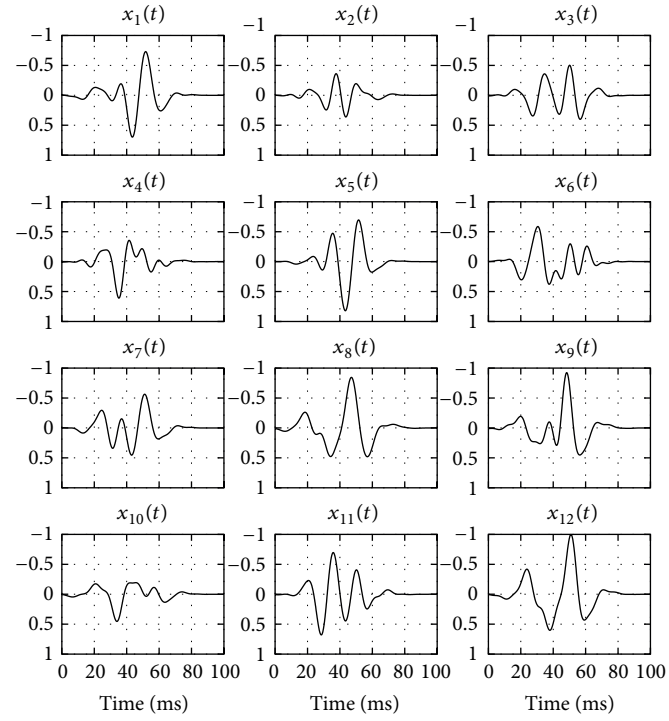

(b)

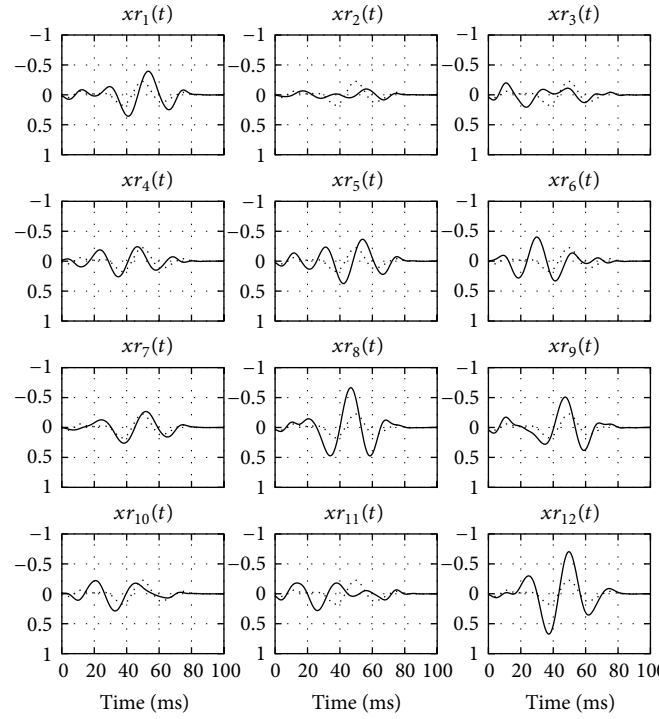

(c)

FIGURE 3: Diagram for "eigenspace filtering". (a) Algorithm flowchart for eigenspace filtering. (b) Set of $x_k(t)$ signals from Figure 1(b) before eigen filtering. (c) Set of $xr_k(t)$ signals after filtering with the extracted SSEP signal, $s(t)$, shown by dotted line superimposed on the signals for easy comparison.

In their structure, (i) the components were arranged in the descending order of their corresponding eigenvalues and (ii) the components that correspond to the eigenvalues, more than one standard deviation above the mean, are the components that contribute to the background brain activity.

(v) These components were identified and removed by zeroing out the components resulting in $\mathbf{Y}_r$.

(vi) The signals were reconstructed from $\mathbf{Y}_r$ with the noise contributing components removed:

$$\mathbf{X}_r = \mathbf{H}^{-1} \cdot \mathbf{Y}_r. \tag{10}$$

2.4.5. Reconstruction and SSEP. We claim that the $\mathbf{X}_r$ signals are the cleanest signals obtained from 12 trials because they are now devoid of

(i) undesired frequency components that are known a priori due to SSEP signal characteristics;

(ii) white Gaussian noise;

(iii) sources estimated to contribute to background brain activity.

The reconstructed components are thus a very close approximation of true SSEP signals corrupted only because of possible brain activity that could not be modeled using second order statistics and not common in all the 12 trials. Performance of signal averaging, using the 12 reconstructed components, like the traditional approach can eliminate this

$$\mathbf{X}_r = \left[xr_1(t) \;\; xr_2(t) \;\; \cdots \;\; xr_{12}(t)\right]^T, \tag{11}$$

where $xr_k(t)$ represents the kth reconstructed trial with 640 time samples arranged along the row:

$$s(t) = \frac{1}{12}\sum_{k=1}^{12} xr_k(t). \tag{12}$$

This signal $s(t)$ represents the SSEP that remains consistent through the 12 trials used in Section 2.4.2 above. Algorithm steps "Window based preconditioning" and "Eigenspace filtering" are continuously carried out while data acquisition is valid and the surgery is proceeding. Since the algorithm requires only 12 trials to extract an SSEP, it requires only a few seconds as opposed to the conventional signal averaging method. As shown in Figure 3, we notice that this eigenspace filtering is able to (1) remove the spurious frequencies, (2) align the most relevant signal components, and (3) preserve the SSEP morphological characteristics extracted by the Chebyshev window-based preconditioning step.

3. Results and Discussion

For IONM using tibial serve SSEP, the peaks that typically occur at 37 ms (positive) and 45 ms (negative) as denoted by P37 and N45, respectively, were monitored. The SSEP obtained just before the surgical procedure is called the baseline signal and was considered as the reference throughout the surgery. It is an established protocol that (1) the time latencies of these peaks should not deviate more than 10% and (2) the peak-to-peak amplitude should not deviate more than 50% from the corresponding baseline values. Any deviation from this protocol is considered a cause for alarm and necessary steps will be undertaken for the safety of the patient.

The algorithm was tested on 12 and the results are presented in Table 1. The algorithm was successful in extracting the SSEP signals throughout all surgeries using only 12 trials that passed the exclusion criterion and checks for the consistencies and any causes for false alarms. The 12 surgical cases did not have any alarms raised during the clinical procedures. The algorithm, however, did raise alarms and these can be termed as "false alarms." This fact assures us that the algorithm is capable of detecting and raising alarms. As such, the accuracy of the algorithm was defined as

$$\%\text{Accuracy} = \left(1 - \frac{\text{no. of false alarms}}{\text{no. of SSEP signals}}\right) \times 100. \tag{13}$$

The sensitivity and accuracy of the algorithm can be analyzed based on the number of detections by the algorithm and the actual alarms raised. In the surgeries performed, there were no alarms raised during the surgeries; however, the algorithm did raise alarms that can be understood as false alarms. It was shown in Table 1 that there are, on an average, 1.6 false alarms per hour. If the false alarms are quantized as the percentage of false alarms occurring per subject for every set of 12 trials used to extract the SSEP, we obtain an average of 0.09% of false alarms.

It is very important to note that since the extracted SSEP signals are obtained every twelve trials and hence the short-term SSEP changes, that would have otherwise gone unnoticed by the conventional averaging method easily detected when using the proposed algorithm. Hence, for a true positive, the changes must persist for 12 successive SSEP signals extracted using the algorithm. No such case was observed in the study confirming that no alarms were raised during the procedures.

On an average, the algorithm raised 1.6 false alarms per hour and presented an accuracy of 91.5%. An example of a typical SSEP extracted using the proposed algorithm for a given subject at five different instances of time during the surgery is shown in Figure 4. Note the merits of using Chebyshev as means to preserve the morphology of the SSEP signal.

In our previous publication, it was observed that even though the automation scheme was shown viable, the IIR filtering applied at the very end might not give an SSEP true to its morphological characteristics to be observed by experienced eyes [14]. We observed, in the present study, that such filtering is more beneficial when applied prior to the eigenspace filtering. Conventional systems also adopt a similar approach of filtering using moving average type filters after signal averaging. These are linear phase filters. Hence, we choose Chebyshev time windowing ante eigenspace filtering. This has the merit of limiting power leakage of the frequency components of SSEP to adjacent frequencies.

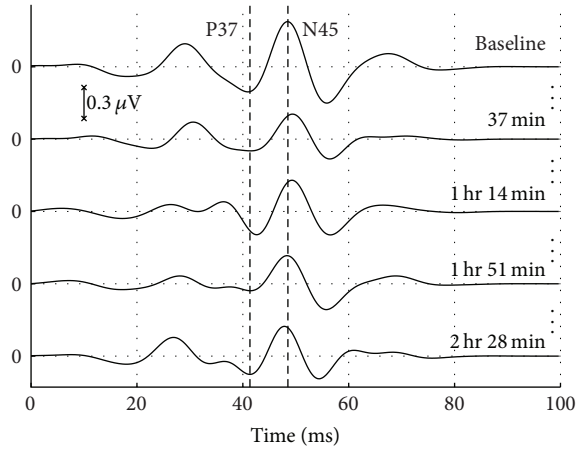

Figure 4: Comparisons of SSEP that were extracted through the surgery with the baseline SSEP at five stages during the surgery of patient number 8.

A rectangular window in the frequency domain eliminates undesired frequency components and preserves those frequencies that contribute most to the SSEP signal. It is also effective in removing the 60 Hz noise introduced by the electrical equipment in the vicinity.

It is a long known fact that EEG sources are nonstationary [19]; however, during the 100 ms time windows, as common in IONM, the EEG sources are considered quasistationary [20, 21] and hence the AMUSE algorithm was able to identify only the known stationary SSEP component. On the other hand, the use of Chebyshev time window made us certain that any other stationary and quasistationary components are eliminated.

4. Conclusions

The current algorithms assume that the SSEP does not change during the time when the 200 or more trials are recorded and rely on the frequency characteristics of the signal rather than the SSEP morphology in time domain. Other proposed approaches also tend to focus on only one aspect of the SSEP characteristics, mainly in the frequency domain. The present approach in retrospect, focuses on preserving the time domain features of SSEP and eliminate the inter-trial variance and extract the SSEP while considering the ongoing brain activity. To ascertain the validity of the algorithm, we present the results of the implementation of the algorithm on 12 surgical procedures that lasted anywhere from 2 to 6 hrs. These surgeries were successful with no resulting neurophysiological disorders. The algorithm also ascertained that the peak latencies and peak-to-peak amplitudes are within the required limits to prove consistency. The algorithm, however, raised 1.6 false alarms per hour. This can be considered as a good sign because this proves that the algorithm is capable of detecting a true alarm, although not experienced in these surgeries. Future study will involve the implementation of this algorithm on patients where a clinical alarm was indeed raised and assess the algorithm's accuracy in detecting the true positives.

Conflict of Interests

The authors declare that there is no conflict of interests regarding the publication of this paper.

Acknowledgments

The authors are thankful for the clinical support provided by the Department of Clinical Neurophysiology at the Oregon Health and Science University (OHSU) and the Ware Foundation. Furthermore, the experimental work of this study was carried out under IRB#052708-03 and IRB#100410-00 and collected data as a routine part of a spine surgery were deidentified at the source.

References

[1] D. S. Dinner, H. Luders, and R. P. Lesser, "Intraoperative spinal somatosensory evoked potential monitoring," *Journal of Neurosurgery*, vol. 65, no. 6, pp. 807–814, 1986.

[2] American Association of Electrodiagnostic Medicine, *Guidelines for Somatosensory Evoked Potentials*, 1999.

[3] C. Strahm, K. Min, N. Boos, Y. Ruetsch, and A. Curt, "Reliability of perioperative SSEP recordings in spine surgery," *Spinal Cord*, vol. 41, no. 9, pp. 483–489, 2003.

[4] D. B. MacDonald, Z. Al Zayed, and B. Stigsby, "Tibial somatosensory evoked potential intraoperative monitoring: recommendations based on signal to noise ratio analysis of popliteal fossa, optimized P37, standard P37, and P31 potentials," *Clinical Neurophysiology*, vol. 116, no. 8, pp. 1858–1869, 2005.

[5] J. I. Aunon, C. D. McGillem, and D. G. Childers, "Signal processing in evoked potential research: averaging and modeling," *Critical Reviews in Bioengineering*, vol. 5, no. 4, pp. 323–367, 1981.

[6] O. Bai, M. Nakamura, T. Nagamine, and H. Shibasaki, "Parametric modeling of somatosensory evoked potentials using discrete cosine transform," *IEEE Transactions on Biomedical Engineering*, vol. 48, no. 11, pp. 1347–1351, 2001.

[7] J. Madhok, A. Maybhate, W. Xiong et al., "Quantitative assessment of somatosensory-evoked potentials after cardiac arrest in rats: prognostication of functional outcomes," *Critical Care Medicine*, vol. 38, no. 8, pp. 1709–1717, 2010.

[8] S. Faul, G. Gregorčič, G. Boylan, W. Marnane, G. Lightbody, and S. Connolly, "Gaussian process modeling of EEG for the detection of neonatal seizures," *IEEE Transactions on Biomedical Engineering*, vol. 54, no. 12, pp. 2151–2162, 2007.

[9] F. Bi, T. Qiu, and N. Yu, "Robust adaptive estimator for evoked potentials based on non-linear transform under impulsive noise environments," *Journal of Medical and Biological Engineering*, vol. 32, no. 6, pp. 443–452, 2012.

[10] X. Kong and T. Oiu, "Latency change estimation for evoked potentials: a comparison of algorithms," *Medical and Biological Engineering and Computing*, vol. 39, no. 2, pp. 208–224, 2001.

[11] H. S. Zhao, Z. G. Zhang, H. T. Liu, K. D. K. Luk, and Y. Hu, "Adaptive signal enhancement of somatosensory evoked potentials based on least mean squares and Kalman filter: a comparative study," in *Proceedings of the 4th International IEEE/EMBS Conference on Neural Engineering (NER '09)*, pp. 738–741, IEEE, May 2009.

[12] Y. Hu, H. Liu, and K. D. Luk, "Time-frequency analysis of somatosensory evoked potentials for intraoperative spinal cord

monitoring," *Journal of Clinical Neurophysiology*, vol. 28, no. 5, pp. 504–511, 2011.

[13] E. Freye and J. V. Levy, "Cerebral monitoring in the operating room and the intensive care unit: an introductory for the clinician and a guide for the novice wanting to open a window to the brain," *Journal of Clinical Monitoring and Computing*, vol. 19, no. 1-2, pp. 1–76, 2005.

[14] K. Vedala, I. Yaylali, M. Cabrerizo, M. Goryawala, and M. Adjouadi, "Peak detection of somatosensory evoked potentials using an integrated principal component analysis-Walsh method," *Journal of Clinical Neurophysiology*, vol. 29, no. 2, pp. 165–173, 2012.

[15] M. Goryawala, I. Yaylali, M. Cabrerizo, K. Vedala, and M. Adjouadi, "An effective intra-operative neurophysiological monitoring scheme for aneurysm clipping and spinal fusion surgeries," *Journal of Neural Engineering*, vol. 9, no. 2, Article ID 026021, 2012.

[16] L. Tong, V. C. Soon, Y. F. Huang, and R. Liu, "AMUSE: a new blind identification algorithm," in *Proceedings of the IEEE International Symposium on Circuits and Systems*, vol. 3, pp. 1784–1787, May 1990.

[17] J. Persson, "Comments on 'Modeling the stationarity and gaussianity of spontaneous electroencephalographic activity'," *IEEE Transactions on Biomedical Engineering*, vol. 24, no. 3, p. 302, 1977.

[18] G. H. Golub and C. Reinsch, "Singular value decomposition and least squares solutions," *Numerische Mathematik*, vol. 14, no. 5, pp. 403–420, 1970.

[19] A. Delorme, J. Palmer, J. Onton, R. Oostenveld, and S. Makeig, "Independent EEG sources are dipolar," *PLoS ONE*, vol. 7, no. 2, Article ID e30135, 2012.

[20] A. Y. Kaplan, A. A. Fingelkurts, A. A. Fingelkurts, S. V. Borisov, and B. S. Darkhovsky, "Nonstationary nature of the brain activity as revealed by EEG/MEG: methodological, practical and conceptual challenges," *Signal Processing*, vol. 85, no. 11, pp. 2190–2212, 2005.

[21] J. Zygierewicz, J. Mazurkiewicz, P. J. Durka, P. J. Franaszczuk, and N. E. Crone, "Estimation of short-time cross-correlation between frequency bands of event related EEG," *Journal of Neuroscience Methods*, vol. 157, no. 2, pp. 294–302, 2006.

Hindawi Publishing Corporation
The Scientific World Journal
Volume 2014, Article ID 907521, 6 pages
http://dx.doi.org/10.1155/2014/907521

Clinical Study

Effect of the Independent Acid Base Variables on Anion Gap Variation in Cardiac Surgical Patients: A Stewart-Figge Approach

Michalis Agrafiotis,[1] Ilias Keklikoglou,[1] Sofia Papoti,[1] George Diminikos,[1] Konstantinos Diplaris,[2] and Vassileios Michaelidis[1]

[1] *2nd Department of Intensive Care Medicine, "G. Papanikolaou" General Hospital of Thessaloniki, G. Papanikolaou Avenue, Exohi, 57010 Thessaloniki, Greece*
[2] *Department of Cardiothoracic Surgery, "G. Papanikolaou" General Hospital of Thessaloniki, G. Papanikolaou Avenue, Exohi, 57010 Thessaloniki, Greece*

Correspondence should be addressed to Michalis Agrafiotis; m.agrafiotis@gmail.com

Received 26 August 2013; Accepted 24 December 2013; Published 3 February 2014

Academic Editors: L. M. Gillman, D. Karakitsos, and A. E. Papalois

Purpose. To determine the effect of each of independent acid base variables on the anion gap (AG) value in cardiac surgical patients. *Methods*. This retrospective study involved 128 cardiac surgical patients admitted for postoperative care. The variation of AG (AG_{var}) between the day of admission and the first postoperative day was correlated via a multiple linear regression model with the respective variations of the independent acid base variables, that is, apparent strong ion difference (SID_a), strong ion gap (SIG), carbon dioxide (PCO_2), and albumin and phosphate concentrations. *Results*. The variations of all the above variables contributed significantly to the prediction of AG_{var} (adjusted $R^2 = 0.9999$, $F = 201890.24$, and $P < 0.001$). According to the standardized coefficients (β), SIG_{var} ($\beta = 0.948$, $P < 0.001$), $[Albumin]_{var}$ ($\beta = 0.260$, $P < 0.001$), and $[Phosphate]_{var}$ ($\beta = 0.191$, $P < 0.001$) were the major determinants of AG_{var} with lesser contributions from $SID_{a,var}$ ($\beta = 0.071$, $P < 0.001$) and $PCO_{2,var}$ ($\beta = -0.067$, $P < 0.001$). *Conclusions*. All the independent acid base variables contribute to the prediction of the AG value. However, albumin and phosphate and SIG variations seem to be the most important predictors, while AG appears to be rather stable with changes in PCO_2 and SID_a.

1. Introduction

The anion gap (AG) is a time-honored acid base variable which has been employed for over 30 years as a scanning tool for the presence of unmeasured ions [1]. It is usually estimated as the difference between the commonly measured cations ($[Na^+] + [K^{(+)}]$) and anions ($[Cl^-] + [HCO_3^-]$) according to the equation:

$$AG = [Na^+] + [K^+] - [Cl^-] - [HCO_3^-] \quad (1)$$

The concept of AG stems from the fundamental principle of electrical neutrality. Hence,

$$\begin{aligned} AG &= [Na^+] + [K^+] - [Cl^-] - [HCO_3^-] \\ &= [UA^-] - [UC^+] + [A^-] \end{aligned} \quad (2)$$

where $[A^-]$ denotes the negative charges contributed by the nonvolatile weak acids, mainly albumin and phosphate; $[UC^+]$ and $[UA^-]$ represent unmeasured cations and anions, respectively. Other ions participating in the equation as $[H^+]$, $[OH^-]$, and $[CO_3^-]$ are quantitatively less important and are ignored [1, 2].

The difference of $[UA^-] - [UC^+]$ quantifies the total charge contributed by the unmeasured ions and incorporates the concentrations of Ca^{2+}, Mg^{2+}, lactate, and sulfate which, under normal conditions, are thought to offset each other. An alternative collective term for unmeasured ions is that of strong ion gap (SIG). Thus, in the absence of significant increases in the concentrations of the unmeasured ions, the AG is formed mainly by the negative charges contributed by the nonvolatile weak acids, mostly albumin and to a lesser extend phosphate [1, 2].

A major limitation in the use of AG for the diagnosis and the evaluation of metabolic acidosis is its dependence on the concentrations of the nonvolatile weak acids, of which albumin is the most important [1, 2]. This shortcoming has long been recognized and addressed by various adjustments or corrections, mainly accounting for the deviation of albumin concentration from its reference value [3–5]. An additional issue of concern is the fact that the charges contributed by weak nonvolatile acids may vary with perturbations in the acid base equilibrium. When acidemia ensues, proteins will titrate the excess protons and therefore their net ionic equivalency will be reduced [6]. Indeed, according to the studies by Figge et al. [7–9], over the physiological pH range, the charges contributed by albumin ($[\text{Albumin}^{z-}]$) and phosphate ($[\text{Phosphate}^{y-}]$) are linear functions of pH:

$$[\text{Albumin}^{z-}] = [\text{Albumin}] \cdot (0.1204 \cdot \text{pH} - 0.625), \quad (3)$$

$$[\text{Phosphate}^{y-}] = [\text{Phosphate}] \cdot (0.309 \cdot \text{pH} - 0.469), \quad (4)$$

where [Albumin] (in g/L) and [Phosphate] (in mmol/L) denote serum albumin and phosphate concentrations, respectively, and charge concentrations are expressed in meq/L.

Therefore, (2) can be recast as

$$\begin{aligned}[\text{AG}] = {} & [\text{UA}^-] - [\text{UC}^+] \\ & + [\text{Albumin}] \cdot (0.1204 \cdot \text{pH} - 0.625) \\ & + [\text{Phosphate}] \cdot (0.309 \cdot \text{pH} - 0.469).\end{aligned} \quad (5)$$

The right side of (5) incorporates three variables: the concentration of unmeasured ions (SIG), the concentrations of the non-volatile weak acids ([Albumin] and [Phosphate], collectively termed A_{tot}), and pH. However, according to the premises of modern quantitative acid base physiology, pH itself is not an independent variable because it is determined by apparent strong ion difference (SID_a), SIG, A_{tot}, and PCO_2 [7–11]. Therefore, both the nonrespiratory (SID_a, SIG, and A_{tot}) and as well the respiratory (PCO_2) component of acid base equilibrium should participate independently in the determination of the AG value. Previous approaches to model AG variation emphasized on the role of the nonvolatile weak acids and they were also based on assumptions or approximations regarding their respective charge concentrations [3–5, 12, 13]. On the other hand, a significant variation of the AG with PCO_2 was observed in an *ex vivo* experiment on whole blood by Morgan et al. [14].

Given the previous considerations, we embarked on this study to assess the impact and the quantitative significance of each of the independent acid base variables on AG variability *in vivo*.

2. Patients and Methods

2.1. Study Design. This retrospective study evaluated routine acid base and biochemical data from cardiac surgical patients admitted to our ICU for postoperative care between January 2010 and March 2011. The local Ethics and Scientific Committee approved the study protocol and waived the requirement for informed consent (Ethics and Scientific Committee session number 5/14.03.2012, Chairperson Dr. Ioannis Zarifis). After reviewing the patients' written medical records and the nurses' flowcharts, the following paired acid base and biochemical data from the day of admission and the first postoperative day were extracted: pH, PCO_2, Na, K, and Cl (from the output of the blood gas machine) and serum albumin and phosphate concentrations (from the biochemical report). A time interval of 16–18 hours intervened between consecutive measurements. In addition, we recorded clinical and demographic data from each patient, including age, sex, type of operation, and logistic Euroscore value.

Blood gas sampling was performed with the use of specifically designed commercially available syringes which come prefilled with dry electrolyte-balanced heparin (PICO sampler; Radiometer, Copenhagen, Denmark); the first 2-3 mL of blood was discarded to avoid contamination with the flushing fluid. Biochemical samples were obtained from the radial artery catheter immediately after the first blood gas samples were drawn. The blood gas samples were analyzed at 37°C for blood gases and electrolytes in the point-of-care blood gas and electrolyte analyzer (ABL800 FLEX analyzer; Radiometer, Copenhagen, Denmark). Albumin and phosphate concentrations were assessed in the hospital central laboratory using colorimetric techniques (Olympus EU 640; Olympus, Center Valley, Pennsylvania, USA).

Following the methodology employed by Park et al. [15], we developed a multiple linear regression model correlating AG variation between admission and first postoperative day with the respective variations of SID_a, SIG, PCO_2, [Albumin], and [Phosphate]. The variation of any acid base variable (e.g., X) between the day of admission and the first postoperative day was defined according to the following formula:

$$X_{\text{var}} = X_1 - X_0, \quad (6)$$

where the suffix var denotes variation and the suffixes 0 and 1 correspond to the day of the admission and the first postoperative day, respectively.

2.2. Mathematical Acid Base Calculations. Quantitative acid base analysis was based on the principles advanced by Stewart [10, 11] and subsequently modified by Figge et al. [7–9] to model the effects of proteins and other nonvolatile weak acids on acid base equilibria. For each patient, the following acid base variables were assessed: AG, bicarbonate concentrations, albumin and phosphate charge concentration, apparent and effective strong ion difference, and strong ion gap (SIG). AG (in meq/L) was calculated by (1), while bicarbonate concentration (in mmol/L) was calculated by the Henderson-Hasselbalch equation:

$$[\text{HCO}_3^-] = 0.0301 \cdot \text{PCO}_2 \cdot 10^{(\text{pH}-6.1)}, \quad (7)$$

where PCO_2 is expressed in mmHg.

Albumin and phosphate charge concentrations were calculated according to (3) and (4), respectively. Since, in the AG formalism Ca^{2+}, Mg^{2+} and lactate are considered unmeasured ions and therefore incorporated into SIG calculation,

the equation for SID_a (in meq/L) was cast in a more simplified form:

$$SID_a = [Na^+] + [K^+] - [Cl^-]. \quad (8)$$

Last, effective strong ion difference (SID_e) and SIG (all in meq/L) were calculated according to the following equations:

$$SID_e = [Albumin^{z-}] + [Phosphate^{y-}] + [HCO_3^-], \quad (9)$$

$$SIG = SID_a - SID_e. \quad (10)$$

2.3. Statistical Analysis. Statistical analysis was performed using the Statistical Package for the Social Sciences software (SPSS Inc., Chicago, Illinois, release 17.0). Continuous variables are expressed as mean ± standard deviation (SD), unless stated otherwise, and dichotomous (categorical) variables are expressed as frequency counts (proportions).

The normality of data distribution was assessed by inspection of histograms. The multiple linear regression model was built in the forward mode with entry and removal criteria of $P = 0.05$ and $P = 0.10$, respectively. Pearson's statistic was employed to assess the presence of single collinearity between the independent variables, with an R value > 0.85 chosen as a single collinearity criterion. Multicollinearity was suggested by a tolerance value less <0.1 and/or a variance inflation factor (VIF) > 10. We plotted the residuals against the dependent and the independent variables to disclose any possible nonlinear relationship. The change in F statistic was used to assess the significance of R^2 improvement by the inclusion of a new variable in the model and a P value less than 0.05 was considered to be significant.

3. Results

One hundred and twenty eight cardiac surgical patients (age 65.8 ± 10 years, 103 males) were included in study. Clinical and demographic characteristics of the patients are summarized in Table 1. The values of AG and of its predictors and their respective variations between admission and the first postoperative day are presented in Table 2.

The output of the multiple linear regression model is summarized in Table 3. According to the standardized correlation coefficients (β) of the model, AG_{var} can be independently predicted by SIG_{var} ($\beta = 0.948, P < 0.001$), $[Albumin]_{var}$ ($\beta = 0.260, P < 0.001$), $[Phosphate]_{var}$ ($\beta = 0.191, P < 0.001$), $SID_{a,var}$ ($\beta = 0.071, P < 0.001$), and $PCO_{2,var}$ ($\beta = -0.067, P < 0.001$). This combination of independent variables virtually explained the whole variance of the dependent variable with an adjusted $R^2 = 0.9999$ ($F = 201890.24, P < 0.001$).

Table 1: Clinical and demographic characteristics of patients ($N = 128$).

Age (years)	65.8 ± 10.0
Males, n/N (%)	103/128 (80.4)
Logistic Euroscore	4.65 (0.88, 78.52)*
Types of operations, n/N (%)	
CABG	90/128 (70.3)
Valvular	16/128 (12.5)
Aortic	8/128 (6.2)
Combined CABG and valvular	7/128 (5.5)
Other	7/128 (5.5)

*Median (range).
CABG: coronary artery bypass grafting.

4. Discussion

In this study we endeavored to identify the independent predictors of AG variation and assess their quantitative importance. The results of our multiple linear regression model suggest that AG variation is determined mainly by two factors: the concentration of the unmeasured ions and the concentrations of nonvolatile weak acids, namely, albumin and phosphate. An important finding of our study is that strong ion difference and PCO_2 also participate independently in the prediction of AG variation although their contributions are quantitatively less important. Indeed, it should be noted that, within the usual clinical settings, the variations of SID_a and PCO_2 are unlikely to be the cause of significant bias in the AG value. For instance, assuming a zero change for the other parameters, a decrease in PCO_2 by 10 mmHg or an increase in SID_a by 10 meq/L would increase AG value by 0.42 and 0.65 meq/L, respectively. Interestingly, in an *ex vivo* experiment on whole blood by Morgan et al. [14], in which PCO_2 was varied from >200 to <20 mmHg, the calculated average increase in AG per mmHg was 0.03 and 0.02 meq/L for normal and diluted blood, respectively (calculations based on mean initial and final values). These values are of the same order with the correlation coefficient for $PCO_{2,var}$ in our model (Table 3).

To our knowledge, this is the first study that evaluated the role of respiratory perturbations on the value of the AG *in vivo*. The results of this study indicate that respiratory acid base disorders do not impact a quantitatively significant bias on the AG value. Therefore, the AG (particularly in its albumin and phosphate-adjusted form) can be reliably used for the assessment of metabolic acid base disorders in patients with respiratory acid base disturbances. Of note, an alternative metabolic acid base index, standard base excess, was recently demonstrated to exhibit a quantitatively significant variability with changes in PCO_2 [15].

On the other hand, the possibility that changes in SID_a may influence the AG value has not been considered so far in quantitative acid base analyses. This fact is likely to be partly related to the persistence of previous firmly established premises of traditional acid base physiology. Thus, the traditional classification of acidosis distinguished between the "hyperchloremic" and the "nonhyperchloremic" types and ignored the other strong ions, while the change in $[Cl^-]$ was thought to be more or less cancelled out by an opposite change in $[HCO_3^-]$, essentially leaving AG unaltered (non-AG acidosis) [16].

Furthermore, although the homeostases of Cl^- and CO_2 are thought to be interlinked at the level of the erythrocytes [17] and the kidneys [18], we have found that the variations of

Table 2: Variation of anion gap and its predictors between admission and first postoperative day ($N = 128$).

Acid base variables	Admission	First postoperative day	Variation
SID_a, meq/L	37.8 ± 4.0	37.4 ± 3.8	−0.4 ± 4.9
PCO_2, mmHg	40.1 ± 5.8	37.7 ± 4.6	−2.4 ± 7.0
Phosphate, mmol/L	1.1 ± 0.4	1.2 ± 0.4	0.05 ± 0.5
Albumin, g/L	31.5 ± 5.0	29.5 ± 4.7	−1.9 ± 4.7
SIG, meq/L	4.0 ± 4.7	2.5 ± 3.8	−1.5 ± 4.5
AG, meq/L	14.3 ± 4.5	12.6 ± 3.5	−1.7 ± 4.5

Table 3: Output of the multiple linear regression model correlating AG_{var} (dependent variable) with SIG_{var}, $[Albumin]_{var}$, $[Phosphate]_{var}$, $PCO_{2,var}$, and $SID_{a,var}$ (independent variables) (adjusted $R^2 = 0.9999$, $F = 201890.24$, and $P < 0.001$).

	Unstandardized coefficients (95% CI)	Standardized coefficients	P value	Tolerance	VIF
Constant	0 (−0.014, 0.012)		0.883		
SIG_{var}, meq/L	0.934 (0.931, 0.938)	0.948	<0.001	0.310	3.228
$[Albumin]_{var}$, g/L	0.251 (0.248, 0.253)	0.260	<0.001	0.680	0.1471
$[Phosphate]_{var}$, mmol/L	1.704 (1.685, 1.723)	0.191	<0.001	0.821	1.218
$PCO_{2,var}$, mmHg	−0.042 (−0.044, −0.041)	−0.067	<0.001	0.623	1.606
$SID_{a,var}$, meq/L	0.065 (0.062, 0.068)	0.071	<0.001	0.283	3.530

CI: confidence intervals.

SID_a and PCO_2 between admission and the first postoperative day predict independently AG variation without significant multicollinearity. This is not surprising since, according to Stewart-Figge theory [7–11], within a single compartment, both PCO_2 and SID_a should be independent predictors of acid base equilibrium, regardless how their values were established. In addition, the opposite correlation coefficients of PCO_2 and SID_a (Table 3) preclude the possibility of renal or tissue compensation.

Based on the output of the model (Table 3), the change of AG value from a reference state can be partitioned into the respective changes of the four independent acid base variables according to the following equation:

$$\begin{aligned}\Delta AG = {} & 0.934 \cdot \Delta SIG + 0.251 \cdot \Delta [Albumin] \\ & + 1.704 \cdot \Delta [Phosphate] + 0.065 \cdot \Delta SID_a \\ & - 0.042 \cdot \Delta PCO_2,\end{aligned} \tag{11}$$

where Δ denotes change or difference.

If the quantitatively minimal contributions from SID_a and PCO_2 are ignored and the correlation coefficients are rounded, our model's master equation (11) can be recast in a more simplified form:

$$\begin{aligned}\Delta AG = {} & \Delta SIG + 0.25 \cdot \Delta [Albumin] \\ & + 1.7 \cdot \Delta [Phosphate].\end{aligned} \tag{12}$$

Alternatively we can write

$$\begin{aligned}\Delta AG - \Delta SIG = {} & 0.25 \cdot \Delta [Albumin] \\ & + 1.7 \cdot \Delta [Phosphate].\end{aligned} \tag{13}$$

Equation (13) quantifies the partition in the change of AG value that is not attributed to the addition of unmeasured ions. Therefore, the AG value can be adjusted to reference conditions according to the following equation:

$$\begin{aligned}AG_{adj} = {} & AG_{ob} + 0.25 \cdot \left([Albumin]_{ref} - [Albumin]_{ob}\right) \\ & + 1.7 \cdot \left([Phosphate]_{ref} - [Phosphate]_{ob}\right),\end{aligned} \tag{14}$$

where the suffixes ref, adj, and ob denote the reference, adjusted, and observed values, respectively. With respect to albumin, this adjustment is identical to the one proposed by Figge et al. [3], although in their study on critically ill patients the contribution of phosphate was not modeled. Alternatively, Carvounis and Feinfeld [5] suggested that the adjustment factor should be expressed either as $1.5 \cdot ([Albumin]_{ref} - [Albumin]_{ob})$ for patients with total $CO_2 > 21$ meq/L or as $2 \cdot ([Albumin]_{ref} - [Albumin]_{ob})$ for patients with total $CO_2 < 22$ meq/L. More recently, the slope of AG versus albumin was found to be equal to 0.23 meq/L per g/L of albumin in study by Feldman et al. [12] involving a large database of in- and outpatients.

If we integrate both sides of (12) and solve for SIG, we can also obtain the unmeasured ion concentration:

$$\begin{aligned}SIG = {} & AG_{ob} - \left(0.25[Albumin]_{ob}\right. \\ & \left. + 1.7[Phosphate]_{ob}\right).\end{aligned} \tag{15}$$

It should be noted here that Kellum proposed a similar empirical calculation rule for the unmeasured ion concentration (termed corrected AG), by averaging albumin and phosphate charges over the acidemic pH range and subtracting them from the observed AG value [4]. Hence,

$$\begin{aligned}AG_{cor} = {} & AG_{ob} - \left(0.2[Albumin]_{ob}\right. \\ & \left. + 1.5[Phosphate]_{ob}\right),\end{aligned} \tag{16}$$

where the suffix cor denotes the corrected AG value. Again, the units for albumin and phosphate concentrations are g/L and mmol/L, respectively.

The validity of Figge's algorithm for the correction (adjustment) of AG value according to albumin concentration has been assessed in several clinical studies. Generally, studies in critically ill [19–21] and in hospitalized patients [22] have demonstrated that albumin-corrected AG (ACAG) is not specific enough for the detection of hyperlactemia although it may rule out its presence [19]. In addition, in a study by Hatherill et al. on critically ill children with shock, the difference between the observed ACAG and its reference value could predict an increase >5 mmol/L in occult tissue ions (lactate plus unmeasured ions) with a sensitivity of 87% and a specificity of 75% [23]. On the other hand, a study by Moviat et al. [21] noted that when the difference between the observed ACAG and its reference value was adjusted for lactate, it performed reasonably well in the prediction of SIG in critically ill adult patients (bias 1.86 and precision 0.96 according to Bland-Altman analysis).

Our approach is limited by the fact that we did not prospectively validate our model on an independent patient population. However the formalisms derived from this model (see (14) and (15)) do not differ significantly from previous approximations employed for the adjustment or the correction of the AG value [3, 4].

In addition, we should point out that this mathematical model is only applicable within the ranges of the independent variable variations observed in this study. On the other hand, a major advantage of our approach is that it does neither require nor resort to assumptions or approximations regarding the pH value or albumin and phosphate charge concentrations. Only the knowledge of the independent variables of acid base equilibrium, that is, SID_a, [Albumin], [Phosphate], SIG, and PCO_2, suffices for the prediction of AG value.

To conclude, we have developed a comprehensive mathematical model which correlates AG variation with the respective variations of SIG, [Albumin], [Phosphate], SID_a, and PCO_2. All the above acid base variables exert an independent influence on the AG value, although SIG, [Albumin], and [Phosphate] are quantitatively the most important predictors. Moreover, the AG seems to be a robust index for the assessment of metabolic acid base disorders in patients with coexistent respiratory or strong ion acid base disturbances.

Conflict of Interests

The authors declare that there is no conflict of interests regarding the publication of this paper.

References

[1] J. A. Kraut and N. E. Madias, "Serum anion gap: its uses and limitations in clinical medicine," *Clinical Journal of the American Society of Nephrology*, vol. 2, no. 1, pp. 162–174, 2007.

[2] J. A. Kellum, "Clinical review: reunification of acid-base physiology," *Critical Care*, vol. 9, no. 5, pp. 500–507, 2005.

[3] J. Figge, A. Jabor, A. Kazda, and V. Fencl, "Anion gap and hypoalbuminemia," *Critical Care Medicine*, vol. 26, no. 11, pp. 1807–1810, 1998.

[4] J. A. Kellum, "Determinants of blood pH in health and disease," *Critical Care*, vol. 4, no. 1, pp. 6–14, 2000.

[5] C. P. Carvounis and D. A. Feinfeld, "A simple estimate of the effect of the serum albumin level on the anion gap," *American Journal of Nephrology*, vol. 20, no. 5, pp. 369–372, 2000.

[6] H. J. Adrogué, J. Brensilver, and N. E. Madias, "Changes in the plasma anion gap during chronic metabolic acid-base disturbances," *American Journal of Physiology—Renal Physiology*, vol. 235, no. 4, pp. F291–F297, 1978.

[7] J. Figge, T. H. Rossing, and V. Fencl, "The role of serum proteins in acid-base equilibria," *Journal of Laboratory and Clinical Medicine*, vol. 117, no. 6, pp. 453–467, 1991.

[8] J. Figge, T. Mydosh, and V. Fencl, "Serum proteins and acid-base equilibria: a follow-up," *Journal of Laboratory and Clinical Medicine*, vol. 120, no. 5, pp. 713–719, 1992.

[9] J. Figge, "Role of the non-volatile weak acids (albumin, phosphate and citrate)," in *Stewart's Textbook of Acid Base*, J. A. Kellum and P. W. G. Elbers, Eds., pp. 217–232, Lulu Enterprises, 2nd edition, 2009.

[10] P. A. Stewart, "Modern quantitative acid-base chemistry," *Canadian Journal of Physiology and Pharmacology*, vol. 61, no. 12, pp. 1444–1461, 1983.

[11] P. A. Stewart, "How to understand acid base," in *Stewart's Textbook of Acid Base*, J. A. Kellum and P. W. G. Elbers, Eds., pp. 29–197, Lulu Enterprises, 2nd edition, 2009.

[12] M. Feldman, N. Soni, and B. Dickson, "Influence of hypoalbuminemia or hyperalbuminemia on the serum anion gap," *Journal of Laboratory and Clinical Medicine*, vol. 146, no. 6, pp. 317–320, 2005.

[13] H. E. Corey, "The anion gap (AG): studies in the nephrotic syndrome and diabetic ketoacidosis (DKA)," *Journal of Laboratory and Clinical Medicine*, vol. 147, no. 3, pp. 121–125, 2006.

[14] T. J. Morgan, D. M. Cowley, S. L. Weier, and B. Venkatesh, "Stability of the strong ion gap versus the anion gap over extremes of PCO_2 and pH," *Anaesthesia and Intensive Care*, vol. 35, no. 3, pp. 370–373, 2007.

[15] M. Park, A. T. Maciel, D. T. Noritomi, L. C. Pontes de Azevedo, L. U. Taniguchi, and L. M. da Cruz Neto, "Effect of $PaCO_2$ variation on standard base excess value in critically ill patients," *Journal of Critical Care*, vol. 24, no. 4, pp. 484–491, 2009.

[16] D. A. Story, "Hyperchloraemic acidosis: another misnomer?" *Critical Care & Resuscitation*, vol. 6, no. 3, pp. 188–192, 2004.

[17] E. A. Westen and H. D. Prange, "A reexamination of the mechanisms underlying the arteriovenous chloride shift," *Physiological and Biochemical Zoology*, vol. 76, no. 5, pp. 603–614, 2003.

[18] L. L. Hamm, "Renal regulation of hydrogen ion balance," in *Acid Base Disorders and Their Treatment*, F. J. Gennari, H. J. Androgue, J. H. Galla, and N. E. Madias, Eds., pp. 79–117, Taylor and Francis, 2005.

[19] L. S. Chawla, S. Shih, D. Davison, C. Junker, and M. G. Seneff, "Anion gap, anion gap corrected for albumin, base deficit and unmeasured anions in critically ill patients: implications on the assessment of metabolic acidosis and the diagnosis of hyperlactatemia," *BMC Emergency Medicine*, vol. 8, article 18, 2008.

[20] L. S. Chawla, D. Jagasia, L. M. Abell et al., "Anion gap, anion gap corrected for albumin, and base deficit fail to accurately diagnose clinically significant hyperlactatemia in critically ill patients," *Journal of Intensive Care Medicine*, vol. 23, no. 2, pp. 122–127, 2008.

[21] M. Moviat, F. van Haren, and H. van der Hoeven, "Conventional or physicochemical approach in intensive care unit patients with metabolic acidosis," *Critical Care*, vol. 7, no. 3, pp. R41–R45, 2003.

[22] C. H. Dinh, R. Ng, A. Grandinetti, A. Joffe, and D. C. Chow, "Correcting the anion gap for hypoalbuminaemia does not improve detection of hyperlactataemia," *Emergency Medicine Journal*, vol. 23, no. 8, pp. 627–629, 2006.

[23] M. Hatherill, Z. Waggie, L. Purves, L. Reynolds, and A. Argent, "Correction of the anion gap for albumin in order to detect occult tissue anions in shock," *Archives of Disease in Childhood*, vol. 87, no. 6, pp. 526–529, 2002.

Hindawi Publishing Corporation
The Scientific World Journal
Volume 2014, Article ID 504248, 10 pages
http://dx.doi.org/10.1155/2014/504248

Research Article

Invasive and Ultrasound Based Monitoring of the Intracranial Pressure in an Experimental Model of Epidural Hematoma Progressing towards Brain Tamponade on Rabbits

Konstantinos Kasapas,[1] Angela Diamantopoulou,[2] Nicolaos Pentilas,[3] Apostolos Papalois,[4] Emmanuel Douzinas,[5] Gregorios Kouraklis,[2] Michel Slama,[6] Abdullah Sulieman Terkawi,[7,8] Michael Blaivas,[9] Ashot Ernest Sargsyan,[10] and Dimitrios Karakitsos[9]

[1] *Department of Neurosurgery, Athens General Hospital "G. Gennimatas", 11527 Athens, Greece*
[2] *2nd Department of Surgery, Athens Medical School, Laiko University Hospital, 11527 Athens, Greece*
[3] *Intensive Care Unit, Athens General Hospital "G. Gennimatas", Athens, Greece*
[4] *Experimental Research Center ELPEN, 19009 Athens, Greece*
[5] *3rd ICU Department, Athens Medical School, Evgenideio University Hospital, 15128 Athens, Greece*
[6] *ICU, Amiens University Hospital, 80054 Amiens, France*
[7] *Department of Anesthesiology, University of Virginia Health System, Charlottesville, VA 22903, USA*
[8] *Department of Anesthesiology, King Fahad Medical City, Riyadh 11525, Saudi Arabia*
[9] *Department of Internal Medicine, School of Medicine, University of South Carolina, Columbia, SC 29225, USA*
[10] *Wyle Science, Technology & Engineering Group/NASA Bioastronautics, Houston, TX 77058, USA*

Correspondence should be addressed to Konstantinos Kasapas; kostaskasapas@gmail.com

Received 30 August 2013; Accepted 12 November 2013; Published 21 January 2014

Academic Editors: H. Morimatsu and O. B. Paulson

Introduction. An experimental epidural hematoma model was used to study the relation of ultrasound indices, namely, transcranial color-coded-Doppler (TCCD) derived pulsatility index (PI), optic nerve sheath diameter (ONSD), and pupil constriction velocity (V) which was derived from a consensual sonographic pupillary light reflex (PLR) test with invasive intracranial pressure (ICP) measurements. *Material and Methods*. Twenty rabbits participated in the study. An intraparenchymal ICP catheter and a 5F Swan-Ganz catheter (SG) for the hematoma reproduction were used. We successively introduced 0.1 mL increments of autologous blood into the SG until the Cushing reaction occurred. Synchronous ICP and ultrasound measurements were performed accordingly. *Results*. A constant increase of PI and ONSD and a decrease of V values were observed with increased ICP values. The relationship between the ultrasound variables and ICP was exponential; thus curved prediction equations of ICP were used. PI, ONSD, and V were significantly correlated with ICP ($r^2 = 0.84 \pm 0.076$, $r^2 = 0.62 \pm 0.119$, and $r^2 = 0.78 \pm 0.09$, resp. (all $P < 0.001$)). *Conclusion*. Although statistically significant prediction models of ICP were derived from ultrasound indices, the exponential relationship between the parameters underpins that results should be interpreted with caution and in the current experimental context.

1. Introduction

The invasive measurement of intracranial pressure (ICP) is an established neuromonitoring tool in patients with traumatic brain injury (TBI) [1–6]. Although the insertion of an intracranial catheter remains the standard method for diagnosing intracranial hypertension, noninvasive monitoring techniques such as computed tomography (CT) scan of the head, ophthalmoscopy, and transcranial color-coded Doppler (TCCD) have been applied on head injured patients in the intensive care unit (ICU) [4, 5, 7]. Apart from TCCD, the development of multipurpose ultrasound systems has

facilitated the assessment of optic nerve sheath diameter (ONSD) as a surrogate measure of ICP and recently the recording of pupillary light reflex (PLR) when visual access to the pupil is impeded [4–10].

Although not yet established, the aforementioned ultrasound methods have been gradually integrated in neuromonitoring strategies due to the availability of ultrasound systems which allowed fast and by-the-bed evaluation in the ICU. Ultrasound methods have various limitations as they remain largely operator-dependent, while the presence of inadequate acoustic windows, especially in the case of TCCD, may prevent their application in all cases [4–10]. Our group has previously suggested the significance of combined measurements of the Doppler derived pulsatility index (PI) in the middle cerebral artery (MCA) and ONSD recordings as surrogate measures of ICP in patients with TBI [4, 5]. PI is calculated by the equation: PI = systolic flow velocity (FVs)—diastolic flow velocity (FVd)/mean flow velocity (FVm) and is a well-known measure of vascular impedance [5, 7]. In previous experimental models of TBI progressing towards brain tamponade and thus cerebral circulatory arrest (CCA), increased PI thresholds over 2 were associated with loss of autoregulation and critically reduced cerebral blood flow [11–16]. CCA can be identified by TCCD as the former is characterized by the presence of systolic spikes or oscillating flow [15, 16]. However, the progression of a brain injury to loss of cerebral autoregulation and finally to CCA may indeed follow variable pathophysiologic pathways dependent on the underlying disorder (i.e., stroke, diffuse brain edema, hematoma, etc.). Moreover, the relationship of noninvasive neuromonitoring indices such as the PI, ONSD, and sonographic PLR to invasive ICP measurements remains a debatable issue in patients with TBI [1–11].

In this experimental study, we have used a previously established model of TBI in rabbits which has been developed by our group [17]. In the aforementioned model, a 5-Fr balloon-tipped catheter is placed in the epidural space of rabbits, while gradual infusion of autologous blood results in the reproduction of a mass effect due to the implanted epidural hematoma [17]. In this model, we have invasively evaluated the ICP, during the epidural hematoma formation until the Cushing reaction was established. Simultaneous combined recordings of ultrasound neuromonitoring indices, namely, PI, ONSD, and pupil constriction velocity (V) during a consensual PLR test were performed. The endpoint was to study the possible relation of the ultrasound neuromonitoring indices to the invasive ICP measurements.

2. Materials and Methods

All animal experiments were approved by the veterinary authorities of East Attica region and were in accordance with European Union regulations and the principles of the Helsinki Declaration. The animals had free access to daily food and drink. Twenty-two adult New Zealand white rabbits (10 males, 3 ± 0.3 Kg) participated in the study. Two animals died during intubation, and thus 20 animals were included in the final analysis.

Figure 1: The offhand three-dimensional frame used to stabilize the head of the rabbit.

Figure 2: An intubated rabbit stabilized by the three-dimensional frame.

In all rabbits, we facilitated the reproduction of an epidural hematoma that consequently resulted in brain tamponade [17]. Briefly, the central auricular artery and marginal ear vein were cannulated. Anesthesia was induced with intravenous Pentobarbital (Dolethal 200 mg/mL) (2 mL diluted in 8 mL N/S) 1–1.5 mL and maintained with 0.3–1 mL/20 min, while for analgesia Fentanyl 0.5 mg/10 mL was infused and maintained at 0.02 mg/kgr/20 min. Adjustments of the anesthesia depth were guided according to the pedal withdrawal, the ear pinch and the eye lid reflexes. Tracheal intubation was performed in 18 animals using a 2.5–3 mm diameter tube. Tracheotomy was performed in two animals which could not be intubated. All animals were ventilated with a volume-controlled ventilator (Tiberius 19, Drogerwerk AG, Lobeck, Germany) using low tidal volumes (set at 5–10 mL/kg) and adjusted respiratory rates to maintain the carbon dioxide pressure in arterial blood (PCO2) between 32 and 35 mmHg.

The head of the animal was stabilized by means of an offhand three-dimensional frame almost similar to the 3-point Mayfield system used in neurological procedures (Figures 1 and 2). This was performed to facilitate the surgical process and the consequent ultrasound measurements. Ten minutes after the administration of anesthesia, a middle-line incision was performed and a burr hole approximately 1 cm lateral to the sagittal suture and 1 cm posterior to the coronal suture of the animal's skull was also performed bilaterally. In the first burr hole, the dura matter was incised carefully

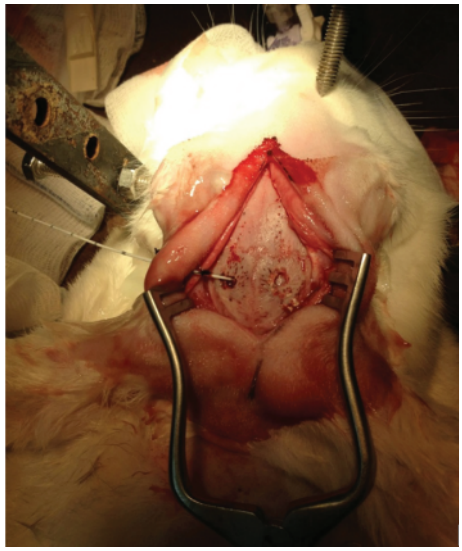

Figure 3: Intraprocedural image of the rabbit's skull depicting the two burr holes and the insertion of the fiberoptic Camino catheter.

with a thick needle and a fiberoptic catheter (Camino Laboratories, San Diego, CA, USA) that was connected to a dedicated monitor was placed in the parenchyma, after being calibrated in the air for continuous ICP monitoring (Figure 3). In the contralateral burr hole, a 5F Swan-Ganz balloon-tipped catheter was placed in the epidural space for the reproduction of the epidural hematoma. The volume of the cranial vault was measured by calculating the volume of an injected hydrophilic gel that was required to fill the intracranial vault [17].

2.1. Study Protocol. When the experimental setup was completed, reference values of ICP, ONSD, TCD, and V were recorded taking into consideration that the volumes of the fiberoptic catheter and the Swan-Ganz balloon catheter were 0.1 and 0.3 mL, respectively. The aforementioned values were entered as baseline values in the statistical analysis. Next, we gradually and successively introduced 0.1 mL increments of autologous blood into the Swan Ganz balloon-tipped catheter that was placed in the epidural space (0.1 mL, 0.2 mL, 0.3 mL, etc.) until the Cushing reaction occurred. Four rabbits exhibited a Cushing reaction at 0.6 to 0.8 mL of infused autologous blood, while the remaining 16 exhibited this reaction when a total volume of 1 mL was reached. Thus, we used the latter as the higher volume reference value of autologous blood infusion in the statistical analysis. We maintained the Cushing reaction for 2-3 minutes in all animals to facilitate a diagnosis of CCA by means of TCCD (see below). Next, the balloon was deflated accordingly.

At each stage of the formation of the epidural hematoma, several minutes (5–10 min) were given to achieve a "steady" state as most animals required additional anesthesia to maintain deep sedation, while intravenous infusion of small amounts of normal saline (10–80 mL) was also necessary to preserve an adequate systolic pressure. During this process, continuous invasive recordings of the ICP were performed, while heart rate and systemic blood pressure were monitored by means of an invasive arterial line which was inserted in the central auricular artery and connected to a dedicated hemodynamic monitor (Edwards monitor, Edwards Lifesciences, Irvine, CA). Electrocardiograms were recorded accordingly. Body temperature was recorded with a rectal temperature probe. At the end of the above-mentioned "steady" state (around 5–10 minutes following each infusion), simultaneous ICP and ultrasound measurements were recorded and included in the analysis. Two sets of three bilateral ultrasound measurements of each ultrasound parameter (PI, ONSD, and V) were performed at each stage of the reproduction of the epidural hematoma and average values were used in the final analysis. Five animals immediately expired after the completion of the experiment, while the remaining 15 were killed with a bolus dose of thiopental. In all animals, the skull was opened and both the dura and the brain were examined for possible procedural lesions that could confound the interpretation of results.

2.2. Ultrasound Measurements. All measurements were performed by one experienced operator to minimize bias. An M-Turbo ultrasonographic system (SonoSite, Bothell, WA) equipped with a high-frequency linear transducer was used for the ONSD and PLR measurements, while a 2.5 MHz wide-phase array transducer with an appropriate software program was utilized to perform TCCD measurements.

TCCD recordings were performed by accessing the anterior and posterior temporal TCCD windows bilaterally [4, 5, 15, 16]. PI values (PI = FVs−FVd/FVm) derived from the Doppler waveform at the area of the insonated middle cerebral artery (MCA) were registered accordingly (Figure 4). The recordings were technically difficult due to the small size of the animal's head and the on-going surgical process. However, the animal's skull was thin, while adjustments of the probe's frequency and intensity (i.e., adjusting the mechanical index) facilitated TCCD recordings in all cases. CCA was diagnosed when systolic spikes or oscillating flow were evident in the MCA as previously described in the literature [4, 5, 15, 16]. CCA was registered on Doppler recordings when the gradually expanding epidural hematoma has created brain tamponade due to its mass effect; moreover, CCA coincided with the occurrence of the Cushing reaction in all animals.

ONSD was measured by using an oblique axial view to access the optic nerve head 2 to 3 mm posterior to the papilla as previously described in the literature [4, 5, 8]. The probe was placed on the upper eyelid and the plane bypassed the anterior structures focusing on the optic nerve head. Unfortunately, the sonographic differentiation (contrast) between the nerve proper and the arachnoid (cerebrospinal fluid space) was not possible. This was mainly due to the fact that in rabbits the optic nerve's size is small and its course rather is oblique. Hence, the ONSD was measured as a "dark stripe" behind the globe (Figure 4). Past studies have suggested increased ONSDs which correlated with invasive ICP measurements and brain computed tomography (CT) findings in patients with severe TBI [4, 5].

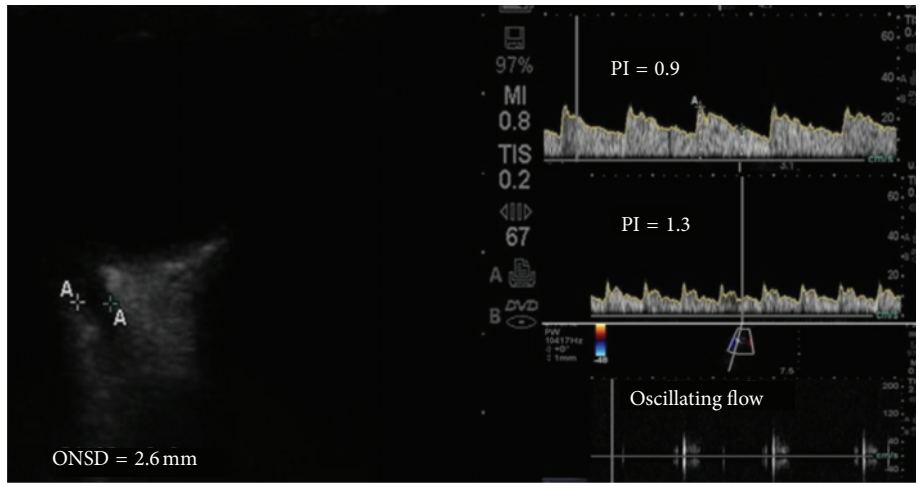

Figure 4: (Left panel) Ultrasound measurements (volume of autologous blood volume infusion = 0.8 mL) by means of the "dark stripe" method depicting an increased ONSD of 2.6 mm in a rabbit with increased ICP (30 mm Hg). (Right panel) TCCD waveforms depicting sequentially: a normal PI (top, volume of autologous blood infusion = 0.1 mL, ICP = 7 mm Hg), an increased PI of 1.3 (middle, volume of autologous blood infusion = 0.6 mL, ICP = 21 mm Hg, and oscillating flow soon after the occurrence of the Cushing reaction (bottom, volume of autologous blood infusion = 1 mL, ICP =40 mm Hg).

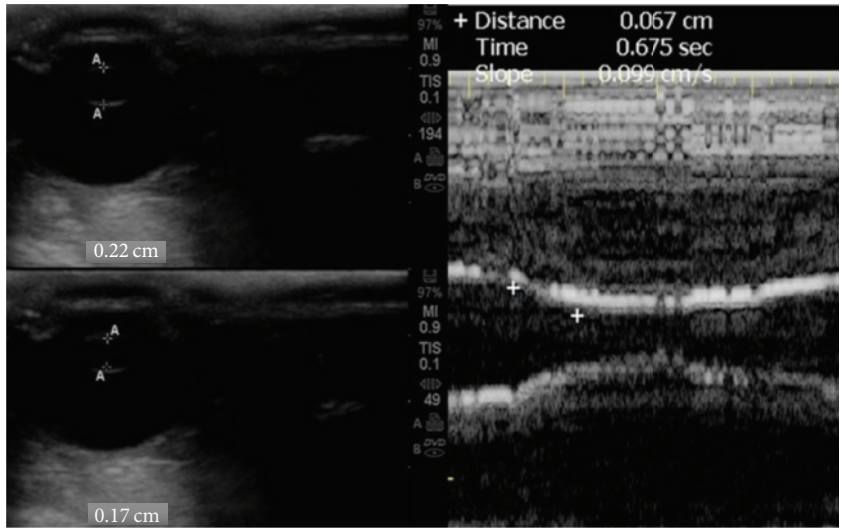

Figure 5: (Left panel) Normal pupillary size at relaxation (top) and following a consensual PLR (bottom) on B-mode. (Right panel) Normal pupil constriction velocity which is calculated by the slope of the M-mode (V = 0.09 cm/s in this example) as the latter can be easily placed on the pupil's center when performing a consensual PLR (volume of autologous blood infusion = 0.1 mL, ICP = 8 mm Hg).

The sonographic examination of pupil's diameter and reactivity to light is a new alternative method to standard pupillometry. Past studies have suggested a relationship, particularly in TBI patients with a mass effect, of ICP and V when performing a consensual PLR test [18]. The sonographic method was initially developed for the U.S. Space Program and is not currently standardized for clinical use [19]. In this study, a consensual PLR was elicited with contralateral transillumination through the eyelids of the rabbits with both eyes closed. The PLR ultrasound test was conducted with a linear array probe at the highest available frequency using a coronal view through the upper eyelid. In rabbits, the pupil's size is relatively large compared to the size of other ocular structures, and thus it was detectable on B-mode. Finally, M-mode recordings were focused on the two-dimensional images of the pupil and were used to evaluate the pupil's V by measuring the slope of the elicited consensual PLR as demonstrated in Figure 5.

2.3. Statistical Analysis. Data are presented as mean ± standard deviation (SD), while 95% confidence intervals (CI) were calculated accordingly. Differences between the values of the studied neuromonitoring indices (PI, ONSD, and V) at baseline compared to our higher volume reference value (1 mL) were evaluated by paired t-test. The relationship

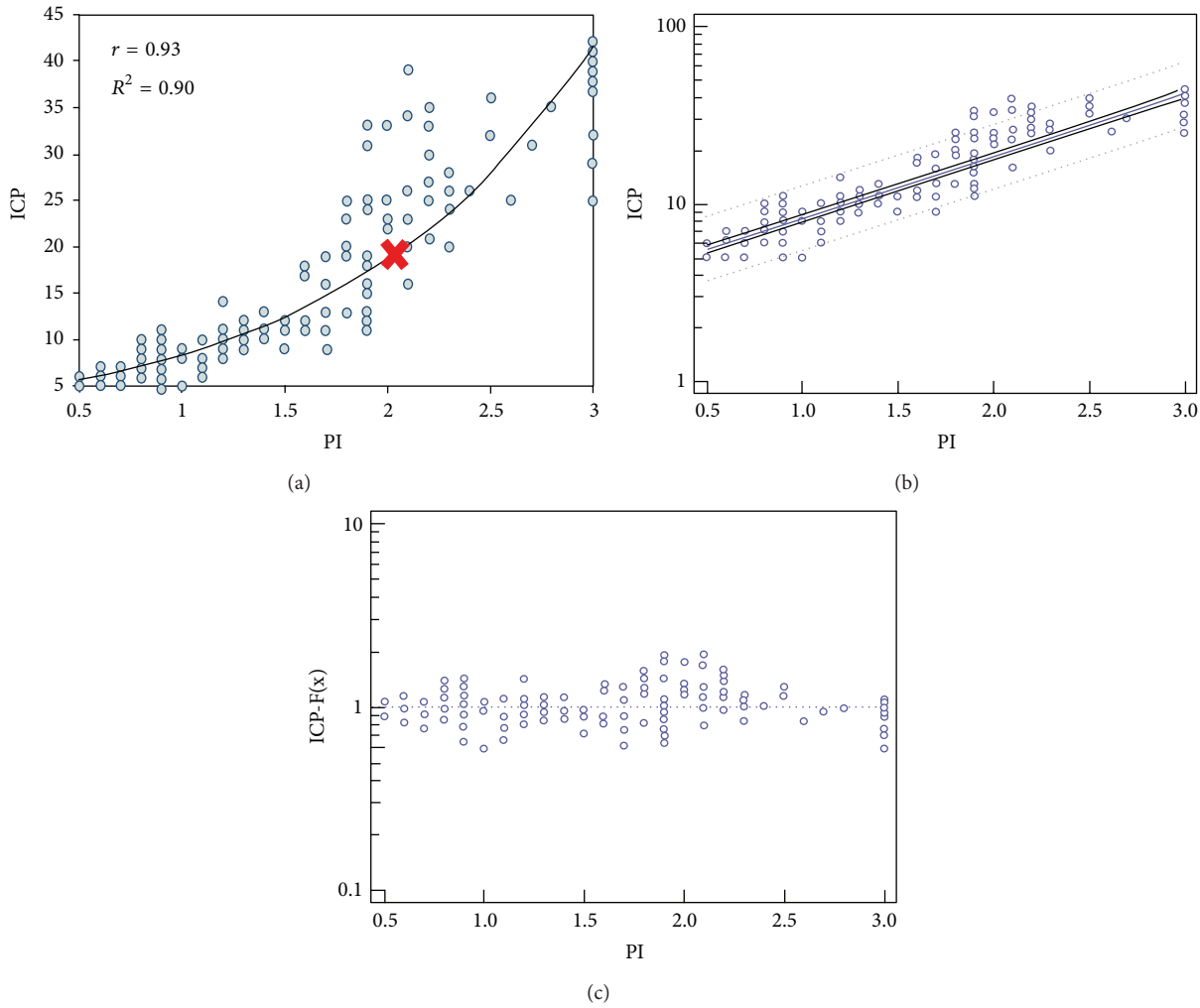

Figure 6: (a) Pulsatility index (PI) plotted versus the ICP (mm Hg); the scatter plot displays a positive exponential relation between the two parameters rather than an exact linear relation. (b) Regression analysis model: the "dots" represent the actual measured values, while the blue line in the middle represents the estimated values by the model and the dashed lines represent 95% confidence intervals. (c) Goodness of fit for the model-driven prediction equation calculating the proximity of the predicted values (dots) to the actual measured values (dashed blue line).

between each ultrasound parameter to the invasive ICP measurements was assessed for linearity using pertinent scatter plots, while the strength and direction of the relationship were evaluated by means of Pearson's correlation coefficient [20, 21]. To evaluate the relative impact of a predictor ultrasound variable (PI, ONSD, and V) on a particular outcome (ICP), we used linear regression analysis and therefore model-driven prediction equations were formulated accordingly [20, 21]. Due to the fact that the aforementioned relations of predictor ultrasound variables and ICP were exponential rather than straight linear, we used the exponential curve equation: $(\log(Y) = b0 + b1 * X)$, where "Y" is the estimated value (i.e., ICP), "$b0$" is the y intercept, "$b1$" is the slope of the line, and "X" is the measured value (PI, ONSD, and V). The resulted model-driven prediction equations were evaluated accordingly by goodness of fit [20, 21]. All tests were two-sided and a P value ≤ 0.05 was considered as statistically significant. Statistical analysis was performed using MedCalc 12 software.

3. Results

No procedure-related lesions were found on the dura or the brain of the rabbits after opening the skulls at the end of the experiment. The estimated intracranial vault volume was approximately 20 mL. Four rabbits exhibited a Cushing reaction at 0.6 to 0.8 mL of infused autologous blood, while the remaining 16 exhibited this reaction when a total blood infusion volume of 1 mL has been reached. The studied ultrasound neuromonitoring indices and other parameters at baseline versus at volume 1 mL of epidural hematoma are presented on Table 1. ICP, ONSD, and PI were all significantly increased at 1 mL volume of epidural hematoma compared to baseline values. PI values at the higher volume (1 mL)

of the experimental mass effect (brain tamponade, ICP > 40 mm Hg) far exceeded 7 and oscillating flow was the main finding which confirmed CCA, while pupils were fixed, dilated, and unresponsive to light ($V = 0$ cm/s).

The relationship of the ultrasound neuromonitoring indices with the invasive ICP measurements was studied by regression analysis models as previously mentioned. PI values were plotted versus the ICP and exhibited an exponential relation (Figure 6(a)). As the volume of the epidural hematoma and consequently ICP values gradually increased, a constant increase in PI values was evident until the point of brain tamponade when oscillating flow was observed (no PI values were registered as these far exceeded the ultrasound scale used in the analysis). Notably, the distribution of PI data appeared to be more scattered for ICP values over 20 mm Hg compared to values less than 20 mm Hg. An overall strong positive relationship between PI and ICP was observed ($r = 0.93$; 95% CI 0.91 to 0.95; $P < 0.001$; Figure 6(b)). The model-driven prediction equation of ICP for PI was log (ICP) = 0.63 + 0.30 × PI. The prediction equation was further confirmed by goodness of fit (coefficient of determination $r^2 = 0.84 \pm 0.076$; $P < 0.001$; Figure 6(c)). Accordingly, ONSD values were plotted versus the ICP and showed a gradual increase as the volume of the epidural hematoma increased. ONSD values also showed an exponential relation to the ICP values (slightly different compared to the PI plot), while an overall strong positive relationship was evident ($r = 0.75$; 95% CI 0.68 to 0.80; $P < 0.001$; Figures 7(a) and 7(b)). The distribution of ONSD data exhibited a rather different pattern compared to PI data as the former also increased gradually but with a "step-like" manner (Figures 6(a) and 7(a)). The model-driven prediction equation of ICP for ONSD was log (ICP) = 0.27 + 0.35 × ONSD. The latter was further evaluated by goodness of fit (coefficient of determination $r^2 = 0.62 \pm 0.119$; $P < 0.001$; Figure 7(c)). Finally, the pupil constriction velocity (V) showed an exponential relation to ICP as well, while the pattern of distribution of V data resembled the ONSD scatter plot (Figure 8(a)). Higher ICP values resulted in slower pupil contraction during the consensual PLR test, and thus V was gradually decreased. A strong negative relationship between V and ICP values was evident ($r = -0.87$; 95% CI −0.90 to −0.83; $P < 0.001$; Figure 8(b)). The model-driven prediction equation of ICP for V was log(ICP) = $1.27 + (-0.45) \times V$ that was further confirmed by goodness of fit (coefficient of determination $r^2 = 0.78 \pm 0.09$; $P < 0.001$; Figure 8(c)). In conclusion, statistically significant model-driven prediction equations of ICP derived from all three studied ultrasound neuromonitoring indices were registered. Using all three ultrasound indices to calculate one combined model-driven prediction equation of ICP was not possible due to the small size of the study group and the limited total number of ultrasound measurements.

4. Discussion

Invasive ICP evaluation is a gold standard neuromonitoring method in patients with severe TBI. ICP should be monitored in all patients with postresuscitation Glasgow Coma Scale <8 and an abnormal brain CT scan. ICP monitoring is also indicated in patients with severe TBI with a normal brain CT scan when two or more of the following features are present upon admission: age over 40 years, unilateral or bilateral motor posturing and systolic blood pressure <90 mmHg. For other patients the indications for invasive ICP monitoring remain debatable [1–5]. Interestingly, a recent multicenter study in patients with severe TBI has suggested that care focused on maintaining monitored ICP at 20 mm Hg or less has not shown as superior to care based on imaging and clinical examination [22]. Complications related to invasive ICP measurements such as hemorrhage and infection can be avoided by the application of noninvasive neuromonitoring methods. In the ICU, invasive ICP monitoring is contraindicated in patients receiving anticoagulants or having thrombocytopenia as well as in scalp or cerebral infection, while lack of neurosurgical expertise is another usual problem [1–3]. Thus, neuromonitoring strategies may indeed be changing in the near future as intensivists and neurosurgeons are gradually driven away from ICP based diagnostic and therapeutic practices to cerebral perfusion pressure (CPP) related clinical strategies. Apart from ultrasound techniques, several other noninvasive methods which estimate ICP based on physiological or anatomical brain features have been described including CT and magnetic resonance imaging, near-infrared spectroscopy, and visual-evoked potentials [1–3]. Ultrasound neuromonitoring techniques are becoming increasingly popular in the ICU setting due to the availability of multipurpose ultrasound systems and the rapid and by-the-bed nature of the sonographic evaluation. However, the application of ultrasound neuromonitoring techniques on patients with TBI is not yet established or standardized [1–5].

In this experimental study, we have reproduced an epidural hematoma model to study the relation of invasive ICP measurements with simultaneous recordings of ultrasound neuromonitoring indices. The gradually expanding hematoma created a mass effect which needed to reach at a volume of 1 mL to produce a Cushing reaction in the vast majority of the studied animals. In our previously published study, the Cushing reaction was achieved at lower hematoma volumes (0.5-0.6 mL) [17]. This discrepancy may be explained by the fact that in this study the experimental setting was modified as all animals were intubated and mechanically ventilated (deeper sedation); moreover the volume of the cranial vault measured in this study was larger compared to the one measured in the previous one (20 versus 13 mL). The current results indicated statistically significant model-driven prediction equations of ICP derived from the ultrasound neuromonitoring indices, namely, PI, ONSD, and V. However, the exponential relationship of all ultrasound data to the ICP measurements (Figures 6, 7, and 8) underpins that the current results should be interpreted with caution and in the context of the specific experimental scenario.

TCCD is a specialized examination which has advantages over the conventional transcranial Doppler examination by showing the images of the intracranial anatomy and arteries by duplex B-mode, while still having the capacity to measure velocities with Doppler. PI is derived from the TCCD waveform as mentioned in previous paragraphs. TCCD may

Table 1: Ultrasound and other parameters in the study group (n = 20 rabbits).

Variable	Baseline		Volume of epidural hematoma = 1 mL	
	Mean (95% CI)	SD	Mean (95% CI)	SD
Intracranial pressure (mm Hg)	5.85 (5.57 to 6.12)	±0.58	42.20 (41.34 to 43.05)*	±1.82
Systolic blood pressure (mm Hg)	83.40 (80.78 to 86.01)	±31.20	199.30 (195.28 to 203.31)*	±8.57
Diastolic blood pressure (mm Hg)	49.10 (48.70 to 49.49)	±0.85	103.40 (101.31 to 105.48)*	±4.45
Pulsatility index (PI)	0.70 (0.64 to 0.76)	±0.13	Oscillating flow (PI > 7)*	
Optic nerve sheath diameter (mm)	1.73 (1.63 to 1.83)	±0.22	2.78 (2.64 to 2.92)*	±0.30
Maximum pupillary diameter (mm)	2.29 (2.24 to 2.33)	±0.10	2.33 (2.26 to 2.40)	±0.15
Minimum pupillary diameter (mm)	1.59 (1.54 to 1.63)	±0.10	2.33 (2.26 to 2.40)	±0.15
Pupil constriction velocity (cm/s)	0.089 (0.084 to 0.098)	±0.10	0.0 (fixed pupil)*	±0

*The differences between values of the neuromonitoring indices at baseline versus at volume of epidural hematoma = 1 mL were all statistically significant (paired t-test; $P < 0.0001$).

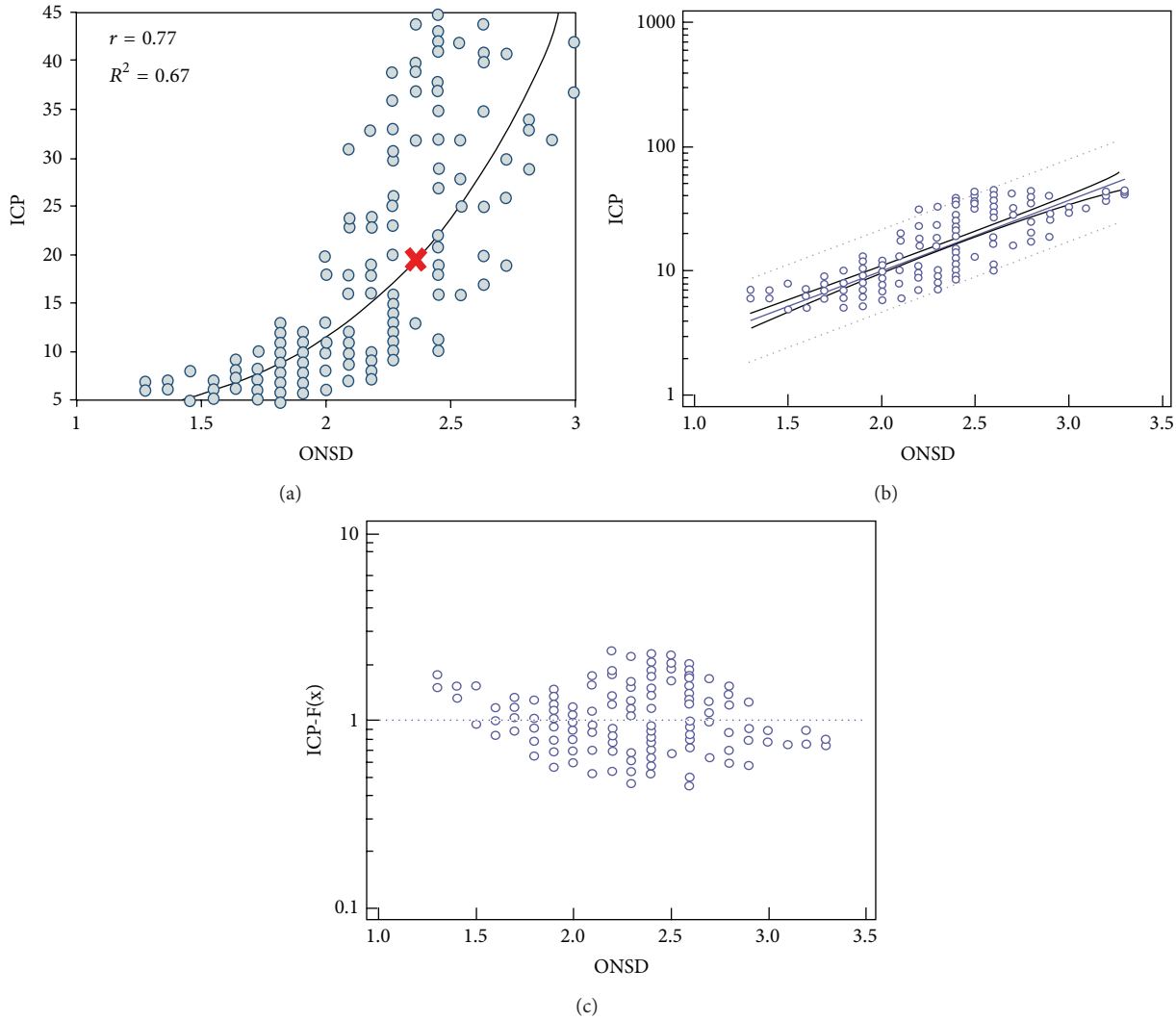

Figure 7: (a) Optic nerve sheath diameter (ONSD) in mm plotted versus the ICP (mm Hg); the scatter plot displays a positive exponential relation (slightly different compared to the PI plot) between the two parameters rather than an exact linear relation. (b) Regression analysis model: the "dots" represent the actual measured values, while the blue line in the middle represents the estimated values by the model and the dashed lines represent 95% confidence intervals. (c) Goodness of fit for the model-driven prediction equation calculating the proximity of the predicted values (dots) to the actual measured values (dashed blue line).

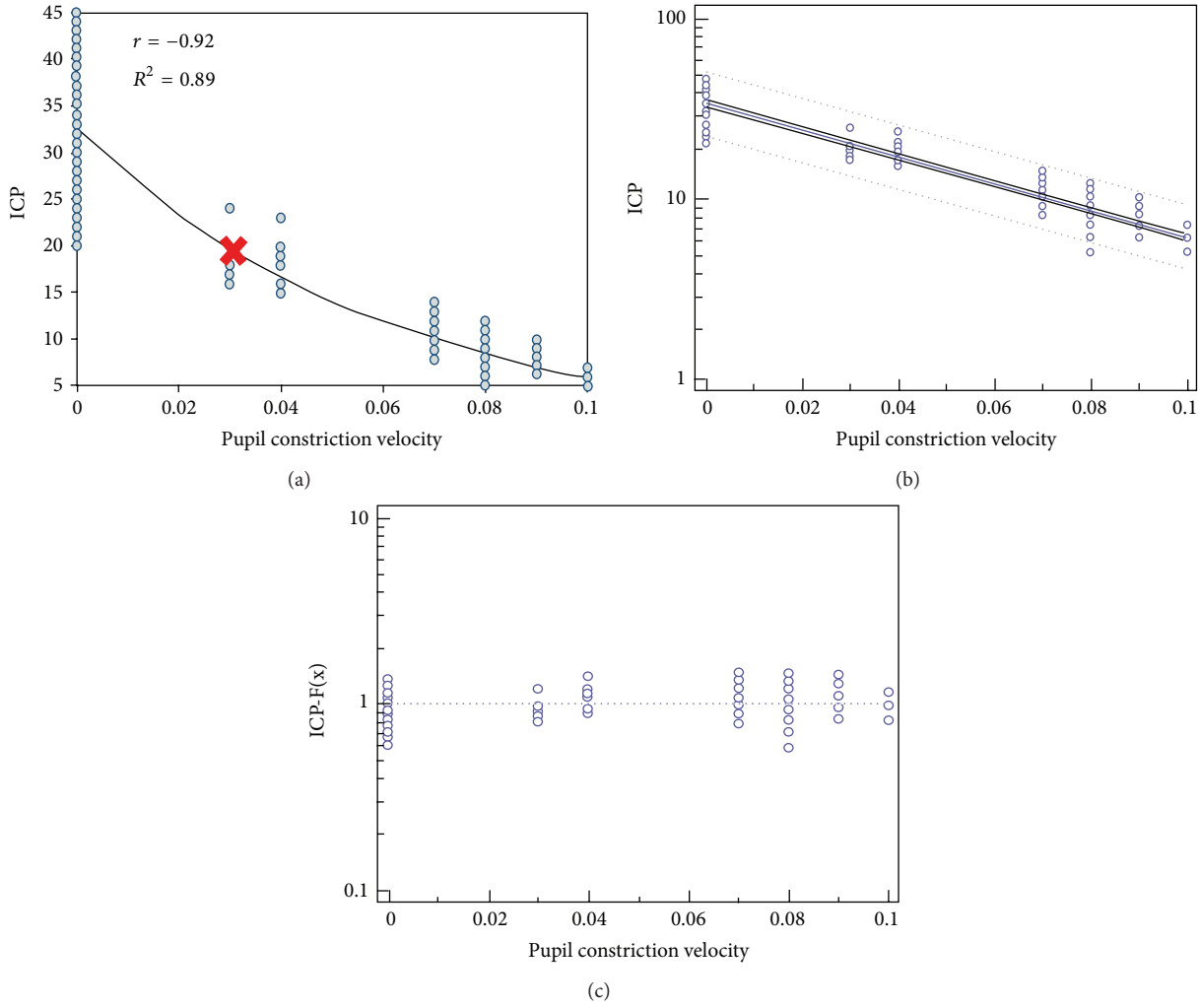

Figure 8: (a) Pupil constriction velocity (V) in cm/s plotted versus the ICP (mm Hg); the scatter plot displays a negative exponential relation (red ribbon corresponds to ICP = 20 mm Hg) between the two parameters rather than an exact linear relation. (b) Regression analysis model: the "dots" represent the actual measured values, while the blue line in the middle represents the estimated values by the model and the dashed lines represent 95% confidence intervals. (c) Goodness of fit for the model-driven prediction equation calculating the proximity of the predicted values (dots) to the actual measured values (dashed blue line).

detect alterations of cerebral blood flow caused by elevated ICP and hence identify patients who are at risk of developing cerebral ischemia and/or edema in the early phases of TBI [1–5]. However, absent sonographic windows may be present in 5 to 13% of cases [16]. Absolute pulsatility is difficult to assess by ultrasound as the amplitude of the pulsatile blood flow velocity is dependent on the angle of insonation. Also, it is well known that TCCD flow velocities do not correspond to cerebral blood flow per se [11–16]. Previous reports have linked the PI with distal cerebrovascular resistance suggesting an increasing PI as a reflection of an increasing resistance and vice versa [23, 24]. Other studies have reported that the aforementioned link was weak suggesting thus that the PI is not an absolute measure of cerebrovascular resistance [25, 26]. Previously published animal models in which cerebrovascular resistance was manipulated in a controlled manner under different physiologic conditions such as an increase in arterial PCO2 or by a decrease in CPP suggested that the PI cannot be interpreted merely as an index of cerebrovascular resistance but in the context of combined changes of cerebrovascular resistance and compliance of large cerebral arteries [11–14, 26]. Our results indicated a gradual and constant increase of PI with higher ICP which is in accordance with previous reports [11–14]. Notably, the distribution of PI data was more scattered in ICP values over 20 mm Hg. This might be explained by a loss of cerebral autoregulation above the aforementioned ICP values as other groups have previously reported [11–14, 26]. The high correlation of PI values to the invasive ICP measurements in this study might be attributed to the specific experimental pathophysiologic scenario: the reproduction of the epidural hematoma has created a mass effect which has gradually progressed to brain tamponade. Taking into account the small volume of the rabbit's brain and cranial vault, the expanding epidural hematoma resulted in

a direct mass effect on the circle of Willis. Thus, blood flow in the insonated MCA was affected in a straightforward manner. However, the pathophysiology of TBI may be extremely variable (i.e., hematoma, edema, ischemia, loss of autoregulation, etc.) in real time clinical scenarios [4, 5, 11–14, 26]. Despite the aforementioned inherent and technical TCCD limitations, PI remains a useful neuromonitoring variable when individual patient and physiologic features are taken into account in order to make context-relevant use of its measurements in various clinical scenarios [1–5].

Our results indicated that ONSD measurements were positively correlated with the increments of ICP. ONSD measurement is performed as a standalone ultrasound examination of eye and orbit in association with known, suspected, or anticipated ICP elevation. The protocol is reasonably simple to allow fast bedside evaluation in acute conditions with rapidly rising ICP (i.e., TBI) [4, 5, 8, 9]. ONSD increments in cases of intracranial hypertension are mainly attributed to the fact that the intraorbital cerebrospinal fluid (CSF) space (i.e., the space between the dural sheath of the optic nerve and the nerve proper) is contiguous with the intracranial CSF space. In this study, the sonographic differentiation between the nerve proper and the CSF space was difficult. In order to standardize measurements and ensure their reproducibility, the "dark stripe" method was applied on all cases. The results suggested a statistically significant model-driven prediction equation of ICP derived by the ONSD measurements. The distribution of ONSD data exhibited a rather different pattern compared to PI data as the former also increased gradually but with a "step-like" manner which is in accordance with previous clinical studies [4, 5].

In this study, we have presented for the first time to the best of our knowledge experimental data regarding the sonographic consensual PLR test. The latter is an established neuromonitoring tool when performed by means of standard pupillometry [18]. The present results showed that the pupil constriction velocity becomes lower (the pupil's reaction to light becomes more sluggish) with increased ICP values and this occurs just before the occurrence of brain tamponade, CCA, or Cushing reaction, which is on accordance with previous reports (Figure 8) [18]. This sonographic method is not yet established in clinical neuromonitoring. The sonographic PLR test has many limitations as it is affected by various factors such as the depth of anesthesia and mechanical ventilation; however, the method has no real alternatives when visual access to the pupil is impossible, and its results are self-explanatory. The method is difficult in unstable gaze. In cases of severe facial trauma, extreme care should be taken to avoid additional damage to the globe and other tissues. The method can be combined with ONSD measurements to evaluate a potentially catastrophic intracranial process [19]. Interestingly, the distribution of pupil constriction velocity data (Figures 7(a) and 8(a)) resembled the pattern of the distribution of ONSD data (a "step-like" manner of distribution). This observation may strengthen the rationale behind a combined ONSD/PLR sonographic method and its relevance in neurocritical monitoring; however, further larger studies are clearly required to study the aforementioned suggestions. Finally, the combination of all studied ultrasound indices in one model-driven prediction equation of ICP was not possible due to the small size of the study group and the limited total number of ultrasound measurements. This remains a future research target of our group. Despite the many inherent and technical limitations of the presented experimental model, our results showed a clear relation of the studied ultrasound neuromonitoring indices with invasive ICP values in this experimental model of epidural hematoma

5. Conclusion

In conclusion, Doppler derived PI, ONSD measurements, and sonographically determined pupil constriction velocity (derived from a consensual PLR test) were all significantly related to invasive ICP increments in an experimental model of epidural hematoma. Statistically significant prediction models of ICP derived from all three ultrasound methods were registered. This observation may further support the rationale of pursuing the concept of a holistic ultrasound protocol (combination of various ultrasound neuromonitoring indices on the same monitoring platform) in the ICU [27]. Undeniably, further research work is clearly necessary to explore the role of ultrasound in modern neurocritical practice.

Conflict of Interests

The authors declare that there is no conflict of interests regarding the publication of this paper.

Acknowledgments

This study was funded by Scholarship by the Experimental-Research Center ELPEN Pharmaceuticals (E.R.C.E), Athens, Greece. The research facilities for this project were provided by the aforementioned institution.

References

[1] P. H. Raboel, J. Bartek Jr., M. Andresen et al., "Intracranial pressure monitoring: invasive versus non-invasive methods-a review," *Critical Care Research and Practice*, vol. 2012, Article ID 950393, 14 pages, 2012.

[2] F. Güiza, B. Depreitere, I. Piper, G. Van den Berghe, and G. Meyfroidt, "Novel methods to predict increased intracranial pressure during intensive care and long-term neurologic outcome after traumatic brain injury: development and validation in a multicenter dataset," *Critical Care Medicine*, vol. 41, no. 2, pp. 554–564, 2013.

[3] J. B. Rosenberg, A. L. Shiloh, R. H. Savel, and L. A. Eisen, "Non-invasive methods of estimating intracranial pressure," *Neurocritical Care*, vol. 15, no. 3, pp. 599–608, 2011.

[4] D. Karakitsos, T. Soldatos, A. Gouliamos et al., "Transorbital sonographic monitoring of optic nerve diameter in patients with severe brain injury," *Transplantation Proceedings*, vol. 38, no. 10, pp. 3700–3706, 2006.

[5] T. Soldatos, D. Karakitsos, K. Chatzimichail, M. Papathanasiou, A. Gouliamos, and A. Karabinis, "Optic nerve sonography in

the diagnostic evaluation of adult brain injury," *Critical Care*, vol. 12, no. 3, article R67, 2008.

[6] P. M. Kochanek, N. Carney, P. D. Adelson et al., "Guidelines for the acute medical management of severe traumatic brain injury in infants, children, and adolescents-second edition," *Pediatric Critical Care Medicine*, vol. 13, supplement 1, pp. S1–S82, 2012.

[7] M. Czosnyka, B. F. Matta, P. Smielewski, P. J. Kirkpatrick, and J. D. Pickard, "Cerebral perfusion pressure in head-injured patients: a noninvasive assessment using transcranial Doppler ultrasonography," *Journal of Neurosurgery*, vol. 88, no. 5, pp. 802–808, 1998.

[8] M. Blaivas, D. Theodoro, and P. R. Sierzenski, "Elevated intracranial pressure detected by bedside emergency ultrasonography of the optic nerve sheath," *Academic Emergency Medicine*, vol. 10, no. 4, pp. 376–381, 2003.

[9] H. C. Hansen and K. Helmke, "The subarachnoid space surrounding the optic nerves: an ultrasound study of the optic nerve sheath," *Surgical and Radiologic Anatomy*, vol. 18, no. 4, pp. 323–328, 1996.

[10] A. E. Sargsyan, D. R. Hamilton, S. L. Melton et al., "Ultrasonic evaluation of pupillary light reflex," *Critical Ultrasound Journal*, vol. 1, pp. 53–57, 2009.

[11] R. J. Nelson, M. Czosnyka, J. D. Pickard et al., "Experimental aspects of cerebrospinal hemodynamics: the relationship between blood flow velocity waveform and cerebral autoregulation," *Neurosurgery*, vol. 31, no. 4, pp. 705–710, 1992.

[12] P. Barzo, T. Doczi, K. Csete, Z. Buza, and M. Bodosi, "Measurements of regional cerebral blood flow and blood flow velocity in experimental intracranial hypertension: infusion via the cisterna magna in rabbits," *Neurosurgery*, vol. 28, no. 6, pp. 821–825, 1991.

[13] J. M. De Bray, J. L. Saumet, M. Berson, G. Lefteheriotis, and L. Pourcelot, "Acute intracranial hypertension and basilar artery blood flow velocity recorded by transcranial Doppler sonography: an experimental study in rabbits," *Clinical Physiology*, vol. 12, no. 1, pp. 19–27, 1992.

[14] K. Ungersbock, D. Tenckhoff, A. Heimann et al., "Transcranial Doppler and cortical microcirculation at increased intracranial pressure and during the Cushing response: an experimental study on rabbits," *Neurosurgery*, vol. 36, no. 1, pp. 147–157, 1995.

[15] J. Poularas, D. Karakitsos, G. Kouraklis et al., "Comparison between transcranial color doppler ultrasonography and angiography in the confirmation of brain death," *Transplantation Proceedings*, vol. 38, no. 5, pp. 1213–1217, 2006.

[16] D. Karakitsos, J. Poularas, A. Karabinis, V. Dimitriou, A. Cardozo, and N. Labropoulos, "Considerations for the utilization of transcranial Doppler sonography in the study of progression towards cerebral circulatory arrest," *Intensive Care Medicine*, vol. 37, no. 2, pp. 368–370, 2011.

[17] E. E. Douzinas, V. Kostopoulos, E. Kypriades et al., "Brain eigenfrequency shifting as a sensitive index of cerebral compliance in an experimental model of epidural hematoma in the rabbit: Preliminary Study," *Critical Care Medicine*, vol. 27, no. 5, pp. 978–984, 1999.

[18] W. R. Taylor, J. W. Chen, H. Meltzer et al., "Quantitative pupillometry, a new technology: normative data and preliminary observations in patients with acute head injury—Technical note," *Journal of Neurosurgery*, vol. 98, no. 1, pp. 205–213, 2003.

[19] A. E. Sargsyan, D. R. Hamilton, S. L. Melton et al., "Ultrasonic evaluation of pupillary light reflex," *Critical Ultrasound Journal*, vol. 1, pp. 53–57, 2009.

[20] M. Scott, D. Flaherty, and J. Currall, "Statistics: are we related?" *Journal of Small Animal Practice*, vol. 54, no. 3, pp. 124–128, 2013.

[21] M. Scott, D. Flaherty, and J. Currall, "Statistics: using regression models," *Journal of Small Animal Practice*, vol. 54, no. 6, pp. 285–290, 2013.

[22] R. M. Chesnut, N. Temkin, N. Carney et al., "A trial of intracranial-pressure monitoring in traumatic brain injury," *The New England Journal of Medicine*, vol. 367, no. 26, pp. 2471–2481, 2012.

[23] K.-F. Lindegaard, P. Grolimund, R. Aaslid, and H. Nornes, "Evaluation of cerebral AVM's using transcranial Doppler ultrasound," *Journal of Neurosurgery*, vol. 65, no. 3, pp. 335–344, 1986.

[24] C. A. Giller, K. Hodges, and H. H. Batjer, "Transcranial Doppler pulsatility in vasodilation and stenosis," *Journal of Neurosurgery*, vol. 72, no. 6, pp. 901–906, 1990.

[25] K. F. Lindegaard, "Indices of pulsatility," in *Transcranial Doppler*, D. W. Newell and R. Aaslid, Eds., pp. 67–82, Raven Press, New York, NY, USA, 1992.

[26] M. Czosnyka, H. K. Richards, H. E. Whitehouse, and J. D. Pickard, "Relationship between transcranial Doppler-determined pulsatility index and cerebrovascular resistance: An Experimental Study," *Journal of Neurosurgery*, vol. 84, no. 1, pp. 79–84, 1996.

[27] P. D. Lumb and D. Karakitsos, "Ocular ultrasound in the intensive care unit," in *Critical Care Ultrasound*, Elsevier, Melville, NY, USA, 1st edition, 2014.

Hindawi Publishing Corporation
The Scientific World Journal
Volume 2014, Article ID 852356, 8 pages
http://dx.doi.org/10.1155/2014/852356

Review Article

PEEP Role in ICU and Operating Room: From Pathophysiology to Clinical Practice

M. Vargas,[1] Y. Sutherasan,[2] C. Gregoretti,[3] and P. Pelosi[4]

[1] *Department of Neurosciences and Reproductive and Odontostomatological Sciences, University of Naples "Federico II," 80100 Naples, Italy*
[2] *Ramathibodi Hospital, Mahidol University, Bangkok 10400, Thailand*
[3] *Department of Critical Care Medicine, "Città della Salute e della Scienza" Hospital, 10121 Turin, Italy*
[4] *Department of Surgical Sciences and Integrated Diagnostics, University of Genoa, 16132 Genoa, Italy*

Correspondence should be addressed to P. Pelosi; ppelosi@hotmail.com

Received 5 October 2013; Accepted 24 December 2013; Published 14 January 2014

Academic Editors: M. Elbarbary, L. M. Gillman, A. E. Papalois, and A. Shiloh

Positive end expiratory pressure (PEEP) may prevent cyclic opening and collapsing alveoli in acute respiratory distress syndrome (ARDS) patients, but it may play a role also in general anesthesia. This review is organized in two sections. The first one reports the pathophysiological effect of PEEP on thoracic pressure and hemodynamic and cerebral perfusion pressure. The second section summarizes the knowledge and evidence of the use of PEEP in general anesthesia and intensive care. More specifically, for intensive care this review refers to ARDS and traumatic brain injured patients.

1. Introduction

Positive end expiratory pressure (PEEP) is applied during the end of expiration to maintain the alveolar pressure above atmospheric pressure. PEEP is different from continuous positive airway pressure (CPAP), because this one refers to a positive pressure maintained during inspiration and expiration phase of spontaneous ventilation. The benefit of PEEP has been demonstrated in terms of preventing cyclic opening and collapsing alveoli in acute respiratory distress syndrome patients (ARDS). Moreover, protective ventilation, even in noninjury lungs, should be considered such as during perioperative period aiming to prevent collapsing of alveoli. However, applying PEEP may affect cardiac function and vital organ perfusion by complex mechanisms (Figure 1). To minimize the adverse effects of PEEP in intensive care unit (ICU) and in operating room, better knowledge and understanding of the interaction between heart, lung, and brain during applying PEEP are required.

The aims of this review are

(1) to clarify the pathophysiology of PEEP on thoracic pressure and hemodynamic and cerebral perfusion;

(2) to clarify the role of PEEP during general anesthesia;

(3) to clarify the role of PEEP in intensive care for ARDS, with a special focus on traumatic brain injured patients.

2. Methods

In the first section of this paper, we considered general issues related to pathophysiology of PEEP. In the second and third parts we focused on randomized clinical trials evaluating the role of PEEP during general anesthesia for different types of surgery and for ARDS patients. The specific search for traumatic brain injured patients was conducted with the best available evidence according the aim of this paper. The research was conducted mainly in PUBMED from 1996 to 2013.

3. Pathophysiology of PEEP

3.1. PEEP and Thoracic Pressure. The intrathoracic pressure (ITP) should be categorized in airway pressure (Paw), pleural

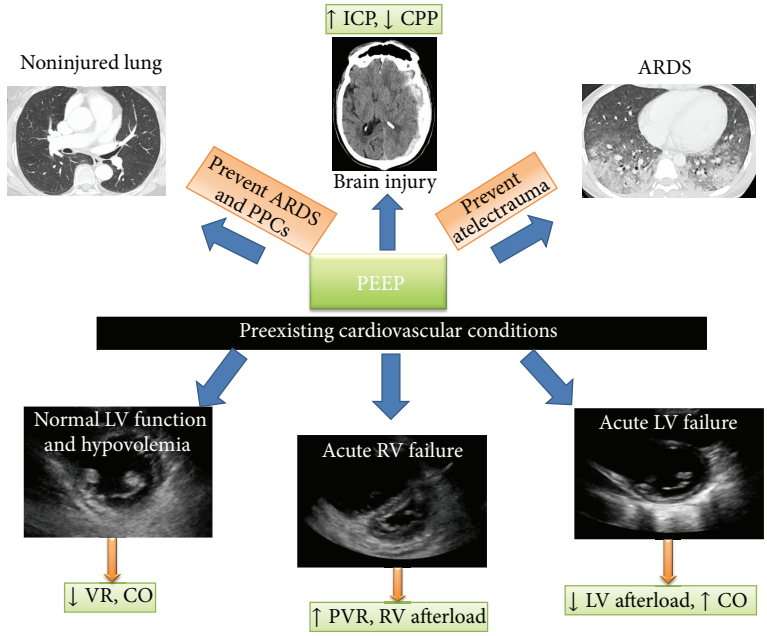

Figure 1: Impact of PEEP on lung and hemodynamic and cerebral perfusion pressure. PEEP: positive end expiratory pressure, ICP: intracranial pressure, CPP: cerebral perfusion pressure, ARDS: acute respiratory distress syndrome, LV: left ventricular, RV: right ventricular, VR: venous return, CO: cardiac output, PVR: pulmonary vascular resistance and PPCs: Postoperative Pulmonary Complications.

pressure (Ppl), and pericardial pressure (Ppc). The main factor affecting the change of Ppl and Ppc was the lung volume [1]. The variation of the lung volume, and not of lung compliance, was the primary determinant of ITP changes [2].

The change in the lung volume was determined by airway resistance and lung and chest wall compliance. The change of Ppl was not identical in each pleural region during positive pressure ventilation (PPV). The Ppl at the diaphragm minimally increased during PPV, whereas the maximum increase of the Ppl was observed at juxtacardiac region [3]. When total lung compliance was normal, 50% of applying Paw was transmitted to intrapleural space; therefore decrease in lung compliance led to a further reduction in the transmission of Paw to intrapleural space [4]. Predicting Paw transmission to Ppc was difficult; during the increase in PEEP the percentage of Paw transmitted to Ppc was not constant [5]. Esophageal pressure may be used as a method estimating pleural pressure and pericardial pressure; however when PEEP increased, this method may underestimate the actual value [6].

3.2. PEEP and Hemodynamics. The main determinants of cardiac output were (1) preload or venous return, (2) right ventricular (RV) output, (3) left ventricular (LV) filling and ventricular interdependence, and (4) LV contractility and afterload (Figure 1).

3.3. Venous Return. Venous system was filled with a certain volume (unstressed volume) that represents approximately 25% of total blood volume. The amount of volume returning to the heart was determined by the relationship between the upstream and downstream pressure gradient. The changing of upstream pressure, so-called mean systemic filling pressure (MSP), influenced the shift between unstressed volume and stressed volume (the volume that caused pressure in filling chamber) that allowed volume of blood returning to the heart. However, the downstream pressure or right atrial pressure (RAP) also affected that volume. The increase in RAP causing lower pressure gradient resulted in decreasing venous return (VR) [2].

In general, elevation of RAP by increasing ITP resulted in decrease of venous return. But impact of ITP rising, especially by PEEP, on VR was not straight forward and did not always lead to a decrease of cardiac output (CO). A study by Jellinek et al. reported that positive airway pressure increases RAP but also MSP; therefore no change in pressure gradient (MSP-RAP) was observed [7].

This debated topic came from the difference of fluid status of the enrolled patients and the increase in intraabdominal pressure associated with compression of the liver and squeezing of the lungs [8]. In ARDS patients with preexisting hypovolemia (RAP $\leq$ 10 mm Hg), applying mechanical ventilation with Paw 30 cm H_2O could decrease greater cardiac index in comparison to those with RAP >10 mm Hg [9]. As well as in sepsis patients, Vieillard-Baron et al. demonstrated that superior vena cava collapsibility index changed along breathing cycle was an accurate index for fluid responsiveness [10]. In this group of patients, volume expansion may improve VR and left ventricular end diastolic volume (LVEDV).

3.4. Right Ventricular Output. PEEP not only decreased RV preload by impeding systemic venous return, but also increased RV afterload. The impact of PEEP on RV afterload was affected through the change of pulmonary vascular resistance (PVR) by several mechanisms. At the first place,

we should take into account the intraparenchymal vessels physiology and how PEEP affected lung volume relative to normal functional residual capacity (FRC). When lung volume increased, intraalveolar vessels were compressed while extraalveolar vessels were exposed by radial interstitial force of the lungs. At lung volume above FRC, the effect of compression on intraalveolar vessels predominated; then the PVR increased. Furthermore intraalveolar pressure may impede right ventricular ejection leading to decrease of right ventricular cardiac output. At lung volume near FRC, the PVR was minimal. At lung volume below FRC, the effects of extraalveolar vessels predominated therefore on the PVR increase. Furthermore, at low end expiratory lung volume that alveoli collapse and atelectasis may be occurred, hypoxia led to pulmonary vasoconstriction causing the rise of PVR. Applying PEEP that recruits collapsed alveoli led to reduce hypoxic pulmonary vasoconstriction and decrease PVR [2, 11].

In summary, PEEP modified PVR in 2 ways. The first one was that PEEP recruiting collapsed alveoli decreases PVR. The second one was that PEEP leading to hyperinflation tends to increase PVR and may lead to acute cor pulmonale.

3.5. LV Filling and Ventricular Interdependence. Changing the volume of blood in the right ventricle may affect the left ventricular filling when pulmonary transit time was reached. As a result of this, the reduction of RV ejection from PEEP may not impact on LV preload at the same time; it may be delayed for 4-5 heartbeats.

During spontaneous breathing, inspirations allowed more amount of VR into the RV that caused the interventricular septum shifting to the left and probably affected the LV ejection. But PPV or PEEP may reduce VR and reverse this negative effect to the LV. However, when PEEP created high level of PVR, this caused a rise of RV pressure and promoted leftward shift of interventricular septum leading to lower LV ejection. In addition, PEEP shifted the left ventricular pressure-volume curve to the left indicating a decrease of left ventricular distensibility and showed the transmission of positive pressure from lungs to heart [2, 11].

Effect of PEEP on LV diastolic function still had conflicting results. Patients with diastolic dysfunction had an increase of LV filling pressure and LV wall tension. PEEP may worsen myocardial perfusion. Recent study by Chin et al. demonstrated that incremental PEEP from 0 cm H_2O to 5 and 10 cm H_2O worsened diastolic dysfunction in patients with preexisting diastolic dysfunction that might take the risk to myocardial infarction [12].

3.6. LV Contractility and Afterload. The effect of PEEP on LV contractility was still controversial due to the difficulty of measuring LV filling pressure and LV volume. Although several authors investigated the relationship between PEEP, CO, and LV end diastolic volume, they failed to demonstrate the decrease in LV function with PEEP [2, 13, 14].

Ventricular afterload was the tension developed in the wall after ventricular systole or the pressure against LV ejection. Ventricular afterload increased with ventricular volume or aortic pressure. Increase of ITP decreased the force necessary to eject the blood from the ventricle. Left ventricular transmural pressure decreased when PEEP was applied. When the heart was small, change of ITP to the pericardial surface was small. On the other hand, when the heart becomes dilated maybe under volume loading condition, pericardial elastic pressure became the major influence of cardiac surface pressure and may result in overestimation of transmural pressure [2, 15]. In poor myocardial function patients, applying PEEP can rise the cardiac output which proved by several clinical studies [16]. However PEEP may limit coronary blood flow because of the increase of epicardial surface pressure [17]. In hypovolemic state, PPV impeded venous return and then led to the decrease of SV. In hypervolemia heart failure state, increase in ITP may decrease LV afterload and increase ejection fraction.

3.7. PEEP and Cerebral Perfusion Pressure. About 20–25% of patients with brain injury developed ARDS, which was associated with high mortality. The proposed mechanisms were massive sympathetic discharge that produced systemic hypertension and edema formation from an increase of hydrostatic pressure. Guideline for MV in ARDS recommended low tidal volume and moderate to high levels of PEEP. Nevertheless, use of PEEP in brain injury led to an increase in ITP, impeded venous return, and reduced cerebral venous drainage from superior vena cava. Finally these effects induced high intracranial pressure (ICP) and reduced cerebral perfusion pressure (CPP) [18]. However, in clinical studies, these effects occurred only when applying PEEP more than 15 cm H_2O in hypovolemic patients. Another study by Caricato et al. reported that the level of PEEP had no effect on intracranial system in patients with low respiratory system compliance [19]. Mascia et al. demonstrated that the effect of PEEP on ICP depended on whether PEEP causes alveolar hyperinflation or alveolar recruitment [20]. When PEEP caused overinflation, the rise of $PaCO_2$ and lung elastance led to an increase in ICP, doppler flow velocity, and cerebral venous hemoglobin oxygen saturation (SjO_2). The increase of $PaCO_2$ caused vasodilation of cerebral arteries and increase in cerebral blood volume. On the contrary, lung recruitment by PEEP had no effect on ICP and CPP (Figure 1).

4. PEEP in Clinical Practice

4.1. PEEP during General Anesthesia: Lines of Evidence from RCT. The role of PEEP in mechanical ventilation was investigated for different types of surgery. Table 1 showed the RCT included in this review. Neumann et al. and Tusman et al. suggested that different levels of PEEP and different tidal volumes were associated with a reduction of postoperative atelectasis but with no difference in oxygenation [21, 22]. According to Reis Miranda et al., high PEEP level with low VT was associated with a reduction of pulmonary inflammation after cardiopulmonary bypass [23]. Wetterrslev et al. investigated the efficacy of PEEP to prevent atelectasis

Table 1: Main characteristics of RCTs for surgical patients included in this study.

Author	Year	Surgery	Low PEEP level	High PEEP level
Tusman et al. [21]	1999	Neurosurgical	0 cm H_2O	10 cm H_2O
Neumann et al. [22]	1999	Abdominal	0 cm H_2O	10 cm H_2O
Wetterslev et al. [24]	2001	Abdominal	0 cm H_2O	Best PEEP
Meininger et al. [25]	2005	Laparoscopic	0 cm H_2O	5 cm H_2O
Whalen et al. [27]	2006	Laparoscopic	4 cm H_2O	12 cm H_2O
Talab et al. [29]	2009	Laparoscopic bariatric	0 cm H_2O	5–10 cm H_2O
Reinius et al. [30]	2009	Bariatric	0 cm H_2O	10 cm H_2O
Kim et al. [26]	2010	Laparoscopic	0 cm H_2O	5 cm H_2O
Futier et al. [31]	2013	Abdominal	0 cm H_2O	6–8 cm H_2O
Severgnini et al. [32]	2013	Abdominal	0 cm H_2O	10 cm H_2O

and to improve oxygenation in patients undergoing abdominal surgery [24]. In this study, perioperative oxygenation significantly improved in PEEP group while postoperative complications were lower, but not statistically significant, in PEEP group [24]. The concept that using PEEP was useful during surgery was also evaluated in laparoscopic surgery. In this surgery, the prolonged insufflation of intraperitoneal gas may enhance the cephalic diaphragm shift and worsen the airway closing capacity, thus, resulting in an increase of lung injury and atelectasis. Meininger et al. evaluated the role of PEEP on arterial oxygenation and hemodynamics in laparoscopic surgery for nonobese patients [25]. PEEP group had a better oxygenation during intraperitoneal gas insufflation than ZEEP group but no hemodynamic significant difference was found between the considered groups [25]. Kim et al. evaluated the efficacy of PEEP to improve oxygenation and dynamic compliance during laparoscopic surgery for nonobese patients [26]. The oxygenation was significantly higher in the PEEP group than ZEEP group during the pneumoperitoneum, but in both groups respiratory system compliance decreased after 40 minutes [26]. Interestingly in obese patients undergoing laparoscopic surgery, PEEP had different effects. Whalen et al. investigated the effect of high PEEP versus low PEEP level on arterial oxygenation in laparoscopic surgery for morbidly obese patients [27]. High PEEP group showed a better arterial oxygenation than low PEEP group during the mechanical ventilation, but it disappeared after the extubation [27]. Thus in bariatric patients undergoing laparoscopic surgery, PEEP had a temporary effect on oxygenation during mechanical ventilation, while it is likely that an alveolar derecruitment could occur at the extubation. The use of PEEP in the intraoperative mechanical ventilation was associated with a reduction of atelectasis in postoperative period as reported by 3 studies using high PEEP level (10 cm H_2O) [28–30]. These studies involved healthy patients undergoing neurosurgical or eye surgery, as well as obese patients for laparoscopic and nonlaparoscopic surgery. Interestingly, the incidence of atelectasis was lower also in bariatric patients demonstrating possible beneficial effects in this category of patients. Recently, two prospective randomized clinical studies investigated the effect of protective ventilation, as low tidal volume and high PEEP, in major abdominal surgery [31, 32]. In both studies, using protective mechanical ventilation improved respiratory function and reduced pulmonary infections. A Cochrane systematic review and meta-analysis assessed the efficacy of PEEP during anaesthesia on postoperative mortality and pulmonary complications [33]. This review finally included 8 randomized clinical trials involving 330 patients treated with intraoperative PEEP or ZEEP. The results showed insufficient evidence to assess the role of intraoperative PEEP on mortality while two secondary outcomes were statistically significant. PEEP group had a higher intraoperative PaO_2/FiO_2 ratio and a lower incidence of postoperative atelectasis [33]. The usefulness of PEEP to improve intraoperative and postoperative outcome is still matter of debate and further studies needed to evaluate the efficacy of PEEP during anaesthesia in healthy and nonhealthy patients. Actually, a worldwide multicenter randomized controlled trial, known as PROVHILO study, had planned to recruit 900 patients randomized in two PEEP arms (12 cm H_2O versus 2 cm H_2O) undergoing open abdominal surgery. This study may add new information about the rational of using protective ventilation with high PEEP during general anaesthesia to prevent pulmonary and extrapulmonary postoperative complications [34].

5. PEEP in Intensive Care

5.1. PEEP in ARDS Patients: Lines of Evidence from RCT. The use of PEEP during mechanical ventilation may improve oxygenation in ARDS patients. This effect was due to the PEEP prevention of the collapse of alveoli and small airway lacking of surfactant [35]. Furthermore, keeping the alveoli open throughout the respiratory cycle, PEEP may prevent the damage produced by the repetitive opening and closing of the small airway and alveoli. PEEP levels used in clinical practice for ARDS patients highly differ. In 90's years, thanks to a new approach for lung injury, it was suggested that the adequate PEEP level for ARDS patients could be chosen by the analysis of pressure-volume curve [36]. During ARDS the pressure-volume curve assumed a sigmoidal shape with two inflection points. According to the sigmoidal curve, the PEEP level at which recruitment of collapsed alveoli began could be set between the lower and the upper inflection point (Figure 2) [37].

Table 2 showed the RCTs included in this review. Amato et al. and Ranieri et al. compared high with low PEEP levels [38, 39]. In these studies, the plateau pressure and mortality

Table 2: Main characteristics of RCTs for ARDS patients included in this study.

Author	Year	Patients	Low PEEP level	High PEEP level
Amato et al. [38]	1998	ARDS	≥5 cm H_2O	16 cm H_2O or Pflex + 2
Ranieri et al. [39]	1999	ARDS	3–15 cm H_2O	15 cm H_2O or Pflex + 3
The NHLBI Institute ARDS Clinical Trial Network [40]	2004	ALI/ARDS	5 cm H_2O	5–24 cm H_2O according FiO_2
Villar et al. [50]	2006	ARDS	≥5 cm H_2O	15 cm H_2O or Pflex + 3
Mercat et al. [41]	2008	ALI/ARDS	5–9 cm H_2O	PEEP according to Plateau 28–30 cm H_2O
Meade et al. [42]	2008	ALI/ARDS	5 cm H_2O	5–24 according FiO_2
Talmor et al. [43]	2008	ALI/ARDS	10 cm H_2O	17 cm H_2O

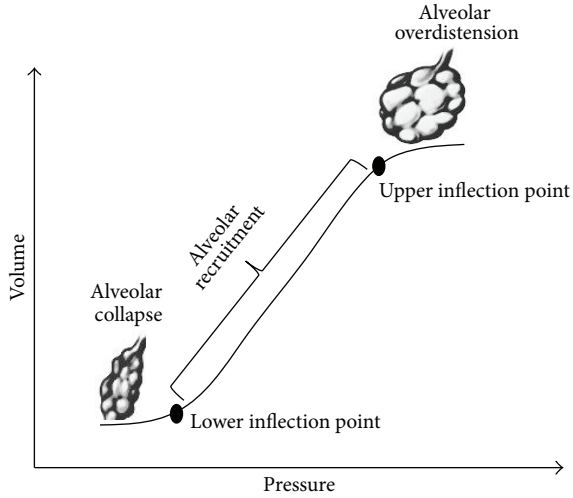

Figure 2: Pressure-volume curve with lower and upper inflection points. According to PEEP level, the recruitment of collapsed alveoli could be set between the lower and the upper inflection points.

were lower in high PEEP group [38, 39]. In 2004 the ARDS network performed a clinical trial with the aim to investigate the role of high PEEP levels on clinical outcome in ARDS patients receiving mechanical ventilation [40]. PEEP levels were set at 8 and 14 cm H_2O during the days. As results, there were no significant differences in mortality, in ventilator free-days, or organ failure between low and high PEEP groups [40]. ARDS network failed to show the best degree of PEEP to be applied during mechanical ventilation for mild to severe ARDS. General consensus exists about the use of PEEP in ARDS to keep open alveoli and small airway. After the ARDS network, Ranieri et al. compared the effect of high PEEP with low PEEP as protective and standard ventilation [39]. In this study the authors found a reduction in plateau pressure and mortality in patients ventilated with high PEEP in a contest of protective ventilation [38]. The role of PEEP in ARDS was also evaluated in association with a fixed tidal volume [41, 42]. In LOVS trial, there was no significant difference in mortality but the incidence of refractory hypoxemia was significantly lower in high PEEP group [40]. In EXPRESS trial, the authors found no difference in mortality, but there was a significant increase in ventilator and organ failure free-days [42]. In a RCT by Talmor et al., PEEP was set at 13 cm H_2O for three days and then changed to 17 or 10 cm H_2O [43]. As results, from the third day oxygenation, respiratory compliance and plateau pressure significantly improved in the high PEEP group [43]. The role of higher PEEP in severe ARDS seems to be established by several RCTs to improve survival or respiratory function even if it was associated with fixed or differ from tidal volume.

In 2010, a meta-analysis evaluating the effect of higher versus lower PEEP in ARDS patients suggested that treatments with different PEEP levels were not associated with an improvement in hospital survival, even if high PEEP level was associated with an improvement of survival in the subgroup of ARDS patients [44]. Recently, the ARDS definition task force proposed a new definition for ARDS, the Berlin definition, categorizing this pathology in three mutual exclusive degrees as mild, moderate, and severe [45]. According to this task force, high PEEP level should be reserved in severe ARDS patients [45].

5.2. PEEP in Traumatic Brain Injured Patients. The use of PEEP in traumatic brain injured (TBI) patient is still controversial. In mechanical ventilation for respiratory disease, mild PEEP levels and recruitment maneuver avoided progressive alveolar collapse and possible lung consolidation, improved arterial oxygenation, and reduced elastance of the respiratory system [46]. As discussed above, the application of PEEP in TBI patients could affect the cerebral circulation by a raised of mean intrathoracic pressure resulting in a reduction of cerebral venous return and then in an increase of ICP [47]. Videtta et al. investigated the variation of ICP and CPP at different levels of PEEP in mechanically ventilated brain injured patients raising PEEP from 5 to 15 cm H_2O with an increase of ICP about 3 mm Hg but no changes in CPP [48]. Young et al. investigated the ICP response to a gradual increment of PEEP in 3 randomized groups of patients with severe brain injured patients with pulmonary dysfunction [45]. Interestingly, the authors reported a decrease in ICP of 6 mm Hg in the group of patients with PEEP from 0 to 5 cm H_2O, of 8 mm Hg in the group with PEEP from 6 to 10 cm H_2O, and of 12 mm Hg in the group of PEEP from 11 to 15 cm H_2O. This study seemed to suggest a useful and safe application of PEEP for mechanical ventilation in brain injury [49]. The effects of PEEP were also investigated by Caricato et al. in comatose patients with severe TBI and normal or low lung compliance [19]. The rise of PEEP reduced CPP and

mean arterial pressure only in the normal compliance group but had no effects on systemic and cerebral hemodynamics in patients with low lung compliance [19]. PEEP level seemed to affect cerebral hemodynamics if it resulted in alveolar hyperinflation; in this case the predominant event was an increase in pulmonary elastance and dead space leading to a rise in $PaCO_2$ and ICP. Mascia et al. evaluated the effects of PEEP on respiratory mechanics, gas exchange, and cerebral perfusion in patients with traumatic brain injury [20]. To test this hypothesis the author included only patients with baseline ICP higher than the applied PEEP levels set to 5 and 10 cm H_2O. In nonrecruiter patients PEEP induced alveolar hyperinflation and rise in $PaCO_2$ and ICP, while in recruiter patients it had no effects on ICP and cerebral perfusion [20]. These data show that, in patients with ICP values higher than applied PEEP, effects of PEEP on cerebral hemodynamics depend on recruitment/hyperinflation of alveolar units and $PaCO_2$ variations may have major impact on brain perfusion [20]. PEEP levels in lung dysfunction after a TBI, compatible with a plateau pressure of 28–30 cm H_2O, may be applied with the aim to improve lung compliance and increase alveolar oxygenation and O_2 saturation. PEEP level in this kind of patients should be safely used with a close control of cardiovascular hemodynamics, respiratory function, gas exchange, and intracranial pressure.

6. Conclusions

PEEP may affect the lung, heart, and brain with several mechanisms. The role of PEEP in clinical practice is still debated but, in selected categories of patients with a careful monitoring, it may play an important role in improving outcome.

Conflict of Interests

The authors declare that there is no conflict of interests regarding the publication of this paper.

References

[1] R. J. O'Quin, J. J. Marini, B. H. Culver, and J. Butler, "Transmission of airway pressure to pleural space during lung edema and chest wall restriction," *Journal of Applied Physiology*, vol. 59, no. 4, pp. 1171–1177, 1985.

[2] T. Luecke and P. Pelosi, "Clinical review: positive end-expiratory pressure and cardiac output," *Critical Care*, vol. 9, no. 6, pp. 607–621, 2005.

[3] R. Novak, G. M. Matuschak, and M. R. Pinsky, "Effect of positive-pressure ventilatory frequency on regional pleural pressure," *Journal of Applied Physiology*, vol. 65, no. 3, pp. 1314–1323, 1988.

[4] J. C. Chapin, J. B. Downs, and M. E. Douglas, "Lung expansion, airway pressure transmission, and positive end-expiratory pressure," *Archives of Surgery*, vol. 114, no. 10, pp. 1193–1197, 1979.

[5] M. Pinsky, J.-L. Vincent, and J.-M. de Smet, "Estimating left ventricular filling pressure during positive end-expiratory pressure in humans," *American Review of Respiratory Disease*, vol. 143, no. 1, pp. 25–31, 1991.

[6] I. Kingma, O. A. Smiseth, M. A. Frais, E. R. Smith, and J. V. Tyberg, "Left ventricular external constraint: relationship between pericardial, pleural and esophageal pressures during positive end-expiratory pressure and volume loading in dogs," *Annals of Biomedical Engineering*, vol. 15, no. 3-4, pp. 331–346, 1987.

[7] H. Jellinek, H. Krenn, W. Oczenski, F. Veit, S. Schwarz, and R. D. Fitzgerald, "Influence of positive airway pressure on the pressure gradient for venous return in humans," *Journal of Applied Physiology*, vol. 88, no. 3, pp. 926–932, 2000.

[8] P. C. M. van den Berg, J. R. C. Jansen, and M. R. Pinsky, "Effect of positive pressure on venous return in volume-loaded cardiac surgical patients," *Journal of Applied Physiology*, vol. 92, no. 3, pp. 1223–1231, 2002.

[9] H. Jellinek, P. Krafft, R. D. Fitzgerald, S. Schwarz, and M. R. Pinsky, "Right atrial pressure predicts hemodynamic response to apneic positive airway pressure," *Critical Care Medicine*, vol. 28, no. 3, pp. 672–678, 2000.

[10] A. Vieillard-Baron, K. Chergui, A. Rabiller et al., "Superior vena caval collapsibility as a gauge of volume status in ventilated septic patients," *Intensive Care Medicine*, vol. 30, no. 9, pp. 1734–1739, 2004.

[11] M. R. Pinsky, "Cardiovascular issues in respiratory care," *Chest*, vol. 128, no. 5, pp. 592S–597S, 2005.

[12] J. H. Chin, E. H. Lee, W. J. Kim et al., "Positive end-expiratory pressure aggravates left ventricular diastolic relaxation further in patients with pre-existing relaxation abnormality," *British Journal of Anaesthesia*, vol. 111, pp. 368–373, 2013.

[13] T. Luecke, H. Roth, P. Herrmann et al., "Assessment of cardiac preload and left ventricular function under increasing levels of positive end-expiratory pressure," *Intensive Care Medicine*, vol. 30, no. 1, pp. 119–126, 2004.

[14] C. Gernoth, G. Wagner, P. Pelosi, and T. Luecke, "Respiratory and haemodynamic changes during decremental open lung positive end-expiratory pressure titration in patients with acute respiratory distress syndrome," *Critical Care*, vol. 13, no. 2, article R59, 2009.

[15] M. Takata and J. L. Robotham, "Ventricular external constraint by the lung and pericardium during positive end-expiratory pressure," *American Review of Respiratory Disease*, vol. 143, no. 4, pp. 872–875, 1991.

[16] S. Nadar, N. Prasad, R. S. Taylor, and G. Y. H. Lip, "Positive pressure ventilation in the management of acute and chronic cardiac failure: a systematic review and meta-analysis," *International Journal of Cardiology*, vol. 99, no. 2, pp. 171–185, 2005.

[17] H. J. Tucker and J. F. Murray, "Effects of end-expiratory pressure on organ blood flow in normal and diseased dogs," *Journal of applied physiology*, vol. 34, no. 5, pp. 573–577, 1973.

[18] S. E. Lapinsky, J. G. Posadas-Calleja, and I. McCullagh, "Clinical review: ventilatory strategies for obstetric, brain-injured and obese patients," *Critical Care*, vol. 13, no. 2, article 206, 2009.

[19] A. Caricato, G. Conti, F. Della Corte et al., "Effects of PEEP on the intracranial system of patients with head injury and subarachnoid hemorrhage: the role of respiratory system compliance," *Journal of Trauma*, vol. 58, no. 3, pp. 571–576, 2005.

[20] L. Mascia, S. Grasso, T. Fiore, F. Bruno, M. Berardino, and A. Ducati, "Cerebro-pulmonary interactions during the application of low levels of positive end-expiratory pressure," *Intensive Care Medicine*, vol. 31, no. 3, pp. 373–379, 2005.

[21] G. Tusman, S. H. Böhm, G. F. Vazquez de Anda, J. L. do Campo, and B. Lachmann, "'Alveolar recruitment strategy' improves

arterial oxygenation during general anaesthesia," *British Journal of Anaesthesia*, vol. 82, no. 1, pp. 8–13, 1999.

[22] P. Neumann, H. U. Rothen, J. E. Berglund, J. Valtysson, A. Magnusson, and G. Hedenstierna, "Positive end-expiratory pressure prevents atelectasis during general anaesthesia even in the presence of a high inspired oxygen concentration," *Acta Anaesthesiologica Scandinavica*, vol. 43, no. 3, pp. 295–301, 1999.

[23] D. Reis Miranda, D. Gommers, A. Struijs et al., "Ventilation according to the open lung concept attenuates pulmonary inflammatory response in cardiac surgery," *European Journal of Cardiothoracic Surgery*, vol. 28, no. 6, pp. 889–895, 2005.

[24] J. Wetterslev, E. G. Hansen, O. Roikjaer, I. L. Kanstrup, and L. Heslet, "Optimizing peroperative compliance with PEEP during upper abdominal surgery: effects on perioperative oxygenation and complications in patients without preoperative cardiopulmonary dysfunction," *European Journal of Anaesthesiology*, vol. 18, no. 6, pp. 358–365, 2001.

[25] D. Meininger, C. Byhahn, S. Mierdl, K. Westphal, and B. Zwissler, "Positive end-expiratory pressure improves arterial oxygenation during prolonged pneumoperitoneum," *Acta Anaesthesiologica Scandinavica*, vol. 49, no. 6, pp. 778–783, 2005.

[26] J. Y. Kim, C. S. Shin, H. S. Kim, W. S. Jung, and H. J. Kwak, "Positive end-expiratory pressure in pressure-controlled ventilation improves ventilatory and oxygenation parameters during laparoscopic cholecystectomy," *Surgical Endoscopy and Other Interventional Techniques*, vol. 24, no. 5, pp. 1099–1103, 2010.

[27] F. X. Whalen, O. Gajic, G. B. Thompson et al., "The effects of the alveolar recruitment maneuver and positive end-expiratory pressure on arterial oxygenation during laparoscopic bariatric surgery," *Anesthesia and Analgesia*, vol. 102, no. 1, pp. 298–305, 2006.

[28] P. Neumann, H. U. Rothen, J. E. Berglund, J. Valtysson, A. Magnusson, and G. Hedenstierna, "Positive end-expiratory pressure prevents atelectasis during general anaesthesia even in the presence of a high inspired oxygen concentration," *Acta Anaesthesiologica Scandinavica*, vol. 43, no. 3, pp. 295–301, 1999.

[29] H. F. Talab, I. A. Zabani, H. S. Abdelrahman et al., "Intraoperative ventilatory strategies for prevention of pulmonary atelectasis in obese patients undergoing laparoscopic bariatric surgery," *Anesthesia and Analgesia*, vol. 109, no. 5, pp. 1511–1516, 2009.

[30] H. Reinius, L. Jonsson, S. Gustafsson et al., "Prevention of atelectasis in morbidly obese patients during general anesthesia and paralysis: a computerized tomography study," *Anesthesiology*, vol. 111, no. 5, pp. 979–987, 2009.

[31] E. Futier, J. M. Constantin, C. P. Burtx et al., "A trial of intraoperative low tidal volume ventilation in abdominal surgery," *The New England journal of medicine*, vol. 369, pp. 428–437, 2013.

[32] P. Severgnini, G. Selmo, C. Lanza et al., "Protective mechanical ventilation during general anestehsia for open abdominal surgery improves postoperative pulmonary function," *Anestehsiology*, vol. 118, pp. 1307–1321, 2013.

[33] G. Imberger, D. McIlroy, N. L. Pace, J. Wetterslev, J. Brok, and A. M. Møller, "Positive End-Expiratory Pressure (PEEP) during anaesthesia for the prevention of mortality and postoperative pulmonary complications," *Cochrane Database of Systematic Reviews*, vol. 9, Article ID CD007922, 2010.

[34] S. N. T. Hemmes, P. Severgnini, S. Jaber et al., "Rationale and study design of PROVHILO—a worldwide multicenter randomized controlled trial on protective ventilation during general anesthesia for open abdominal surgery," *Trials*, vol. 12, article 111, 2011.

[35] C. R. Bernard, "Acute respiratory distress syndrome: a historical perspective," *American Journal of Respiratory and Critical Care Medicine*, vol. 172, no. 7, pp. 798–806, 2005.

[36] L. M. Bigatello and W. M. Zapol, "New approaches to acute lung injury," *British Journal of Anaesthesia*, vol. 77, no. 1, pp. 99–109, 1996.

[37] E. Roupie, M. Dambrosio, G. Servillo et al., "Tritation of tidal volume and induced hypercapnia in acute respiratory distress syndrome," *American Journal of Respiratory and Critical Care Medicine*, vol. 149, pp. 533–537, 1994.

[38] M. B. P. Amato, C. S. V. Barbas, D. M. Medeiros et al., "Effect of a protective-ventilation strategy on mortality in the acute respiratory distress syndrome," *The New England Journal of Medicine*, vol. 338, no. 6, pp. 347–354, 1998.

[39] V. M. Ranieri, P. M. Suter, C. Tortorella et al., "Effect of mechanical ventilation on inflammatory mediators in patients with acute respiratory distress syndrome: a randomized controlled trial," *Journal of the American Medical Association*, vol. 282, no. 1, pp. 54–61, 1999.

[40] The NHLBI Institute ARDS Clinical Trial Network, "Higher versus lower positive end-expiratory pressures in patients with the acute respiratory distress syndrome," *The New England Journal of Medicine*, vol. 351, pp. 327–336, 2004.

[41] A. Mercat, J.-C. M. Richard, B. Vielle et al., "Positive end-expiratory pressure setting in adults with acute lung injury and acute respiratory distress syndrome: a randomized controlled trial," *Journal of the American Medical Association*, vol. 299, no. 6, pp. 646–655, 2008.

[42] M. O. Meade, D. J. Cook, G. H. Guyatt et al., "Ventilation strategy using low tidal volumes, recruitment maneuvers, and high positive end-expiratory pressure for acute lung injury and acute respiratory distress syndrome: a randomized controlled trial," *Journal of the American Medical Association*, vol. 299, no. 6, pp. 637–645, 2008.

[43] D. Talmor, T. Sarge, A. Malhotra et al., "Mechanical ventilation guided by esophageal pressure in acute lung injury," *The New England Journal of Medicine*, vol. 359, no. 20, pp. 2095–2104, 2008.

[44] P. Pelosi, A. Barassi, P. Severgnini et al., "Prognostic role of clinical and laboratory criteria to identify early ventilator-associated pneumonia in brain injury," *Chest*, vol. 134, no. 1, pp. 101–108, 2008.

[45] N. Young, J. K. J. Rhodes, L. Mascia, and P. J. D. Andrews, "Ventilatory strategies for patients with acute brain injury," *Current Opinion in Critical Care*, vol. 16, pp. 45–52, 2010.

[46] M. Briel, M. Meade, A. Mercat et al., "Higher vs lower positive end-expiratory pressure in patients with acute lung injury and acute respiratory distress syndrome: systematic review and meta-analysis," *Journal of the American Medical Association*, vol. 303, no. 9, pp. 865–873, 2010.

[47] The ARDS definition task force, "Acute respiratory distress sybdrome: the Berlin definition," *Journal of the American Medical Association*, vol. 307, no. 23, pp. 6–33, 2012.

[48] W. Videtta, F. Villarejo, M. Cohen et al., "Effects of positive end-expiratory pressure on intracranial pressure and cerebral perfusion pressure," *Acta Neurochirurgica, Supplement*, no. 81, pp. 93–97, 2002.

[49] T. Huynh, M. Messer, R. F. Sing et al., "Positive end-expiratory pressure alters intracranial and cerebral perfusion pressure in severe traumatic brain injury," *Journal of Trauma*, vol. 53, no. 3, pp. 488–493, 2002.

[50] J. Villar, R. M. Kacmarek, L. Pérez-Méndez, and A. Aguirre-Jaime, "A high positive end-expiratory pressure, low tidal volume ventilatory strategy improves outcome in persistent acute respiratory distress syndrome: a randomized, controlled trial," *Critical Care Medicine*, vol. 34, no. 5, pp. 1311–1318, 2006.

Hindawi Publishing Corporation
The Scientific World Journal
Volume 2013, Article ID 683685, 15 pages
http://dx.doi.org/10.1155/2013/683685

Review Article

Ultrasound for the Anesthesiologists: Present and Future

Abdullah S. Terkawi,[1,2] Dimitrios Karakitsos,[3] Mahmoud Elbarbary,[4] Michael Blaivas,[5] and Marcel E. Durieux[1]

[1] *Department of Anesthesiology, University of Virginia Health System, Charlottesville, VA 22903, USA*
[2] *Department of Anesthesiology, King Fahad Medical City, Riyadh, Saudi Arabia*
[3] *Department of Internal Medicine, University of South Carolina, School of Medicine, Columbia, SC, USA*
[4] *Department of Cardiac Sciences, Critical Care & National and Gulf Center for Evidence Base Health Practice, King Saud bin Abdulaziz University for Health Sciences, Riyadh, Saudi Arabia*
[5] *Department of Emergency Medicine, University of South Carolina, School of Medicine, Columbia, SC, USA*

Correspondence should be addressed to Abdullah S. Terkawi; asterkawi@gmail.com

Received 12 August 2013; Accepted 26 September 2013

Academic Editors: B. Bein, A. Kotanidou, and E. O. Martin

Ultrasound is a safe, portable, relatively inexpensive, and easily accessible imaging modality, making it a useful diagnostic and monitoring tool in medicine. Anesthesiologists encounter a variety of emergent situations and may benefit from the application of such a rapid and accurate diagnostic tool in their routine practice. This paper reviews current and potential applications of ultrasound in anesthesiology in order to encourage anesthesiologists to learn and use this useful tool as an adjunct to physical examination. Ultrasound-guided peripheral nerve blockade and vascular access represent the most popular ultrasound applications in anesthesiology. Ultrasound has recently started to substitute for CT scans and fluoroscopy in many pain treatment procedures. Although the application of airway ultrasound is still limited, it has a promising future. Lung ultrasound is a well-established field in point-of-care medicine, and it could have a great impact if utilized in our ORs, as it may help in rapid and accurate diagnosis in many emergent situations. Optic nerve sheath diameter (ONSD) measurement and transcranial color coded duplex (TCCD) are relatively new neuroimaging modalities, which assess intracranial pressure and cerebral blood flow. Gastric ultrasound can be used for assessment of gastric content and diagnosis of full stomach. Focused transthoracic (TTE) and transesophageal (TEE) echocardiography facilitate the assessment of left and right ventricular function, cardiac valve abnormalities, and volume status as well as guiding cardiac resuscitation. Thus, there are multiple potential areas where ultrasound can play a significant role in guiding otherwise blind and invasive interventions, diagnosing critical conditions, and assessing for possible anatomic variations that may lead to plan modification. We suggest that ultrasound training should be part of any anesthesiology training program curriculum.

1. Introduction

Anesthesiologists require quick and accurate diagnostic tools for the effective management of emergencies. Ultrasound (US) is a safe, easily accessible point-of-care imaging modality that is being increasingly adopted in modern anesthesiology practice. As physician-performed ultrasound becomes more practical and practiced, it is important to assure that anesthesiologists are aware of the expanding applications of this technology and the status of its use. Current and potential future applications of US in anesthesiology are summarized as follows:

(1) regional anesthesia;
(2) neuraxial and chronic pain procedures;
(3) vascular access;
(4) airway assessment;
(5) lung ultrasound;
(6) ultrasound neuro-monitoring;
(7) gastric ultrasound;
(8) focused transthoracic echo (TTE);
(9) transesophageal echo (TEE) and Doppler (Beyond the scope of discussion in this paper).

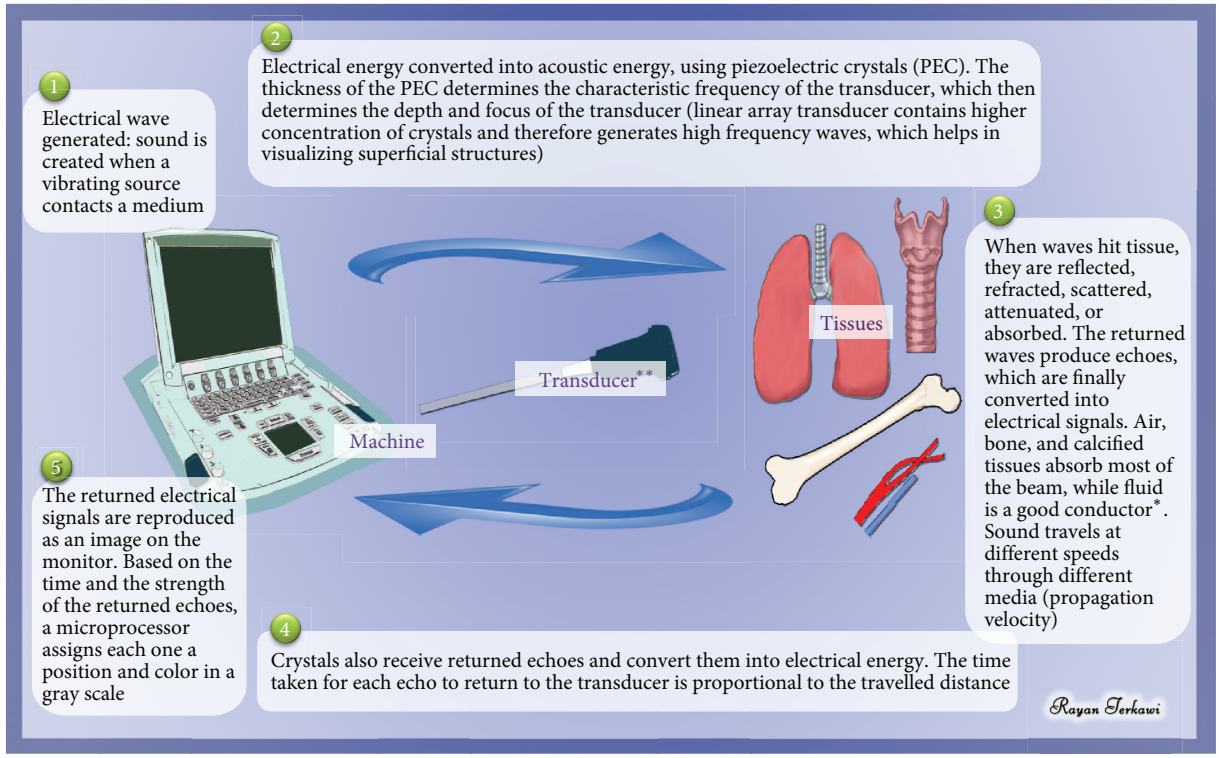

Figure 1: Concept of ultrasonography: *tissues that allow the beam to pass easily (e.g., containing fluids or blood) create only little echo (hypoechoic) and appear black on the screen, while tissues that allows less beam to pass (e.g., fat and bone) create stronger echoes (hyperechoic) and thus appear white on the screen; **linear transducers have a higher frequency (10–15 MHz) and are usually used for superficial structures; curved transducers have a lower frequency (4–8 MHz) and are usually used for deeper structures.

This paper highlights current and potential future applications of ultrasound in the field of anesthesiology. Our objective is to increase awareness of the current benefits and limitations of selected ultrasound applications that may be relevant to anesthesiologists. We aim to encourage practitioners to acquire appropriate training that will allow them to apply well-established ultrasound techniques in their routine practice, to assure that they are aware of constraints and limitations in various settings, and to remain alert for the development of ultrasound techniques that are a focus of ongoing research.

2. Principles of Ultrasound

Ultrasound ("extrasound") refers to the use of sound waves (typically from 2 to 15 MHz, but in modern probes up to 22 MHz), which are above the frequency of those sound waves that can be heard by the human ear (20 to 20,000 Hz range). The concept of ultrasound is explained in Figure 1 [1–3].

Several basic and advanced modes of ultrasound imaging exist, but B-mode, M-mode, and color-Doppler are those most commonly used in anesthesiology [3]. B-mode (brightness) is the main mode of any ultrasound machine. Each gray scale tomographic image in B-mode is composed of pixels with brightness depending on the intensity of the echo that is received from the corresponding location in the body. This mode is used to evaluate and scan organs in real time [4, 5]. M-mode (motion) displays the movement of structures along a single line (axis of the ultrasound beam) chosen by the operator. M-mode is used for evaluation of heart wall or valve motion (echocardiography), hemodynamic status (vena cava analysis), and documentation of lung sliding or movement of the diaphragm [5].

Doppler modes detect frequency shifts that are created by sound reflections of a moving target (Doppler effect). It uses the change in pitch of the sound waves to provide information about blood flow [6]. Three Doppler techniques are commonly used. (1) Color flow Doppler: this gives an image of the blood vessel that represents the speed and direction of blood flow through the vessel. The colors (usually red and blue) denote flow towards and away from the transducer, regardless of the vessel's nature (artery or vein). Power Doppler is a special type of color Doppler. (2) Pulsed wave Doppler (PWD) transmits short pulses of ultrasound and Doppler signals. It allows measurements of blood velocity from a small region, by converting the Doppler sounds into a graph that gives information about the speed and direction of blood flow through the blood vessel. (3) Continuous wave Doppler (CWD) transmits and receives continuous ultrasound waves. The region from which Doppler signals are obtained is determined by the overlap of the transmitted

and received ultrasound beams. It is useful for measuring high velocities but with poor ability to localize a flow signal accurately, since the signal can originate from any point along the ultrasound beam.

3. Regional Anesthesia

Ultrasound-guided peripheral nerve blockade is perhaps the most popular ultrasound application used by anesthesiologists. It might be the gold standard for regional anesthesia; it allows anesthesiologists to perform regional anesthesia more accurately, and it expands the ability to block smaller nerves and those in more difficult anatomic locations.

Ultrasound-guided peripheral nerve blocks offer the following advantages: direct observation of the nerves and surrounding structures (e.g., vessels), thus decreasing complications (e.g., accidental intraneural or intravascular injection), and direct observation of local anesthetic spread. The more accurate deposition leads to faster onset and longer duration of block, improves block quality, and allows dose reduction of local anesthetics [7–9]. It has been shown that when peripheral nerves are adequately imaged by ultrasound, the simultaneous use of the nerve stimulator offers no further advantages [7].

In children, ultrasound guidance carries similar advantages as for adults and has become more popular recently. However, there is still a shortage of clinical studies comparing the advantages of ultrasound guidance over traditional techniques (nerve stimulation), particularly with respect to safety; ilioinguinal blocks may be an exception. Further studies are warranted [10, 11].

4. Neuraxial and Chronic Pain Procedures

Ultrasound has become a commonly used modality in the performance of chronic pain interventions and has begun to substitute for CT scans and fluoroscopy in many chronic pain procedures. It allows direct visualization of tissue structure while allowing real-time guidance of needle placement and medication administration. The following list summarizes some of current and potential applications of ultrasound in neuraxial and chronic pain procedures:

(1) neuraxial blocks;

(2) nerve root blocks (e.g., cervical and lumber);

(3) stellate ganglion block;

(4) lumber transforaminal injections for radicular pain;

(5) facet joint block;

(6) epidural blood patch;

(7) intra-articular joint injections;

(8) ultrasound guidance for peripheral nerve stimulator implantation;

(9) interventional procedures for patients with chronic pelvic pain (e.g., pudendal neuralgia, piriformis syndrome, and "border nerve" syndrome).

Ultrasound can aid in neuraxial blocks in two ways: (1) ultrasound-assisted neuraxial technique and (2) real-time ultrasound-guided neuraxial technique. It helps in identification of landmarks and midline structures, estimating epidural space depth, and facilitating epidural catheter insertion [12]. Improvement in efficacy of epidural analgesia and technique difficulties are two other advantages of preprocedural ultrasound [13].

Karmakar et al. [14] in 14 out of 15 patients demonstrated successful use of real-time ultrasound-guided paramedian epidural access with in-plane needle insertion, without inadvertent dural punctures or complications. Real-time technique requires more expert personnel and a minimum of three hands, which may make it unpractical.

Willschke et al. [15] evaluated ultrasound guidance for epidural catheter placement in children below six years, found that ultrasonography is helpful in reducing bone contacts, faster epidural placement, and offered direct visualization of neuraxial structures and the spread of local anesthetic inside the epidural space. Again, it needs highly skilled hands.

Nerve root blocks under US guidance can be as effective as those placed using a fluoroscopy-guided method [16]. US facilitates identifying critical vessels at unexpected locations, thereby avoiding injury [17]. Transforaminal injection is a commonly used technique in management of spinal radicular pain. Ultrasound-guided transforaminal injection can be accurate and feasible in the preclinical setting, and it carries an advantage over traditional fluoroscopy or CT scan technique by avoiding radiation exposure and the ability to be performed as an outpatient procedure [18].

Ultrasound-guided facet joint block is another application that provides a minimal invasive procedure, with less time consumed, lower expenses, and fewer complications, in comparison with fluoroscopy-guided technique [19, 20].

Ultrasound-guided epidural blood patch allows confirmation of proper placement of injectate into the epidural space [21]. Clendenen et al. [22] presented a case series of six patients who were treated with 4-dimensional ultrasound-guided epidural blood patch for symptomatic postlaminectomy cerebrospinal fluid leak; all of them had relief of their headache.

Ultrasound guidance of intra-articular joint injections (mainly the knee joint) improves needle placement and injection accuracy in comparison with palpation/anatomic landmark techniques, which improves patient-reported clinical outcomes and cost-effectiveness [23, 24]. Ultrasound-guided interventional procedures for patients with chronic pelvic pain (e.g., pudendal neuralgia, piriformis syndrome, and "border nerve" syndrome) were also reported [25].

5. Vascular Access

Advantages of ultrasound-guided central venous catheterization include identification of the vein, detection of variable anatomy and intravascular thrombi, and avoidance of inadvertent arterial puncture. It is safer and less time consuming than the traditional landmark technique [26,

27]. It is of particular benefit when used in patients with underlying coagulopathy or platelet dysfunction, by reducing the number of puncture attempts. Ultrasound can also be used for localization of central vein catheters and detection of postprocedural pneumothorax, as an alternative to chest radiography [28]. Ultrasound-guided vascular access has helped in various challenging patient positions: in sitting patients, patient with kyphosis and fixed chin-on-chest deformity [29], and in the prone position [30].

Ultrasound arterial cannulation helps in reducing the number of attempts, shortening the procedure time, and increasing the success rate, even in children [26]. A linear or hockey-stick probe can be used. However, it requires training to achieve a level of consistent proficiency.

There is a marked reduction in complication rates after implementation of US-guided central venous cannulation approaches. Although some complications still happen, rates of 4.6% have been reported, comparing with 10.5% when using landmark technique, which represents an absolute risk reduction of 5.9% (95% CI 0.5–11.3%) [31]. Most of these complications occur due to inadequate operator's experience; "overshooting" the needle to exit the vein or failing to differentiate between vein and artery. French et al. [32] suggested a new 4-dimensional imaging (real-time 3-dimensional imaging) approach, using a matrix arrays transducer, for central venous cannulation, which shows promising results in preventing "overshooting" the needle and provides better visualization of anatomy.

Peripheral vascular access in pediatrics can be very challenging especially in small, obese, or dehydrated children or in those with previously failed venipuncture. Studies showed that ultrasound-guided peripheral vascular access may improve the success rate of difficult vascular access when performed by well-trained physicians [33]. Recently, the High-frequency UltraSound in Kids studY (HUSKY) group, suggested that high-frequency (50 MHz) micro-ultrasound (HFMU) may allow better visualization for the sub-10 mm space. This could be a valuable tool for difficult vascular access in pediatric patients [34].

6. Airway Assessment

Airway ultrasound can visualize and assess the tongue, oropharynx, hypopharynx, epiglottis, larynx, vocal cords, cricothyroid membrane, cricoid cartilage, trachea, and cervical esophagus [4, 35, 36]. The posterior pharynx, posterior commissure, and posterior wall of the trachea cannot be visualized due to artifacts that are created by the intraluminal air column [35]. In comparison with computed tomography (CT scan), it has been found that ultrasound can reliably image all the structures that are visualized by CT scan and provides almost identical infrahyoid parameter measurements and minimal differences in suprahyoid anatomic parameter measurements, as the latter may be affected by the unintentional head extension [37].

Superficial structures can be scanned by linear high-frequency transducer, while deep structures are better visualized in sagittal and parasagittal views using the curved low-frequency transducer [4]. Current and potential applications of airway ultrasound are summarized as follows.

(1) prediction of difficult airway;

(2) confirmation of proper endotracheal tube placement and ventilation;

(3) evaluation of airway pathologies that may affect the choice of airway management (e.g., subglottic hemangiomas and stenosis), or mandate urgent securing of airway (e.g., Epiglottitis);

(4) prediction of obstructive sleep apnea;

(5) prediction of size of endotracheal, endobronchial, and tracheostomy tubes;

(6) airway related nerve blocks;

(7) assessing and guidance for proper percutaneous dilatational tracheostomy (PDT);

(8) prediction of successful extubation:

   (a) prediction of airway edema;

   (b) assessment of the diaphragm movement;

   (c) assessment of vocal cord movements.

Prediction of the difficult airway is a research area of great interest, with promising preliminary findings. Adhikari et al. [38] recently have reported that measurements of anterior soft neck tissue thickness at the level of the hyoid bone and thyrohyoid membrane can be used to predict difficult laryngoscopies, even though no significant correlation is found between sonographic measurements and clinical screening tests. An early study with a smaller sample size by Komatsu et al. [39] measured the distance from the skin to the anterior aspect of the airway at the level of the vocal cords, anterior to the thyroid cartilage, and failed to show a prediction of difficult laryngoscopy in obese patients. Thus, further studies are still needed in this area.

Confirmation of proper endotracheal tube placement can be done by two methods, direct and indirect [4, 40]. One direct method is the use of a real-time ultrasound probe placed transversely on the neck at the level of the suprasternal notch during intubation to observe whether the tube enters the trachea or esophagus. An indirect method is by observing bilateral lung sliding with ventilation as the probe is placed in the midaxillary line. Marciniak et al. [41] describe some characteristic ultrasonographic findings in the pediatric airway (e.g., shape changes of the glottis as the tracheal tube passes, enhanced posterior shadowing of the trachea, visualization of the vocal cords, and confirmation of bilateral lung movements) that could help during tracheal intubation. Recently, Fiadjoe et al. [42] reported an ultrasound-guided tracheal intubation in a 14-month-old baby, using a 15 MHz linear ultrasound probe at the level of the thyrohyoid membrane. They introduced (without laryngoscope) the tracheal tube containing a malleable stylet until it was visualized by ultrasound at the glottis level and then further adjusted the position and direction into the glottis until widening of the vocal cords was observed.

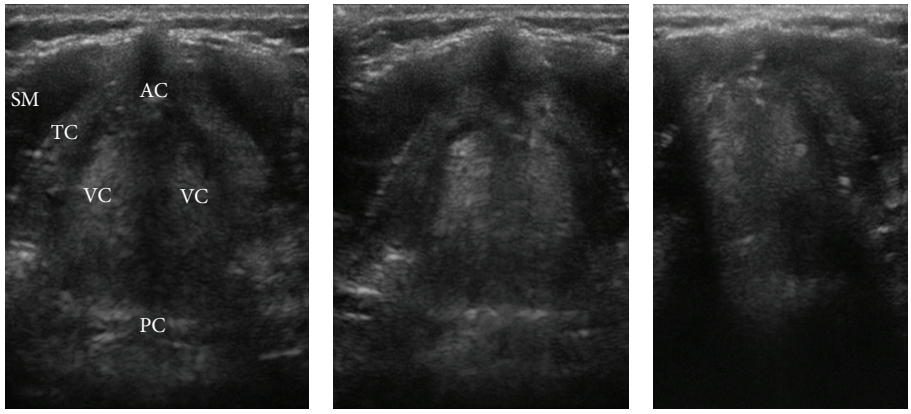

Figure 2: Vocal cords assessment: SM: strap muscles; TC: thyroid cartilage; AC: anterior commissure; PC: posterior commissure; and VC: vocal cords. (a) Vocal cords are abducted on inspiration, (b) adducted partially during expiration, (c) and are tightly closed when asking the patient to say "Eeeee." Linear transducer was placed transversely on the midline of the cricothyroid membrane.

Preliminary results of bedside ultrasonography show that it is a safe and effective tool to diagnose acute epiglottitis. In two recent studies, Hung et al. [43] visualized the "P sign" in a longitudinal view through the thyrohyoid membrane. Ko et al. [44] found a significant difference in the anteroposterior diameter of the epiglottis in acute epiglottitis patients. These findings can facilitate early and proper airway management.

Diagnosis and prediction of obstructive sleep apnea is a challenge, as many patients come for surgery undiagnosed. Lahav et al. [45] found that tongue base width, measured by ultrasound, may influence the severity of obstructive sleep apnea, including the patients' sensation of choking during night. Another important correlation, found by Liu et al. [46], is the lateral parapharyngeal wall thickness. Further studies are still needed in this area.

Ultrasonography has been used successfully to guide the choice of the appropriate size of endotracheal tube [4, 47], tracheostomy tube [4, 36], and even double-lumen tube [48, 49]. Ultrasound is successfully improving the performance of airway related nerve blocks [36], including superior laryngeal nerve, deep cervical plexus, alveolar nerve, and superficial trigeminal nerve. Kaur et al. [50] recently published their preliminary results in ultrasound-guided superior laryngeal nerve block for upper airway anesthesia, using a hockey stick-shaped 8 to 15 MHz transducer and concluded that it is a feasible approach.

Percutaneous dilatational tracheostomy (PDT) is a frequent procedure in intensive care units [36], with possible potential complications, like hemorrhage from local vessels and tracheal stenosis, due to a higher placement of the tracheostomy. Advantages of ultrasound in this setting include [4, 36, 51] identification of possible vessels in the field and localization of the midline and the tracheal rings for optimal intercartilaginous space selection, to avoid any possible laryngotracheal stenosis. The distance from the skin to the surface of the trachea can also be measured in order to estimate the required length of the puncture cannula. Another approach for using real-time ultrasonic guidance with visualization of the needle has been reported [52] and appears to be feasible, accurate, and safe. Selecting the good candidate seems to be the main advantage of ultrasound PDT.

Prediction of successful extubation is another challenge, especially in long-term intubated patients and in those who have a high risk of airway edema and vocal cord injuries (e.g., after thyroid surgery). A pilot study by Ding et al. [53] reported a useful method for predicting postextubation stridor. They found that the air-column width during cuff deflation at the level of the cricothyroid membrane is a potential predictor of postextubation stridor that reflects laryngeal edema. Jiang et al. [54] found that the cranio-caudal displacement of the liver and spleen with a cut-off value of 1.1 cm during spontaneous breathing trials, measured by ultrasonography, is a good predictor for extubation outcome.

Laryngeal ultrasound (Figure 2) to assess vocal fold paralysis in children has been suggested as a useful adjunct to endoscopy in diagnosis of vocal cord palsy [55]. Shaath et al. [56] assessed the accuracy of US in detection the vocal cord mobility in children after cardiac surgery in comparison with standard fiber-optic laryngoscopy and reported a sensitivity of 100% and specificity of 80% in 10 patients with persistent significant upper airway obstruction. A recent case report [57] shows a successful detection of recurrent laryngeal nerve palsy in the immediate postoperative period after thyroid surgery. Although endoscopy is still considered the gold standard for diagnosis of vocal cord palsy, the noninvasive nature and portability make ultrasound a good screening tool pre- and postthyroidectomy.

7. Lung Ultrasound

In a number of emergency situations, hypoxia will require urgent and appropriate diagnosis for its management. Pneumothorax, pulmonary edema, pulmonary embolism, and ARDS are situations where ultrasound can be an important tool for diagnosis (as shown in the following list). Lichtenstein et al. [58] introduced a quick and accurate ultrasound

protocol (BLUE protocol) for a rapid diagnosis and differentiating the cause of acute respiratory failure in critical care settings. We believe that a similar protocol could possibly be applied to our anesthetized patients. Lung ultrasound has a higher diagnostic yield than chest X-ray for most of the aforementioned conditions [59]; it is easier to carry out and less time consuming. However, it has some limitations when used in patients with subcutaneous emphysema, pleural calcifications, and in the obese [5]. Current and potential applications of lung ultrasound are as follows.

(1) diagnosis of pneumothorax;

(2) diagnosis of interstitial syndrome;

(3) diagnosis and differentiation of underlying cause of Pleural effusion, and selecting the optimal puncture site for pleurocentesis;

(4) diagnosis of pulmonary consolidation and pneumonia;

(5) diagnosis of atelectasis

(6) diagnosis of pulmonary edema and differentiate it from acute respiratory distress syndrome (ARDS);

(7) diagnosis of pulmonary embolism;

(8) monitoring of lung disease (severity, progress, and response to therapy);

(9) optimizing mechanical ventilation.

A high frequency (7.5 to 10 MHz) transducer is an appropriate choice for detecting pleural line abnormalities, while lower frequency (3.5 MHz) convex and microconvex transducers can be used to diagnose pleural effusions and lung parenchymal abnormalities. [5]. B- and M-mode may be used during lung ultrasound scanning and the produced sonographic images are a virtual interplay of two elements: air and fluid. Lung ultrasound interprets mainly the presence or absence of various artifacts since air is an acoustic barrier.

7.1. Normal Lung Aeration Patterns Reflect Specific Sonographic Signs [5] (Figures 3(a) and 3(b))

(i) "Lung sliding" signs are sliding of visceral and parietal layers of pleura with respiration.

(ii) Seashore sign is a complex picture of parallel lines signifying the static thoracic wall and sandy "granulous" pattern, which reflect the normal pulmonary parenchyma.

(iii) A-lines are a basic artifact of normally aerated lung.

7.2. Pathological Lung Signs and Patterns Include the following [5]

(i) B-lines represent discrete laser-like vertical hyperechoic lines that arise from the pleural line and extend to the bottom of the screen. These lines are consistent with interlobular pulmonary edema and can be found in both ARDS and cardiogenic pulmonary edema.

(ii) Dynamic and static air bronchograms which consist of hyperechoic punctiform elements within the lung parenchyma can be used to diagnose consolidation and atelectasis, respectively.

(iii) Lung pulse is an early and dynamic diagnostic sign of complete atelectasis, in which US perceives the vibrations of heart activity, along with the absence of lung sliding [60].

The International Liaison Committee on Lung Ultrasound (ILC-LUS) has recommended the following signs for the detection of various lung abnormalities [59].

(i) Pneumothorax (Figures 3(c) and 3(d)). Absence of lung sliding, presence of lung point(s), absence of B-lines, and absence of lung pulse. Lung ultrasound rules out the diagnosis of pneumothorax more accurately than a supine anterior chest X-ray (evidence level A).

(ii) Interstitial Syndrome (Figures 3(e) and 3(f)). Presence of a B-profile consisting of more than 3 B-lines on a longitudinal scanning plane. Interstitial syndrome includes pulmonary edema, interstitial lung disorders and ARDS (evidence level B). [59, 61].

(iii) Lung Consolidation. Sonographic signs are a subpleural echo-poor region or one with tissue-like echotexture. Lung ultrasound can differentiate between consolidation of pulmonary embolism, pneumonia, and atelectasis (evidence level A).

(iv) Pleural Effusion. A hypoechoic or anechoic space between sonoanatomical boundaries (i.e., chest wall, the diaphragm and subdiaphragmatic organs). Lung ultrasound is more accurate than chest X-ray (evidence level A).

(v) Monitoring Interstitial Syndrome. The number of B-lines is directly proportional to the severity of pulmonary congestion. This could be used as a monitoring parameter of severity and response to therapy (evidence level A). Pulmonary edema can be diagnosed, quantified, and monitored by detection of B-lines [62].

Pulmonary embolism (PE) (Figure 4), "mainly peripheral" can be diagnosed sonographically by the recognition of a peripheral, triangular, and pleural based hypoechoic lesion [5]. Mathis et al. [63], in a multicenter study that involves 352 patients, defined diagnostic criteria as (1) PE confirmed: two or more typical triangular or rounded pleural-based lesions; (2) PE probable: one typical lesion with pleural effusion; (3) PE possible: small (<5 mm) subpleural lesions or a single pleural effusion only. The sensitivity was 74%, specificity 95%, positive predictive value 95%, negative predictive value 75%, and accuracy 84%.

Laursen et al. [64] have studied the utility of lung ultrasound in near-drowning victims. Lung ultrasound showed multiple B-lines on the anterior and lateral surfaces of both lungs, consistent with pulmonary edema. These findings may encourage anesthesiologists to consider lung ultrasound for diagnosing aspiration pneumonia during anesthesia.

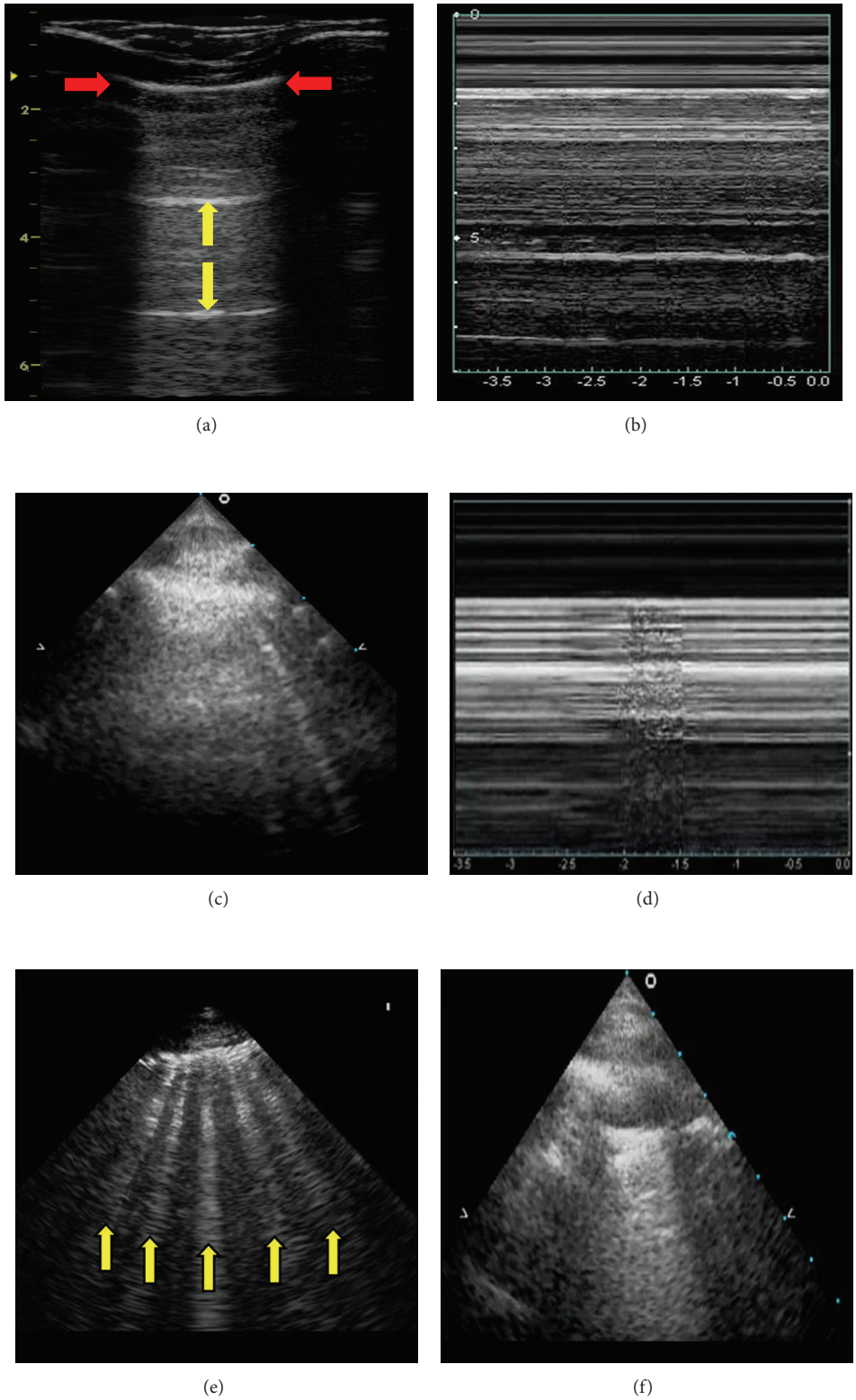

(a) (b)

(c) (d)

(e) (f)

Figure 3: Normal lung ultrasound: (a) 2D "red arrows" point to the pleura, where the normal "sliding sign" should be seen, while the "yellow arrows" represent the A-lines that are normal reverberation from the pleura. (b) M-mode shows the "seashore sign." Pneumothorax: (c) 2D; absence of lung sliding, (d) M-mode; "stratosphere sign" or "barcode sign," lung point may also be seen during inspiration and represents the border between pneumothorax and normal pleura. Cardiac pulmonary edema: (e) homogeneous distribution of B-lines (yellow arrows), normal sliding, and no spared areas. *Acute* respiratory distress syndrome (ARDS): (f) "patchy" distribution of B-lines, reduced/abolished sliding, spared areas, and peripheral consolidations.

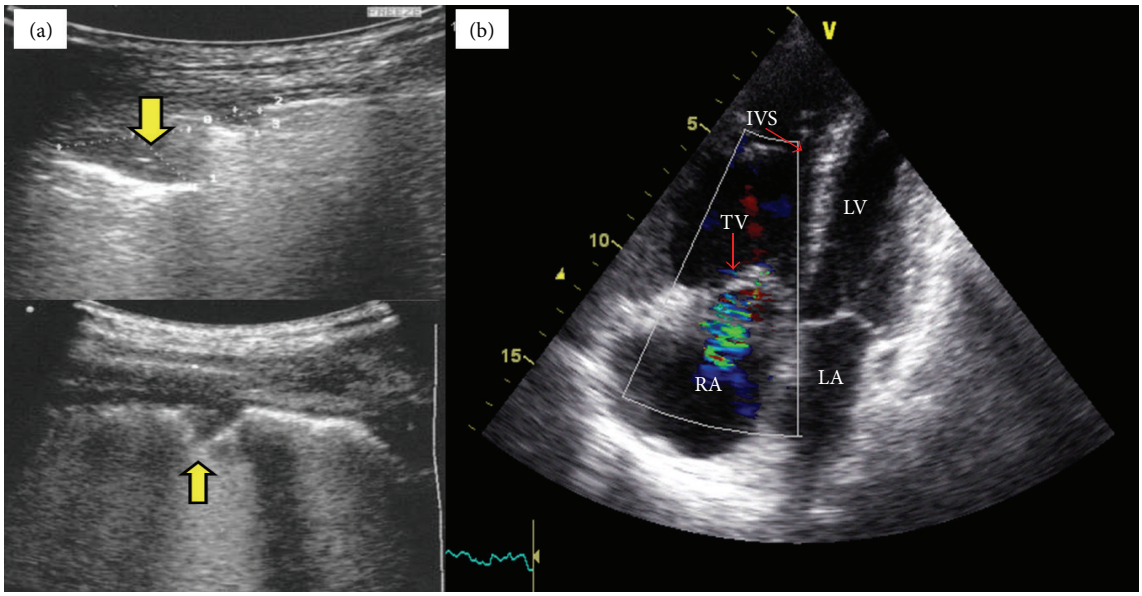

Figure 4: Pulmonary embolism: ((a) lung ultrasound) peripheral, triangular, and pleural based hypoechoic lesions (yellow arrows); ((b) transthoracic echo, apical view) it shows right ventricular (RV) dilation, RV hypokinesia, septal flattening, and tricuspid regurgitation. IVS: interventricular septum; TV: tricuspid valve; LV: left ventricle; RA: right atrium; LA: left atrium.

During positive pressure ventilation (PPV) a quantitative assessment of B-lines may aid in guiding diuretic or optimizing ventilator settings, particularly in conditions such as pulmonary edema or increased lung water content [65]. In general, PPV supports the function of an impaired left ventricular (LV) by reducing the transmural pressure across the LV free wall (LV afterload is reduced). In contrast, PPV is usually a functional burden on an already impaired right ventricle (RV) function, due to the reduction of preload and increase in afterload, respectively. Ultrasound can help in optimizing PPV to achieve the maximum benefit in oxygenation while avoiding its side effects on cardiac function. Ultrasound-guided optimization of positive end-expiratory pressure (PEEP) [66] is a clear example of this beneficial tool. PEEP can be titrated up and followed by quantifying the number of B-lines while watching RV filling and assuring that this PEEP is not causing any decrease in RV filling. Thus chest ultrasound (lung and cardiac ultrasound) evaluation can guide both ventilator and circulatory support. The optimization of heart-lung interaction can enhance the therapeutic effect of mechanical ventilation and facilitates the weaning process as well [67].

8. Ultrasound Neuromonitoring

Elevated intracranial pressure (ICP) requires special precautions by the anesthesiologist, such as avoiding particular medications, ventilation settings, and neuraxial anesthesia. Ultrasound is useful in assessing elevated ICP and cerebral perfusion. Current and potential applications of neuroultrasound are as follows:

(1) optic nerve sheath diameter (ONSD) measurement;

(2) transcranial Doppler ultrasound (TDU);

(3) pupillary light reflex (PLR).

Measurement of optic nerve sheath diameter (ONSD) (Figures 5(a) and 5(b)) has been found to reflect intracranial pressure, as an increase in ICP will be transmitted through the subarachnoid space that surrounds the optic nerve within its sheath and has been proposed as noninvasive and reliable means of assessing ICP in neurocritically ill patients [68].

In a recent systematic review and meta-analysis [69], ONSD measurements exhibited a pooled sensitivity of 0.90 (95% CI 0.80–0.95) and specificity 0.85 (95% CI 0.73–0.93) in detecting elevated ICP, while the area under the summary receiver-operating characteristic (SROC) curve was 0.94 (95% CI 0.91–0.96).

Soldatos et al. [70] found that 5.7 mm is a cut-off value for elevated ICP with sensitivity of 74.1% and specificity of 100%. The main drawbacks to this technique are operator dependence and measurement of relatively small structures, while technical improvements may be necessary.

Dubost et al. [71] measured ONSD in transverse and sagittal plane in patients with preeclampsia and compared the findings with those obtained in healthy pregnant women. They found that median ONSD values were significantly greater in preeclamptic patients at delivery (5.4 mm (95% CI 5.2, 5.7) versus 4.5 mm (95% CI 4.3, 4.8), $P < 0.0001$). In about 20% of preeclamptic patients, ONSD reflected compatible values with intracranial pressure above 20 mmHg. Further studies are required to improve the technique of this useful ultrasound methodology.

It has been thought [72] that intracranial hypotension, as in a setting of dural leak, might be associated with decreased ONSD, as the optic nerve is surrounded by cerebrospinal fluid and dura mater, which form the optic nerve sheath. Dubost et al. [73], in a preliminary report of 10 patients with lumbar epidural blood patch (EBP) for postdural puncture headache,

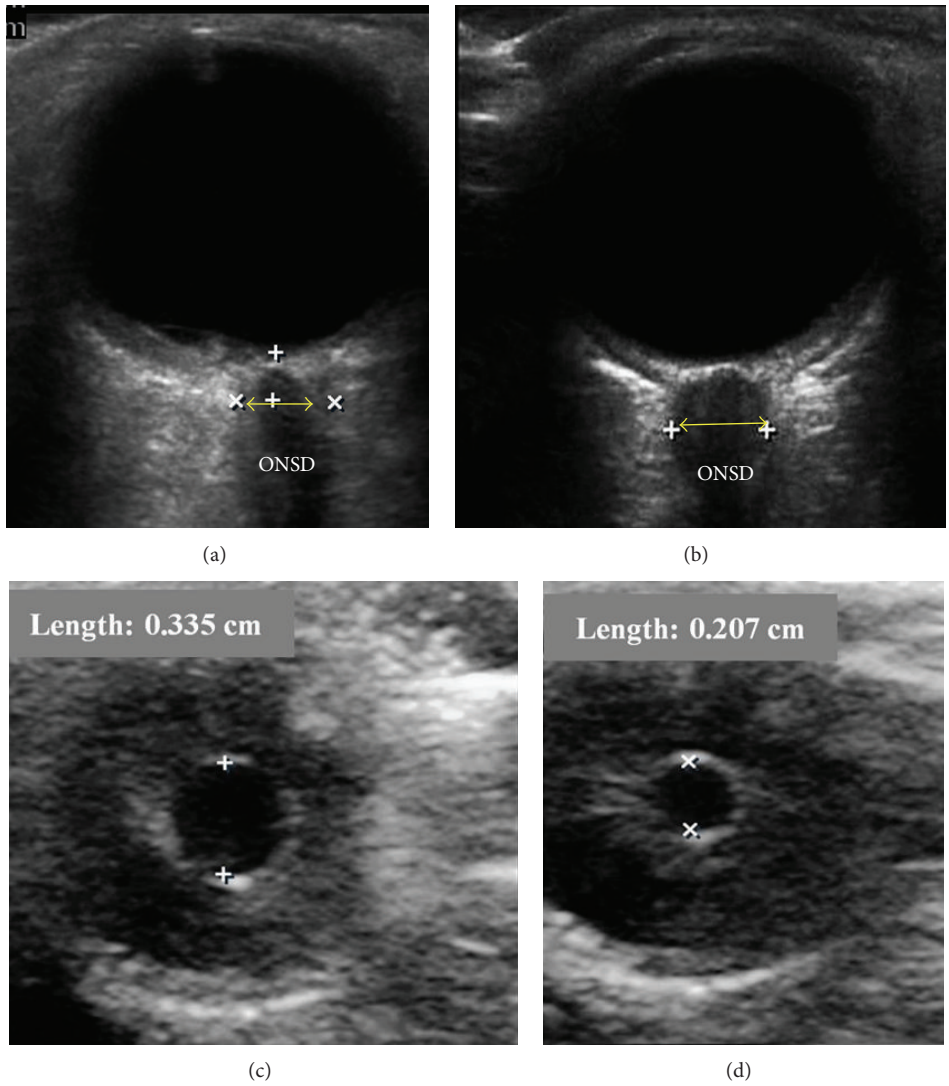

(a) (b)

(c) (d)

Figure 5: Optic nerve sheath: (a) normal diameter and (b) large diameter that represents increase intracranial pressure. ONSD: optic nerve sheath diameter. It is usually measured 3 mm behind the retina. Ultrasound pupillary light reflex: (c) diameter of the pupil before shining light to the contralateral eye and (d) the pupil constricted after shining the light.

indeed found that successful EBP was followed by ONSD enlargement.

Ultrasound assessment of the pupillary light reflex (PLR) was initially developed for the U.S. Space Program (NASA) and is not standardized for clinical use. However, the method can be used even when visual access to the pupil is impossible, and interpreting its results is straightforward [74]. Consensual pupillary light reflex is elicited with contralateral transillumination through the eyelids with both eyes closed (Figures 5(c) and 5(d)). The pupillary light reflex ultrasound test can be conducted with a linear array probe at the highest available frequency (e.g., 12–15 MHz), using the coronal primary view, while M-mode measurements are used to measure the constriction velocity of the PLR [75]. This method might be used as pupillometry as well.

Transcranial color coded duplex (TCCD) (Figure 6) is an accurate, real-time, noninvasive (permits bedside examination), and inexpensive tool used for the study of the intracranial circulation and the diagnosis of nonthrombosed aneurysms, largely due to its ability to reveal flow phenomena [76]. The main limitation of TCCD is the few available ultrasonic windows, which can limit the area of insonation of the cerebral arteries including their proximal branching and lower spatial resolution and can obstruct transtemporal insonation [77]. TCCD has advantages over transcranial Doppler (TCD) by showing the images of the intracranial anatomy and arteries throughout duplex B-mode, while still having the capacity to measure velocities using Doppler. In other words, different from TCD technology, TCCD shoots multiple ultrasound beams to expose a larger brain area at dual emitting frequencies, one for gray scale imaging and one for Doppler imaging. Thus this tool can illustrate arterial position on color flow imaging as well as on B-mode ultrasonography [78]. TCD and TCCD measured velocities are comparable using zero angle correction, resulting in more accurate measurement of flow velocities and allowing for

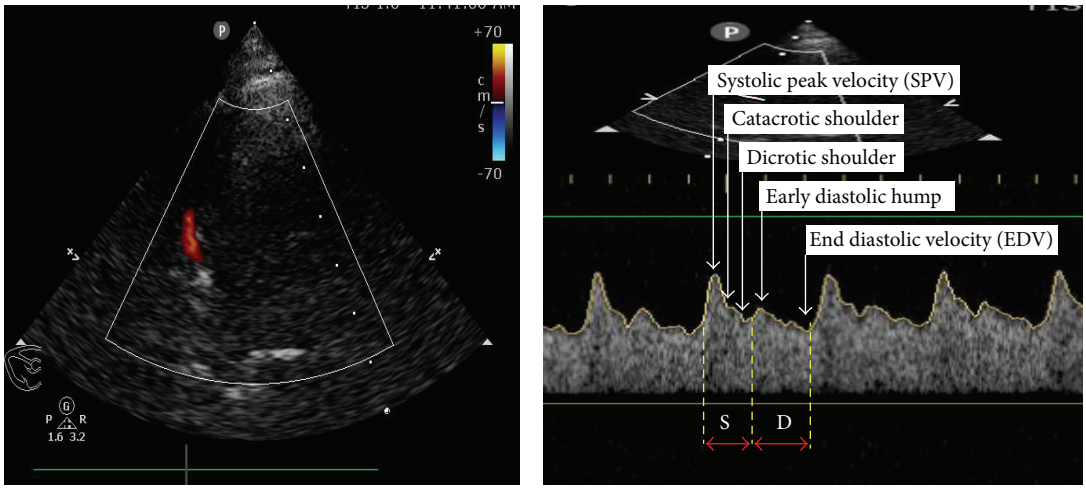

(a) (b)

Figure 6: Transcranial color coded duplex (TCCD): (a) middle cerebral artery (MCA) color Doppler and (b) MCA pulsed wave Doppler. S: systole, D: diastole.

superior precision in order to define intracranial arterial narrowing. TCCD can be used for monitoring of cerebral blood flow alterations which follow traumatic brain injury and in patients with sickle cell anemia. It also can be used in the detection of patent foramen ovale and in the diagnosis of cerebral circulatory arrest which is a component of brain death [79].

9. Gastric Ultrasound

A full stomach may lead to aspiration pneumonia and subsequent morbidities. Anesthesiologists may encounter patients with unknown prandial status, and even fasting "sufficient" time cannot guarantee an empty stomach in many cases (e.g., in the elderly or in patients with gastroparesis). Ultrasound can help in this setting, and the perioperative evaluation of bowel motility is also feasible by means of sonography. Current and potential applications of Gastric ultrasound are as follows:

(1) assessment of gastric content and diagnosis of full stomach;

(2) confirmation of gastric tube placement.

Bouvet et al. [80], measured the antral cross-sectional area (CSA) in 180 patients after intubation and analyzed the relationship between antral CSA and the volume of gastric contents. The cut-off value of antral CSA of 340 mm^2 for the diagnosis of "at risk" stomach was associated with a sensitivity of 91% and a specificity of 71%. The area under the receiver operating characteristic (ROC) curve for the diagnosis of "at-risk" stomach was 90%. ("At risk" stomach was defined as the presence of solid particles and/or gastric fluid volume more than 0.8 mL/kg.) These findings show that antral CSA volume assessment can be important in minimizing the risk of pulmonary aspiration of gastric contents. Perlas et al. [81] performed gastric sonography in 86 patients before anesthetic induction, and patients were classified using a 3-point grading system; grade 0 (empty antrum); grade 1 (minimal fluid volume detected only in the right lateral decubitus position (16 +/− 36 mL, within normal ranges expected for fasted patients); and grade 2 (antrum clearly distended with fluid visible in both supine and lateral positions (180 +/− 83 mL, beyond previously reported "safe" limits). One patient with a grade 2 antrum had an episode of a significant regurgitation of gastric contents on emergence from anesthesia. They concluded that this grading system could be a promising "biomarker" to assess perioperative aspiration risk. Perlas et al. [82], in another work, validated a mathematical model for quantitative US assessment of gastric volume. Arzola et al. [83] found that anesthesiologists will achieve a 95% success rate in bedside qualitative ultrasound assessment after performing approximately 33 examinations, with appropriate training and supervision.

Confirmation of a gastric tube placement is also possible using ultrasound [84], which might replace the conventional radiography method unless sonography is inconclusive.

10. Focused Transthoracic Echo (TTE)

Focus assessed transthoracic echo (FATE) was introduced by Jensen et al. [85] for cardiopulmonary monitoring in the intensive care unit. This approach basically involves four standardized acoustic views for cardiopulmonary screening and monitoring (Figure 7). Recent studies show a great impact of FATE in preoperative assessment [86, 87] when it is performed by anesthesiologists. Dennis and Stenson [88], recently presented a case that shows how anesthesiologists, using basic TTE skills, can diagnose and save a patient with postpartum hemorrhage by using a rapid obstetric screening echocardiography approach [89]. Learning the basic skills to perform focused transthoracic echo allows assessing the global function of the heart and diagnosing certain pathologies (e.g., pulmonary embolism). Cowie [90] presented their 3-year experience of focused cardiovascular ultrasound in

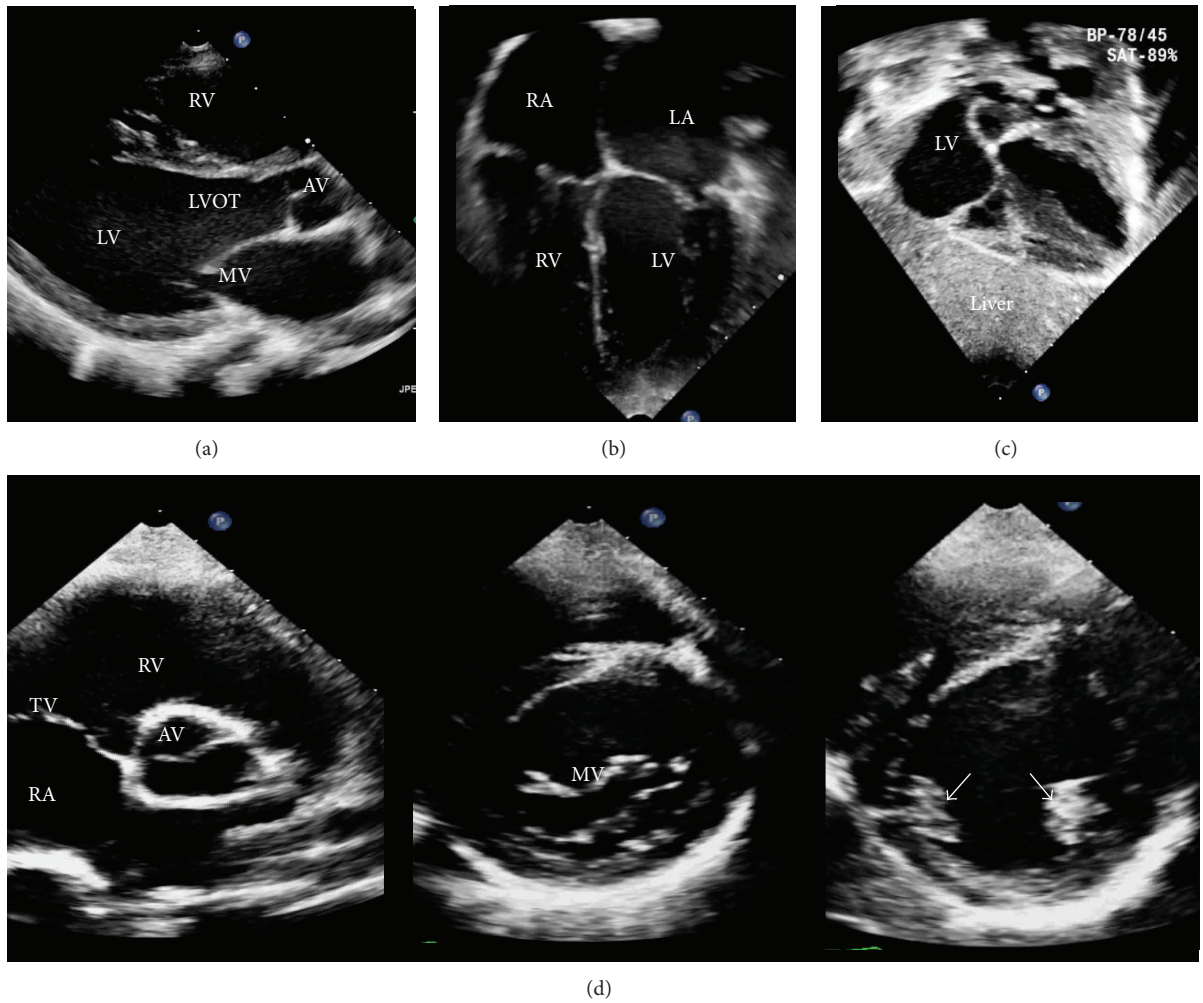

(a) (b) (c)

(d)

Figure 7: Basic transthoracic echo views: (a) left parasternal long axis, (b) apical, (c) subcostal, and (d) left parasternal short axis; aortic valve "Mercedes sign," mitral valve "fish mouth sign," and papillary muscles (two arrows), respectively, from left to right. RV: right ventricle, LV: left ventricle, LVOT: left ventricular outlet, RA: right atrium, LA: left atrium, AV: aortic valve, MV: mitral valve, and TV: tricuspid valve.

the perioperative period, which shows that focused cardiovascular ultrasound performed by anesthesiologists in the perioperative period accurately detects major cardiac pathology and significantly alters perioperative management. Neelankavil et al. [91] suggested a simulation method to train anesthesiologists in basic transthoracic echocardiography skills. Tanzola et al. [92] have suggested that implementation of a focused bedside TTE curriculum within anesthesia residency training is feasible, quantifiable, and effective for increasing anesthesia residents' TTE knowledge.

Recent studies show that preoperative excess testing and consultation are common, adding to the cost of care without noticeably improving patient outcome. These findings must encourage anesthesiologists to play an effective role in the preoperative assessment field by implementing clinically innovative approaches and developing training curricula as well as performing research [93]. Therefore, we strongly encourage the use of a focused protocol for perioperative assessment and incorporation of a training curriculum in residency training.

11. Technological Advances

New technologies have greatly improved the image quality, diagnostic abilities, and size of the US machine. These include advances in transducers, scanning schemes, three- and four-dimensional visualization, contrast agents (microbubbles), strain imaging, and others [94].

The matrix array is a new transducer with improved resolution; it has a lens that is placed in front of the piezoelectric element to allow a mechanical focusing in the Y- and Z-planes. Four-dimensional ultrasound provides real-time 3D images (the 4th "D" is time) and currently is used for fetal imaging, where it provides remarkable images. It may have potential applications in our field. Endobronchial and endoscopic ultrasounds are two other new modalities with great and potential implications [95].

Recently, the use of three-dimensional high resolution ultrasound was reported [96] for nerve blockade, providing better visualization of local anesthetic spread and catheter tip location. Small and portable ultrasound systems have

become increasingly available, even a mobile ultrasound-guided peripheral nerve block has been developed [97]. The SonixGPS needle guidance system (Ultrasonix, Richmond, BC, Canada) is a GPS technology with a new needle tracking system, using sensors in both the needle and transducer to obtain a real-time image of needle shaft and tip position related to the ultrasound beam that is based on the needle trajectory. This can be used for vascular access and nerve blocks. Recently, it has been used for real-time thoracic paravertebral block [98] and spinal anesthesia [99] in pilot studies.

12. Conclusion

Ultrasound is a unique tool which provides the anesthesiologist with diagnostic and monitoring capabilities enabling optimization of perioperative management. Indeed, ultrasound has an important role in problem-based management of various anesthesiology emergencies such as hypoxia, hypotension, dyspnea, and cardiopulmonary arrest. Finally, procedural ultrasound applications in the field of anesthesiology are numerous and improve the quality of care.

We believe that ultrasound can be the third eye of the anesthesiologist that helps in the performance of previously blind procedures and allows discovery of many hidden spaces to uncover their mysteries. Anesthesiologists, in the near future, may need to carry a portable ultrasound around their neck instead of a stethoscope.

Conflict of Interests

The authors declare no conflict of interests.

Acknowledgment

The authors are thankful to Dr. Rayan S. Terkawi, an intern medical doctor at King Fahad Medical City, Riyadh, Saudi Arabia, who designed (Figure 1) in this paper.

References

[1] J. P. Kline, "Ultrasound guidance in anesthesia," *AANA Journal*, vol. 79, no. 3, pp. 209–217, 2011.

[2] C. R. Falyar, "Ultrasound in anesthesia: applying scientific principles to clinical practice," *AANA Journal*, vol. 78, no. 4, pp. 332–340, 2010.

[3] A. Hatfield and A. Bodenham, "Ultrasound: an emerging role in anaesthesia and intensive care," *British Journal of Anaesthesia*, vol. 83, no. 5, pp. 789–800, 1999.

[4] M. S. Kristensen, "Ultrasonography in the management of the airway," *Acta Anaesthesiologica Scandinavica*, vol. 55, no. 10, pp. 1155–1173, 2011.

[5] K. Stefanidis, S. Dimopoulos, and S. Nanas, "Basic principles and current applications of lung ultrasonography in the intensive care unit," *Respirology*, vol. 16, no. 2, pp. 249–256, 2011.

[6] S. Kaddoura, *Echo Made Easy*, Elsevier, 2009.

[7] Z. J. Koscielniak-Nielsen, "Ultrasound-guided peripheral nerve blocks: what are the benefits?" *Acta Anaesthesiologica Scandinavica*, vol. 52, no. 6, pp. 727–737, 2008.

[8] J. Griffin and B. Nicholls, "Ultrasound in regional anaesthesia," *Anaesthesia*, vol. 65, supplement 1, pp. 1–12, 2010.

[9] S. S. Liu, J. Ngeow, and R. S. John, "Evidence basis for ultrasound-guided block characteristics: onset, quality, and duration," *Regional Anesthesia and Pain Medicine*, vol. 35, no. 2, pp. S26–S35, 2010.

[10] G. Ivani and V. Mossetti, "Pediatric regional anesthesia," *Minerva Anestesiologica*, vol. 75, no. 10, pp. 577–583, 2009.

[11] K. Rubin, D. Sullivan, and S. Sadhasivam, "Are peripheral and neuraxial blocks with ultrasound guidance more effective and safe in children?" *Paediatric Anaesthesia*, vol. 19, no. 2, pp. 92–96, 2009.

[12] A. Perlas, "Evidence for the use of ultrasound in neuraxial blocks," *Regional Anesthesia and Pain Medicine*, vol. 35, no. 2, pp. S43–S46, 2010.

[13] K. J. Chin and A. Perlas, "Ultrasonography of the lumbar spine for neuraxial and lumbar plexus blocks," *Current Opinion in Anaesthesiology*, vol. 24, no. 5, pp. 567–572, 2011.

[14] M. K. Karmakar, X. Li, A. M.-H. Ho, W. H. Kwok, and P. T. Chui, "Real-time ultrasound-guided paramedian epidural access: evaluation of a novel in-plane technique," *British Journal of Anaesthesia*, vol. 102, no. 6, pp. 845–854, 2009.

[15] H. Willschke, P. Marhofer, A. Basenberg et al., "Epidural catheter placement in children: comparing a novel approach using ultrasound guidance and a standard loss-of-resistance technique," *British Journal of Anaesthesia*, vol. 97, no. 2, pp. 200–207, 2006.

[16] H. Jee, J. H. Lee, J. Kim, K. D. Park, W. Y. Lee, and Y. Park, "Ultrasound-guided selective nerve root block versus fluoroscopy-guided transforaminal block for the treatment of radicular pain in the lower cervical spine: a randomized, blinded, controlled study," *Skeletal Radiology*, vol. 42, no. 1, pp. 69–78, 2012.

[17] S. N. Narouze, A. Vydyanathan, L. Kapural, D. I. Sessler, and N. Mekhail, "Ultrasound-guided cervical selective nerve root block A fluoroscopy-controlled feasibility study," *Regional Anesthesia and Pain Medicine*, vol. 34, no. 4, pp. 343–348, 2009.

[18] M. Gofeld, S. J. Bristow, S. C. Chiu, C. K. McQueen, and L. Bollag, "Ultrasound-guided lumbar transforaminal injections: feasibility and validation study," *Spine*, vol. 37, no. 9, pp. 808–812, 2012.

[19] D. H. Ha, D. M. Shim, T. K. Kim, Y. M. Kim, and S. S. Choi, "Comparison of ultrasonography- and fluoroscopy-guided facet joint block in the lumbar spine," *Asian Spine Journal*, vol. 4, pp. 15–22, 2010.

[20] H. Jung, S. Jeon, S. Ahn, M. Kim, and Y. Choi, "The validation of ultrasound-guided lumbar facet nerve blocks as confirmed by fluoroscopy," *Asian Spine Journal*, vol. 6, pp. 163–167, 2012.

[21] I. Khayata, J. Lance Lichtor, and P. Amelin, "Ultrasound-guided epidural blood patch," *Anesthesiology*, vol. 114, no. 6, Article ID 1453, 2011.

[22] S. R. Clendenen, S. Pirris, C. B. Robards, B. Leone, and E. W. Nottmeier, "Symptomatic postlaminectomy cerebrospinal fluid leak treated with 4-dimensional ultrasound-guided epidural blood patch," *Journal of Neurosurgical Anesthesiology*, vol. 24, pp. 222–225, 2012.

[23] D. J. Berkoff, L. E. Miller, and J. E. Block, "Clinical utility of ultrasound guidance for intra-articular knee injections: a review," *Clinical Interventions in Aging*, vol. 7, pp. 89–95, 2012.

[24] C. A. Gilliland, L. D. Salazar, and J. R. Borchers, "Ultrasound versus anatomic guidance for intra-articular and peri-articular injection: a systematic review," *The Physician and Sportsmedicine*, vol. 39, no. 3, pp. 121–131, 2011.

[25] P. W. H. Peng and P. S. Tumber, "Ultrasound-guided interventional procedures for patients with chronic pelvic pain: a description of techniques and review of literature," *Pain Physician*, vol. 11, no. 2, pp. 215–224, 2008.

[26] A. Kumar and A. Chuan, "Ultrasound guided vascular access: efficacy and safety," *Best Practice and Research*, vol. 23, no. 3, pp. 299–311, 2009.

[27] M. Lamperti, A. R. Bodenham, M. Pittiruti et al., "International evidence-based recommendations on ultrasound-guided vascular access," *Intensive Care Medicine*, vol. 38, pp. 1105–1117, 2012.

[28] A. Vezzani, C. Brusasco, S. Palermo, C. Launo, M. Mergoni, and F. Corradi, "Ultrasound localization of central vein catheter and detection of postprocedural pneumothorax: an alternative to chest radiography," *Critical Care Medicine*, vol. 38, no. 2, pp. 533–538, 2010.

[29] D. Castillo, D. S. McEwen, L. Young, and J. Kirkpatrick, "Micropuncture needles combined with ultrasound guidance for unusual central venous cannulation: desperate times call for desperate measures: a new trick for old anesthesiologists," *Anesthesia and Analgesia*, vol. 114, no. 3, pp. 634–637, 2012.

[30] K. Sofi and S. Arab, "Ultrasound-guided central venous catheterization in prone position," *Saudi Journal of Anaesthesia*, vol. 4, pp. 28–30, 2010.

[31] T. J. Wigmore, J. F. Smythe, M. B. Hacking, R. Raobaikady, and N. S. MacCallum, "Effect of the implementation of NICE guidelines for ultrasound guidance on the complication rates associated with central venous catheter placement in patients presenting for routine surgery in a tertiary referral centre," *British Journal of Anaesthesia*, vol. 99, no. 5, pp. 662–665, 2007.

[32] J. L. H. French, N. J. Raine-Fenning, J. G. Hardman, and N. M. Bedforth, "Pitfalls of ultrasound guided vascular access: the use of three/four-dimensional ultrasound," *Anaesthesia*, vol. 63, no. 8, pp. 806–813, 2008.

[33] E. Oakley and A.-M. Wong, "Ultrasound-assisted peripheral vascular access in a paediatric ED: paediatric emergency medicine," *Emergency Medicine Australasia*, vol. 22, no. 2, pp. 166–170, 2010.

[34] G. J. Latham, M. L. Veneracion, D. C. Joffe, A. T. Bosenberg, S. H. Flack, and D. K. Low, "High-frequency micro-ultrasound for vascular access in young children: a feasibility study by the High-frequency UltraSound in Kids studY (HUSKY) group," *Paediatric Anaesthesia*, vol. 23, no. 6, pp. 529–535, 2013.

[35] M. Singh, K. J. Chin, V. W. S. Chan, D. T. Wong, G. A. Prasad, and E. Yu, "Use of sonography for airway assessment: an observational study," *Journal of Ultrasound in Medicine*, vol. 29, no. 1, pp. 79–85, 2010.

[36] J. S. Green and B. C. H. Tsui, "Applications of ultrasonography in ENT: airway assessment and nerve blockade," *Anesthesiology Clinics*, vol. 28, no. 3, pp. 541–553, 2010.

[37] A. Prasad, E. Yu, D. T. Wong, R. Karkhanis, P. Gullane, and V. W. S. Chan, "Comparison of sonography and computed tomography as imaging tools for assessment of airway structures," *Journal of Ultrasound in Medicine*, vol. 30, no. 7, pp. 965–972, 2011.

[38] S. Adhikari, W. Zeger, C. Schmier et al., "Pilot study to determine the utility of point-of-care ultrasound in the assessment of difficult laryngoscopy," *Academic Emergency Medicine*, vol. 18, no. 7, pp. 754–758, 2011.

[39] R. Komatsu, P. Sengupta, A. Wadhwa et al., "Ultrasound quantification of anterior soft tissue thickness fails to predict difficult laryngoscopy in obese patients," *Anaesthesia and Intensive Care*, vol. 35, no. 1, pp. 32–37, 2007.

[40] P. Rudraraju and L. A. Eisen, "Confirmation of endotracheal tube position: a narrative review," *Journal of Intensive Care Medicine*, vol. 24, no. 5, pp. 283–292, 2009.

[41] B. Marciniak, P. Fayoux, A. Hébrard, R. Krivosic-Horber, T. Engelhardt, and B. Bissonnette, "Airway management in children: ultrasonography assessment of tracheal intubation in real time?" *Anesthesia and Analgesia*, vol. 108, no. 2, pp. 461–465, 2009.

[42] J. E. Fiadjoe, P. Stricker, H. Gurnaney et al., "Ultrasound-guided tracheal intubation: a novel intubation technique," *Anesthesiology*, vol. 117, pp. 1389–1391, 2012.

[43] T.-Y. Hung, S. Li, P.-S. Chen et al., "Bedside ultrasonography as a safe and effective tool to diagnose acute epiglottitis," *The American Journal of Emergency Medicine*, vol. 29, no. 3, pp. 351.e1–353.e1, 2011.

[44] D. R. Ko, Y. E. Chung, I. Park et al., "Use of bedside sonography for diagnosing acute epiglottitis in the emergency department," *Journal of Ultrasound in Medicine*, vol. 31, no. 1, pp. 19–22, 2012.

[45] Y. Lahav, E. Rosenzweig, Z. Heyman, J. Doljansky, A. Green, and Y. Dagan, "Tongue base ultrasound: a diagnostic tool for predicting obstructive sleep apnea," *Annals of Otology, Rhinology and Laryngology*, vol. 118, no. 3, pp. 179–184, 2009.

[46] K.-H. Liu, W. C. W. Chu, K.-W. To et al., "Sonographic measurement of lateral parapharyngeal wall thickness in patients with obstructive sleep apnea," *Sleep*, vol. 30, no. 11, pp. 1503–1508, 2007.

[47] A. Šustić, "Role of ultrasound in the airway management of critically ill patients," *Critical Care Medicine*, vol. 35, no. 5, pp. S173–S177, 2007.

[48] J. B. Brodsky, A. Macario, and J. B. D. Mark, "Tracheal diameter predicts double-lumen tube size: a method for selecting left double-lumen tubes," *Anesthesia and Analgesia*, vol. 82, no. 4, pp. 861–864, 1996.

[49] J. B. Brodsky, K. Malott, M. Angst, B. G. Fitzmaurice, S. P. Kee, and L. Logan, "The relationship between tracheal width and left bronchial width: implications for left-sided double-lumen tube selection," *Journal of Cardiothoracic and Vascular Anesthesia*, vol. 15, no. 2, pp. 216–217, 2001.

[50] B. Kaur, R. Tang, A. Sawka, C. Krebs, and H. Vaghadia, "A method for ultrasonographic visualization and injection of the superior laryngeal nerve: volunteer study and cadaver simulation," *Anesthesia and Analgesia*, vol. 115, no. 5, pp. 1242–1245, 2012.

[51] A. Hatfield and A. Bodenham, "Portable ultrasonic scanning of the anterior neck before percutaneous dilatational tracheostomy," *Anaesthesia*, vol. 54, no. 7, pp. 660–663, 1999.

[52] V. Rajajee, J. J. Fletcher, L. R. Rochlen, and T. L. Jacobs, "Real-time ultrasound-guided percutaneous dilatational tracheostomy: a feasibility study," *Critical Care*, vol. 15, no. 1, article R67, 2011.

[53] L.-W. Ding, H.-C. Wang, H.-D. Wu, C.-J. Chang, and P.-C. Yang, "Laryngeal ultrasound: a useful method in predicting post-extubation stridor: a pilot study," *European Respiratory Journal*, vol. 27, no. 2, pp. 384–389, 2006.

[54] J.-R. Jiang, T.-H. Tsai, J.-S. Jerng, C.-J. Yu, H.-D. Wu, and P.-C. Yang, "Ultrasonographic evaluation of liver/spleen movements and extubation outcome," *Chest*, vol. 126, no. 1, pp. 179–185, 2004.

[55] A. Vats, G. A. Worley, R. De Bruyn, H. Porter, D. M. Albert, and C. M. Bailey, "Laryngeal ultrasound to assess vocal fold paralysis in children," *Journal of Laryngology and Otology*, vol. 118, no. 6, pp. 429–431, 2004.

[56] G. A. Shaath, A. Jijeh, A. Alkurdi, S. Ismail, M. Elbarbary, and M. S. Kabbani, "Ultrasonography assessment of vocal cords mobility in children after cardiac surgery," *Journal of the Saudi Heart Association*, vol. 24, pp. 187–190, 2012.

[57] P. Kundra, K. Kumar, V. Allampalli, R. Anathkrishnan, S. Gopalakrishnan, and S. Elangovan, "Use of ultrasound to assess superior and recurrent laryngeal nerve function immediately after thyroid surgery," *Anaesthesia*, vol. 67, no. 3, pp. 301–302, 2012.

[58] D. A. Lichtenstein and G. A. Mezière, "Relevance of lung ultrasound in the diagnosis of acute respiratory failure: the BLUE protocol," *Chest*, vol. 134, no. 1, pp. 117–125, 2008.

[59] G. Volpicelli, M. Elbarbary, M. Blaivas et al., "International evidence-based recommendations for point-of-care lung ultrasound," *Intensive Care Medicine*, vol. 38, pp. 577–591, 2012.

[60] D. A. Lichtenstein, N. Lascols, S. Prin, and G. Mezière, "The "lung pulse": an early ultrasound sign of complete atelectasis," *Intensive Care Medicine*, vol. 29, no. 12, pp. 2187–2192, 2003.

[61] R. Copetti, G. Soldati, and P. Copetti, "Chest sonography: a useful tool to differentiate acute cardiogenic pulmonary edema from acute respiratory distress syndrome," *Cardiovascular Ultrasound*, vol. 6, article 16, 2008.

[62] G. Volpicelli, L. A. Melniker, L. Cardinale, A. Lamorte, and M. F. Frascisco, "Lung ultrasound in diagnosing and monitoring pulmonary interstitial fluid," *La Radiologia Medica*, vol. 118, no. 2, pp. 196–205, 2012.

[63] G. Mathis, W. Blank, A. Reissig et al., "Thoracic ultrasound for diagnosing pulmonary embolism: a prospective multicenter study of 352 patients," *Chest*, vol. 128, no. 3, pp. 1531–1538, 2005.

[64] C. B. Laursen, J. R. Davidsen, and P. H. Madsen, "Utility of lung ultrasound in near-drowning victims," *BMJ Case Reports*, vol. 2012, 2012.

[65] R. Copetti, L. Cattarossi, F. Macagno, M. Violino, and R. Furlan, "Lung ultrasound in respiratory distress syndrome: a useful tool for early diagnosis," *Neonatology*, vol. 94, no. 1, pp. 52–59, 2008.

[66] T. Luecke, F. Corradi, and P. Pelosi, "Lung imaging for titration of mechanical ventilation," *Current Opinion in Anaesthesiology*, vol. 25, no. 2, pp. 131–140, 2012.

[67] N. Xirouchaki, E. Magkanas, K. Vaporidi et al., "Lung ultrasound in critically ill patients: comparison with bedside chest radiography," *Intensive Care Medicine*, vol. 37, no. 9, pp. 1488–1493, 2011.

[68] R. Moretti and B. Pizzi, "Ultrasonography of the optic nerve in neurocritically ill patients," *Acta Anaesthesiologica Scandinavica*, vol. 55, no. 6, pp. 644–652, 2011.

[69] J. Dubourg, E. Javouhey, T. Geeraerts, M. Messerer, and B. Kassai, "Ultrasonography of optic nerve sheath diameter for detection of raised intracranial pressure: a systematic review and meta-analysis," *Intensive Care Medicine*, vol. 37, no. 7, pp. 1059–1068, 2011.

[70] T. Soldatos, D. Karakitsos, K. Chatzimichail, M. Papathanasiou, A. Gouliamos, and A. Karabinis, "Optic nerve sonography in the diagnostic evaluation of adult brain injury," *Critical Care*, vol. 12, no. 3, article R67, 2008.

[71] C. Dubost, A. Le Gouez, V. Jouffroy et al., "Optic nerve sheath diameter used as ultrasonographic assessment of the incidence of raised intracranial pressure in preeclampsia: a pilot study," *Anesthesiology*, vol. 116, pp. 1066–1071, 2012.

[72] M. Rollins and P. Flood, "Imaging intracranial pressure: an introduction to ultrasonography of the optic nerve sheath," *Anesthesiology*, vol. 116, pp. 983–984, 2012.

[73] C. Dubost, A. Le Gouez, P. J. Zetlaoui, D. Benhamou, F. J. Mercier, and T. Geeraerts, "Increase in optic nerve sheath diameter induced by epidural blood patch: a preliminary report," *British Journal of Anaesthesia*, vol. 107, no. 4, pp. 627–630, 2011.

[74] L. Chiao, S. Sharipov, A. E. Sargsyan et al., "Ocular examination for trauma; clinical ultrasound aboard the International Space Station," *Journal of Trauma*, vol. 58, no. 5, pp. 885–889, 2005.

[75] A. E. Sargsyan, D. R. Hamilton, S. L. Melton, D. Amponsah, N. E. Marshall, and S. A. Dulchavsky, "Ultrasonic evaluation of pupillary light reflex," *Critical Ultrasound Journal*, vol. 1, no. 2, pp. 53–57, 2009.

[76] M. Nedelmann, E. Stolz, T. Gerriets et al., "Consensus recommendations for transcranial color-coded duplex sonography for the assessment of intracranial arteries in clinical trials on acute stroke," *Stroke*, vol. 40, no. 10, pp. 3238–3244, 2009.

[77] F. A. Rasulo, E. De Peri, and A. Lavinio, "Transcranial Doppler ultrasonography in intensive care," *European Journal of Anaesthesiology*, vol. 25, no. 42, pp. 167–173, 2008.

[78] E. Bor-Seng-Shu, R. Hirsch, M. J. Teixeira, A. F. De Andrade, and R. Marino Jr., "Cerebral hemodynamic changes gauged by transcranial Doppler ultrasonography in patients with post-traumatic brain swelling treated by surgical decompression," *Journal of Neurosurgery*, vol. 104, no. 1, pp. 93–100, 2006.

[79] M. A. Topcuoglu, "Transcranial Doppler ultrasound in neurovascular diseases: diagnostic and therapeutic aspects," *Journal of Neurochemistry*, vol. 123, supplement 2, pp. 39–51, 2012.

[80] L. Bouvet, J.-X. Mazoit, D. Chassard, B. Allaouchiche, E. Boselli, and D. Benhamou, "Clinical assessment of the ultrasonographic measurement of antral area for estimating preoperative gastric content and volume," *Anesthesiology*, vol. 114, no. 5, pp. 1086–1092, 2011.

[81] A. Perlas, L. Davis, M. Khan, N. Mitsakakis, and V. W. S. Chan, "Gastric sonography in the fasted surgical patient: a prospective descriptive study," *Anesthesia and Analgesia*, vol. 113, no. 1, pp. 93–97, 2011.

[82] A. Perlas, N. Mitsakakis, L. Liu et al., "Validation of a mathematical model for ultrasound assessment of gastric volume by gastroscopic examination," *Anesthesia and Analgesia*, vol. 116, pp. 357–363, 2013.

[83] C. Arzola, J. C. Carvalho, J. Cubillos, X. Y. Ye, and A. Perlas, "Anesthesiologists' learning curves for bedside qualitative ultrasound assessment of gastric content: a cohort study," *Canadian Journal of Anaesthesia*, vol. 60, no. 8, pp. 771–779, 2013.

[84] C. Vigneau, J.-L. Baudel, B. Guidet, G. Offenstadt, and E. Maury, "Sonography as an alternative to radiography for nasogastric feeding tube location," *Intensive Care Medicine*, vol. 31, no. 11, pp. 1570–1572, 2005.

[85] M. B. Jensen, E. Sloth, K. M. Larsen, and M. B. Schmidt, "Transthoracic echocardiography for cardiopulmonary monitoring in intensive care," *European Journal of Anaesthesiology*, vol. 21, no. 9, pp. 700–707, 2004.

[86] D. J. Canty, C. F. Royse, D. Kilpatrick, L. Bowman, and A. G. Royse, "The impact of focused transthoracic echocardiography in the pre-operative clinic," *Anaesthesia*, vol. 67, pp. 618–625, 2012.

[87] D. J. Canty, C. F. Royse, D. Kilpatrick, D. L. Williams, and A. G. Royse, "The impact of pre-operative focused transthoracic echocardiography in emergency non-cardiac surgery patients

with known or risk of cardiac disease," *Anaesthesia*, vol. 67, pp. 714–720, 2012.

[88] A. Dennis and A. Stenson, "Echo rounds: the use of transthoracic echocardiography in postpartum hypotension," *Anesthesia and Analgesia*, vol. 115, pp. 1033–1037, 2012.

[89] A. T. Dennis, "Transthoracic echocardiography in obstetric anaesthesia and obstetric critical illness," *International Journal of Obstetric Anesthesia*, vol. 20, no. 2, pp. 160–168, 2011.

[90] B. Cowie, "Three years' experience of focused cardiovascular ultrasound in the peri-operative period," *Anaesthesia*, vol. 66, no. 4, pp. 268–273, 2011.

[91] J. Neelankavil, K. Howard-Quijano, T. C. Hsieh et al., "Transthoracic echocardiography simulation is an efficient method to train anesthesiologists in basic transthoracic echocardiography skills," *Anesthesia and Analgesia*, vol. 115, pp. 1042–1051, 2012.

[92] R. C. Tanzola, S. Walsh, W. M. Hopman, D. Sydor, R. Arellano, and R. V. Allard, "Brief report: focused transthoracic echocardiography training in a cohort of Canadian anesthesiology residents: a pilot study," *Canadian Journal of Anesthesia*, vol. 60, pp. 32–37, 2013.

[93] M. F. Newman, J. P. Mathew, and S. Aronson, "The evolution of anesthesiology and perioperative medicine," *Anesthesiology*, vol. 118, pp. 1005–1007, 2013.

[94] P. N. T. Wells, H.-D. Liang, and T. P. Young, "Ultrasonic imaging technologies in perspective," *Journal of Medical Engineering and Technology*, vol. 35, no. 6-7, pp. 289–299, 2011.

[95] R. T. O'Brien and S. P. Holmes, "Recent advances in ultrasound technology," *Clinical Techniques in Small Animal Practice*, vol. 22, no. 3, pp. 93–103, 2007.

[96] O. Choquet and X. Capdevila, "Case report: three-dimensional high-resolution ultrasound-guided nerve blocks: a new panoramic vision of local anesthetic spread and perineural catheter tip location," *Anesthesia and Analgesia*, vol. 116, pp. 1176–1181, 2013.

[97] C. L. Jeng, T. M. Torrillo, M. R. Anderson, R. S. Morrison, K. H. Todd, and M. A. Rosenblatt, "Development of a mobile ultrasound-guided peripheral nerve block and catheter service," *Journal of Ultrasound in Medicine*, vol. 30, no. 8, pp. 1139–1144, 2011.

[98] B. Kaur, H. Vaghadia, R. Tang, and A. Sawka, "Real-time thoracic paravertebral block using an ultrasound-guided positioning system," *British Journal of Anaesthesia*, vol. 110, pp. 852–853, 2013.

[99] S. W. Wong, A. U. Niazi, K. J. Chin, and V. W. Chan, "Real-time ultrasound-guided spinal anesthesia using the SonixGPS(R) needle tracking system: a case report," *Canadian Journal of Anesthesia*, vol. 60, pp. 50–53, 2013.

Hindawi Publishing Corporation
The Scientific World Journal
Volume 2013, Article ID 519080, 11 pages
http://dx.doi.org/10.1155/2013/519080

Research Article

Nexfin Noninvasive Continuous Hemodynamic Monitoring: Validation against Continuous Pulse Contour and Intermittent Transpulmonary Thermodilution Derived Cardiac Output in Critically Ill Patients

Koen Ameloot,[1] Katrijn Van De Vijver,[1] Ole Broch,[2] Niels Van Regenmortel,[1] Inneke De laet,[1] Karen Schoonheydt,[1] Hilde Dits,[1] Berthold Bein,[2] and Manu L. N. G. Malbrain[1]

[1] *Department of Intensive Care Medicine, Ziekenhuis Netwerk Antwerpen, ZNA Stuivenberg, Lange Beeldekensstraat 267, 2060 Antwerp, Belgium*
[2] *Department of Anaesthesiology and Intensive Care Medicine, University Hospital Schleswig-Holstein, Campus Kiel, Schwanenweg 21, 24105 Kiel, Germany*

Correspondence should be addressed to Manu L. N. G. Malbrain; manu.malbrain@skynet.be

Received 13 July 2013; Accepted 15 September 2013

Academic Editors: L. M. Gillman, D. Karakitsos, A. E. Papalois, and A. Shiloh

Introduction. Nexfin (Bmeye, Amsterdam, Netherlands) is a noninvasive cardiac output (CO) monitor based on finger arterial pulse contour analysis. The aim of this study was to validate Nexfin CO (NexCO) against thermodilution (TDCO) and pulse contour CO (CCO) by PiCCO (Pulsion Medical Systems, Munich, Germany). *Patients and Methods*. In a mix of critically ill patients (n = 45), NexCO and CCO were measured continuously and recorded at 2-hour intervals during the 8-hour study period. TDCO was measured at 0–4–8 hrs. *Results*. NexCO showed a moderate to good (significant) correlation with TDCO (R^2 0.68, $P < 0.001$) and CCO (R^2 0.71, $P < 0.001$). Bland and Altman analysis comparing NexCO with TDCO revealed a bias (± limits of agreement, LA) of 0.4 ± 2.32 L/min (with 36% error) while analysis comparing NexCO with CCO showed a bias (±LA) of 0.2 ± 2.32 L/min (37% error). NexCO is able to follow changes in TDCO and CCO during the same time interval (level of concordance 89.3% and 81%). Finally, polar plot analysis showed that trending capabilities were acceptable when changes in NexCO (ΔNexCO) were compared to ΔTDCO and ΔCCO (resp., 89% and 88.9% of changes were within the level of 10% limits of agreement). *Conclusion*. we found a moderate to good correlation between CO measurements obtained with Nexfin and PiCCO.

1. Introduction

The true value of continuous hemodynamic monitoring in critically ill patients becomes clear in the light of beat-to-beat changing hemodynamics due to either continuously improving or deteriorating cardiac and disease status [1, 2]. Therefore, the critically ill patient must be resuscitated to a continuously changing optimal left ventricular end-diastolic volume. This should be titrated together with an accurate dose of vasopressor agents and inotropes to optimize circulation and restore end-organ perfusion without causing harm due to excessive fluids [3]. Also, for further decision making, we often want to measure in real-time the hemodynamic effects of ongoing therapeutic interventions. The PiCCO system (PiCCO2, Pulsion Medical Systems, Munich, Germany) uses a dedicated PiCCO thermistor-tipped arterial catheter to analyze the patient's heart rate and arterial pressure waveform continuously [4]. Due to the unique properties of each patient's arterial tree, initial calibration of the monitoring system using transpulmonary thermodilution CO measurement (TDCO) improves accuracy of the beat-to-beat cardiac output (CO) obtained by pulse contour analysis (CCO) [5]. The PiCCO device has been validated in numerous studies including burns, medical, and surgical critically ill

patients [6–12]. However, PiCCO remains a relative invasive technique that requires both an arterial and a central venous catheter and therefore increases the risk of iatrogenic complications such as pneumothorax, bleeding, catheter sepsis, and deep venous thrombosis [13–15]. Moreover, the need for calibration by transpulmonary thermodilution may delay the initial measurement and is time consuming, and the system is cost intensive and cannot be used prehospital or in a regular ward. The Nexfin (BMEYE, Amsterdam, The Netherlands) device is a totally noninvasive continuous blood pressure and CO (NexCO) monitor based on finger arterial pressure pulse contour analysis. Potential advantages include its noninvasiveness and ease of use. Questions rose on the accuracy of Nexfin measurements in critically ill patients, as there is no initial calibration of the monitoring system to adjust for the unique mechanical properties of each patient's arterial tree. Moreover, there are concerns about the reliability of continuous noninvasive finger blood pressure derived pulse contour analysis in patients with reduced perfusion of the hand due to high systemic vascular resistance (SVR) or hypothermia. We performed an open observational study in a mix of medical/surgical and burns critically ill patients to validate Nexfin against both TDCO and CCO obtained by PiCCO.

2. Methods

2.1. Study Population. We prospectively studied 47 critically ill patients admitted to the intensive care units of our hospital. Inclusion criteria were hemodynamic instability with need for continuous hemodynamic monitoring and the presence of a central venous (jugular or subclavian) catheter and a PiCCO femoral arterial catheter already in place before inclusion in the study.

2.2. Nexfin Technique. The Nexfin (BMEYE, Amsterdam, The Netherlands) method is based on the measurement of finger arterial pressure by an inflatable cuff around the middle phalange of the finger. The pulsating finger artery is clamped to a constant volume by applying a varying counter pressure equivalent to the arterial pressure using a built-in photoelectric plethysmograph and an automatic algorithm (Physiocal). The resulting finger arterial pressure waveform is reconstructed into a brachial artery pressure waveform by a generalized algorithm. NexCO is calculated by a pulse contour method (CO-TREK) using the measured systolic pressure time integral and the heart's afterload determined from the Windkessel model [16].

2.3. Measurements. In an 8-hour period, simultaneous CCO and NexCO measurements were obtained every 2 hours (0–2–4–6–8 hrs, in total 225 paired measurements) while simultaneous TDCO and NexCO were obtained every 4 hours (0–4–8 hrs, in total 135 paired measurements). The CCO and NexCO values were recorded simultaneously by hand 5 min before TDCO was determined by 3 repeated injections of 20 mL of sterile ice-cold saline via the central venous line. Blood pressure measurements were recorded continuously by Nexfin and PiCCO and were by each device used to calculate the continuous CO. Subanalysis was performed for patients with a low MAP (defined as MAP $\leq$ 70 mmHg), low and high TDCO (defined as $\leq$ 4 L/min and $\geq$ 8 L/min), low and high SVRI (defined as an SVRI obtained by PiCCO $\leq$ 1700 dyne·s·cm^{-5}/m^2 and $\geq$ 3000 dyne·s·cm-5/m^2), and patients on high dose norepinephrine ($\geq$0.3 μg/kg/min) and hypothermia (T°C $\leq$ 35°C). To assess the ease of use, we measured the time to initial measurement, the number of repositions needed in the 8-hours observation period and also the nurses filled in a questionnaire (see addendum) (n = 27 patients).

2.4. Data Analysis and Statistics. Results are presented as mean (±SD) unless otherwise stated. Mean values were compared using student's t-test. Paired CO measurements by 2 different methods were compared statistically using 4 different methods. First, we used Pearson correlation and linear regression analysis. Two methods are considered equal if the line of identity crosses the origin of x and y-axis and if R^2 (R = Pearson's correlation coefficient) is > 0.6. Second, we calculated bias, precision and limits of agreement (Bland-Altman analysis [17, 18]), and the percentage error (PE, defined as two times SD of the bias over the mean TDCO or CCO) as described by L. A. H. Critchley and J. A. J. H. Critchley [19]. If the differences within bias ±1.96 SD (limits of agreement, LA) are not clinically important, if the precision of the new technique is comparable to the reference technique and if the percentage error is less than 30%, the two methods may be used interchangeably [20]. Third, the ability of NexCO to track changes or trends in TDCO or CCO was assessed by plotting ΔTDCO or ΔCCO against ΔNexCO during the same time interval (four quadrants trend plot). The concordance is calculated as the percentage of pairs with the same direction of change. Based on previous reports, the concordance should be > 90% when pairs with both a ΔTDCO or ΔCCO and ΔNexCO $\leq$ ±1 L/min (or less than 15% of change) are excluded for analysis [21]. Finally trending capability of the NexCO compared to TDCO and CCO was assessed by polar plots as suggested by Critchley et al. [22]. Concordance analysis looking at direction of changes is a very simple but crude measure of how well 2 measurements trend. Important aspects of the measurement, such as the magnitude of the underlying CO change (ΔCO) and the degree of agreement, are totally ignored. Therefore, Critchley et al. suggested converting the x-y values to polar coordinates, where agreement is shown by the angle the vector makes with the line of identity ($y = x$) and magnitude of change by the length of the vector [22]. Thus, statistical measures that fully represent the magnitude of ΔCO and its degree of agreement are retained. From these data, a new polar plot that shows agreement as the angle $\boldsymbol{\theta}$ (angle made by ΔCO vector with the line of identity [$y = x$]) against the change in CO as the radian (distance of data point from center of polar plot) can be drawn. Conversion of the Cartesian data with regard to change in cardiac output (ΔCO) into a (x, y) polar coordinate format was performed using an Excel spreadsheet (Microsoft Office Excel 2007; Microsoft Corp.),

Table 1: Patient characteristics.

	Mean ± SD	n = 45 (100%)
Demographics		
Age (yrs)	57.6 ± 19.4	
Male		32 (71%)
Reason of admission		
Medical		27 (60%)
Surgical		9 (20%)
Trauma		5 (11%)
Burns		4 (9%)
Shock		31 (69%)
Septic		18 (58%)
Cardiogenic		6 (19%)
Other		7 (23%)
ICU scores		
APACHE II	25.3 ± 10.3	
SOFA	9.4 ± 3.3	
SAPS II	51.5 ± 16.9	

APACHE II: acute physiology and chronic health evaluation.
SAPS II: simplified acute physiology score.
SOFA: sequential organ failure assessment.

with the formulas for calculation of absolute value of mean ΔCO, quadrant, radians, and angle as suggested by Critchley et al. [22].

2.5. Ethics. The study was conducted in accordance with the ICU protocol, the declaration of Helsinki, and applicable regulatory requirements as approved by the institutional review board and the local institutional ethics committee (approval number 3789). In view of the nature of the study being purely observational, not demanding a deviation from standard clinical ICU care and since the results obtained by Nexfin were not used for clinical decision making, informed consent from the patient or the next of kin was not deemed essential. We merely analysed the existing situation and did nothing to influence events. Only treating ICU physicians accessed the medical records. All data were pseudonymized before analysis.

3. Results

3.1. Study Population. In 2 patients (4.3%) it was impossible to obtain Nexfin values from any of 10 fingers, and they were therefore excluded from final analysis. Baseline characteristics of the 45 remaining patients are summarized in Table 1. Thirty-one patients (69%) were in shock (reflected by an elevated arterial lactate) with the majority in septic shock (n = 18, 58%). Only a minority was in cardiogenic shock (n = 6, 19%). A total of 35 patients (78%) received norepinephrine at a mean (±SD) dose of 0.20 ± 0.17 (range 0.02–1) μg/kg/min, while 27 patients (60%) received dobutamine at a dose of 4.30 ± 2.10 (range 1–10) μg/kg/min (range 1–10). Forty-tree patients (96%) were mechanically ventilated, and the 2 remaining patients were noninvasively ventilated. The critical illness of the patient sample is reflected by high scores on 3 different ICU scoring systems (APACHE II, SOFA, and SAPS II). In-hospital mortality was 57.8%. The neurological, respiratory and hemodynamic parameters, and the dose of the infused drugs did not show significant changes during the entire study period (Table 2).

3.2. Cardiac Output. Mean NexCO was comparable to mean TDCO (6.1 ± 2.3 versus 6.6 ± 2.2 L/min, P = 0.10) and to mean CCO (6.1 ± 2.3 versus 6.4 ± 2.3 L/min, P = 0.30). Correlation, regression, and the Bland and Altman analysis are shown in Tables 3 and 4 and Figures 1 and 2. Pearson correlation coefficients comparing NexCO with TDCO (R^2 0.68) and NexCO with CCO (R^2 0.71) were comparable and showed a highly significant (both P values <0.001) correlation between all obtained CO measurements. Bland and Altman analysis comparing NexCO with TDCO revealed a mean bias ±LA of 0.4 ± 2.32 L/min (with 36% error) while analysis comparing NexCO with CCO showed a bias (±LA) of 0.2 ± 2.32 L/min (37% error). TDCO was highly correlated with CCO (R^2 0.95, P < 0.001) with a bias (±LA) of 0.2 ± 0.86 L/min (13.3% error).

Subanalysis for patients with a low MAP, high TDCO, low SVRI, and high dose norepinephrine consistently showed a very good correlation between NexCO and TDCO or CCO. NexCO was less reliable in patients with hypothermia and not reliable in patients with low TDCO and high SVRI (Tables 3 and 4).

The four quadrants concordance plots are shown in Figure 3. From the 90 initial paired ΔNexCO/ΔTDCO measurements, 34 pairs was excluded because either ΔNexCO or ΔTDCO was ≤ ±1 L/min (or ≤15% change) or because ΔNexCO or ΔTDCO were equal to zero (panel (a)). The calculated level of concordance was 89.3% (50/56). The absolute amplitude correlation of these changes was clinically sufficient (R^2 0.63, P < 0.001). From the 180 initial paired ΔNexCO/ΔCCO measurements, 75 pairs were excluded because either ΔNexCO or ΔCCO was ≤ ±1 L/min (or ≤15% change) or because ΔNexCO or ΔCCO was equal to zero (panel (b)). The calculated level of concordance was only 81% (85/105). The absolute amplitude correlation of these changes was clinically insufficient but still significant (R^2 0.31, P = 0.006).

The polar trending plots are shown in Figure 4. From the 90 initial data 98.9% of the data points were within the 20% lines and 89% within the 10% lines, suggesting acceptable trending capabilities (Figure 4(a)). From the 180 initial data 98.3% of the data points were within the 20% lines and 88.9% within the 10% lines, suggesting acceptable trending capabilities (Figure 4(b)).

3.3. Ease of Use. Data on ease of use were collected in 27 patients. There were no local signs of disturbed circulation in the middle finger due to the application of the finger cuff. The time between the decision to apply Nexfin and the first measurement was less than 5 minutes in 23/27 patients (85%) and between 5 and 10 minutes in 4/27 patients (15%). In 9/27 patients (33%) we were able to do measurements with the first application, while 13/27 patients (48%) needed 1–5 and 5/27

Table 2: Comparison of several neurological, respiratory, and hemodynamic variables and dose of the used drugs between the start and the end (at 8 hours) of the study period.

	Number (%)	Start	8 hours	*P*-value
Neurological				
Propofol (mg/kg/hr)	35 (71%)	2.3 ± 0.9	2.3 ± 1.0	0.99
Midazolam (mg/kg/hr)	31 (69%)	0.2 ± 0.1	0.2 ± 0.1	0.81
Remifentanil (μg/kg/min)	39 (87%)	0.2 ± 0.1	0.2 ± 0.1	0.80
Cisatracurium (mg/kg/hr)	9 (20%)	0.1 ± 0.1	0.1 ± 0.05	0.77
SAS (1–7)	45 (100%)	1.9 ± 1.1	1.6 ± 1.1	0.28
GCS (3–15)	45 (100%)	4.5 ± 3.1	4.8 ± 3.7	0.67
Respiratory system				
pO2/FIO2	45 (100%)	290 ± 171	274 ± 149	0.64
Minute ventilation (L/min)	45 (100%)	11.3 ± 3.5	11.2 ± 4.0	0.92
pH	45 (100%)	7.3 ± 0.1	7.3 ± 0.1	0.45
EVLWI (mL/kg)	45 (100%)	10.2 ± 3.7	10.3 ± 3.4	0.89
Hemodynamics				
Norepinephrine (μg/kg/min)	35 (78%)	0.2 ± 0.2	0.2 ± 0.2	0.90
Dobutamine (μg/kg/min)	27 (60%)	4.1 ± 1.8	4.5 ± 2.2	0.49
MAP (mmHg)	45 (100%)	79.6 ± 16.9	82.9 ± 21.1	0.41
Heart rate (BPM)	45 (100%)	90.3 ± 25.4	88.0 ± 23.7	0.66
CVP (mmHg)	45 (100%)	10.5 ± 5.3	10.1 ± 3.7	0.65
TDCO (L/min)	45 (100%)	6.2 ± 2.1	6.9 ± 2.2	0.14
GEF (%)	45 (100%)	22.8 ± 8.2	24.2 ± 8.6	0.45
GEDVI (mL/BSA)	45 (100%)	715 ± 192	737 ± 162	0.56
SVRI (dyne·s·cm^{-5}/m^2)	45 (100%)	1868 ± 764	1877 ± 793	0.56
SVV (%)	45 (100%)	15.0 ± 8.8	12.3 ± 7.3	0.12
PPV (%)	45 (100%)	14.6 ± 9.7	12.1 ± 7.9	0.17
Other				
IAP (mmHg)	45 (100%)	7.9 ± 2.9	8.8 ± 3.4	0.15
Body Temperature (°C)	45 (100%)	35.4 ± 1.7	35.5 ± 1.7	0.76

CVP: central venous pressure.
EVLWI: extravascular lung water index.
GCS: Glasgow coma scale.
GEDVI: global end-diastolic volume index.
GEF: global ejection fraction.
IAP: intra-abdominal pressure.
MAP: mean arterial pressure.
PPV: pulse pressure variation.
SAS: sedation and agitation scale.
SVRI: systemic vascular resistance index.
SVV: stroke volume variation.
TDCO: thermodilution cardiac output.

(19%) needed more than 5 repositions. Nurse questionnaires revealed a mean score of 1.4 ± 0.5 for the set-up of the device, 1.7 ± 0.7 for set-up placement, 1.8 ± 0.5 for measurements, and 1.9 ± 0.5 for ease of use (1 = very easy to 4 = very difficult).

4. Discussion

We performed an open observational study in 45 mixed surgical/medical and burns critically ill patients to validate the Nexfin against transpulmonary thermodilution and continuous femoral arterial pulse contour derived CO by the PiCCO. To the best of our knowledge, this is the second Nexfin CO validation study conducted in mainly medical ICU patients, the first being published last year by Monnet and coworkers [23].

First, we found moderate to good CO correlation coefficients with TDCO (R^2 0.68) and CCO (R^2 0.71). The overall calculated PEs were however too high to meet the criteria for general interchangeability as suggested by Critchley et al. [22]. These results are in line with previous Nexfin CO validation studies against TEE and PiCCO during abdominal and cardiac surgery [24, 25] and against PAC in a small sample of 10 postsurgical ICU patients [14]. In 2 studies a PE < 30% was reported [14, 25]. Our PE in critically ill patients was lower than the one reported previously by Monnet et al. who found an unacceptable PE of 51% [23]. Second,

Table 3: Comparison of TDCO versus NexCO including subgroup analysis for patients with low MAP, low and high TDCO, low and high SVRI, and high dose norepinephrine and hypothermia.

		Overall	Low MAP ≤70 mmHg	Low TDCO ≤4 L/min	High TDCO ≥8 L/min	Low SVRI ≤1700 dyne·s·cm^{-5}/m^2	High SVRI ≥3000 dyne·s·cm^{-5}/m^2	Norepinephrine ≥0,3 μg/kg/min	Hypothermia ≤35°C
No. of patients		45	19	9	18	29	6	11	22
No. of paired measurements		135	27	16	32	58	14	27	63
Mean TDCO	L/min	6.6	6.2	3.8	8.2	7.2	4.5	6.7	6.5
R^2		0.67	0.82	0.01	0.67	0.74	0.81	0.89	0.70
P value		<0.001	<0.001	NS	<0.001	<0.001	<0.001	<0.001	<0.001
Bias	L/min	0.4	0.9	−0.4	0.9	0.6	−0.1	0.4	0.1
Precision	L/min	1.2	1.1	1.5	1.1	1.3	1.3	1	1.3
Lower LA	L/min	−1.9	−1.2	−3.2	−1.3	−2	−2.7	−1.5	−2.4
Upper LA	L/min	2.7	3	2.5	3	3.2	2.4	2.3	2.6
Percentage error	%	36	34	78	26	37	57	29	39

TDCO: thermodilution cardiac output.
R^2: Pearson correlation coefficient.
LA: limits of agreement.
MAP: mean arterial pressure.
SVRI: systemic vascular resistance index.

Table 4: Comparison of CCO versus NexCO including subgroup analysis for patients with low MAP, low and high TDCO, low and high SVRI, and high dose norepinephrine or hypothermia.

		Overall	Low MAP ≤70 mmHg	Low TDCO ≤4 L/min	High TDCO ≥8 L/min	Low SVRI ≤1700 dyne·s·cm^{-5}/m^2	High SVRI ≥3000 dyne·s·cm^{-5}/m^2	Norepinephrine ≥0.3 μg/kg/min	Hypothermia ≤35°C
No. of patients		45	19	9	18	29	6	11	22
No. of paired measurements		135	50	27	51	104	22	44	63
Mean TDCO	L/min	6.4	5.9	3.8	7.8	7.0	4.5	6.4	6.3
R^2		0.71	0.87	0.1	0.73	0.81	0.78	0.94	0.67
P value		<0.001	<0.001	NS	<0.001	<0.001	<0.001	<0.001	<0.001
Bias	L/min	0.2	0.4	0.0	0.6	0.4	0.0	0.0	0.0
Precision	L/min	1.2	0.9	1.4	1.1	1.0	1.2	0.5	1.3
Lower LA	L/min	−2.1	−1.4	−2.7	−1.7	−1.6	−2.4	−1.1	−2.7
Upper LA	L/min	2.5	2.2	2.7	2.8	2.3	2.3	1.0	2.6
Percentage error	%	36	30	71	29	29	53	16	42

TDCO: thermodilution cardiac output.
R^2: Pearson correlation coefficient.
LA: limits of agreement.
MAP: mean arterial pressure.
SVRI: systemic vascular resistance index.

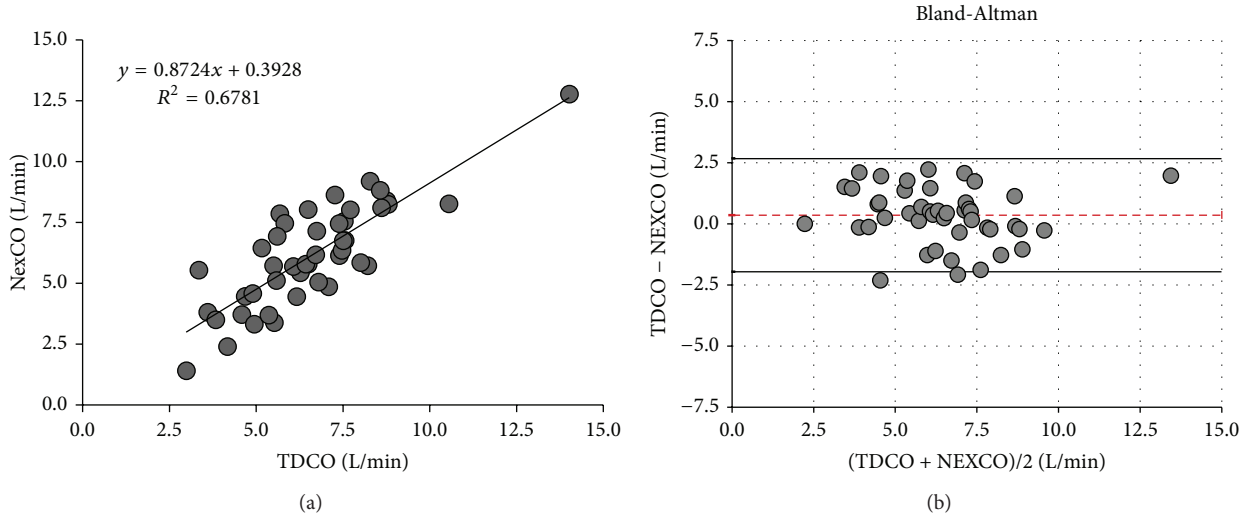

Figure 1: Cardiac output measurements: TDCO versus NexCO. Only one average value per patient is plotted. (a) Regression analysis. (b) Bland-Altman analysis. Patient averages with the mean cardiac output ranges (x-axis) and bias errors (y-axis) during the 8-hour study period. Dotted line indicates bias and solid lines indicate lower and upper limit of agreement. NexCO: Nexfin cardiac output. TDCO: thermodilution cardiac output.

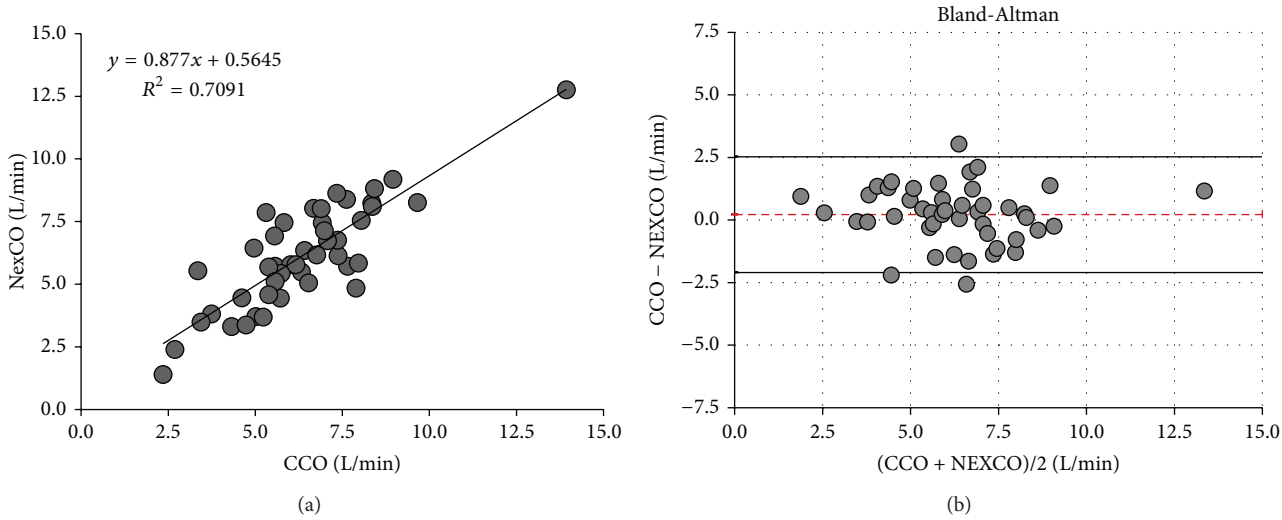

Figure 2: Cardiac output measurements: CCO versus NexCO. Only one average value per patient is plotted. (a) Regression analysis. (b) Bland-Altman analysis. Patient averages with the mean cardiac output ranges (x-axis) and errors (y-axis) during the 8-hour study period. Dotted line indicates bias and solid lines indicate lower and upper limit of agreement. CCO: pulse contour continuous cardiac output NexCO: Nexfin cardiac output.

we found that Nexfin is most accurate in the subgroup of patients with a high CO and low SVRI; however, it was least accurate in patients with low CO and high SVRI. In contrast to other uncalibrated monitoring devices, NexCO keeps comparable reliability in unstable patients with severe hypotension and in patients with reduced vessel compliance due to high dose norepinephrine. In septic patients with the well-known inverse TDCO/SVR hemodynamic profile, with severe hypotension or on high dose norepinephrine the calculated PE was below 30% and all criteria for interchangeability with CCO were met. Since determination of CO was only possible with invasive monitoring in the past, CO is not a target for goal directed therapy guidelines for septic patients [26]. However, since tissue perfusion and oxygen delivery are determined directly by CO and only indirectly by MAP, we strongly believe that with the development and future fine-tuning of noninvasive CO measurement devices like Nexfin, determination of target therapy guidelines for CO should be considered [27]. Third, we found an acceptable concordance (89.3%) between the direction of changes in TDCO and NexCO during the same time interval. This was also shown in previous studies [22, 26]. Although this analysis is based on only 3 time points and 2 values of ΔTDCO/ΔNexCO within an 8-hour time interval, this might be an indication

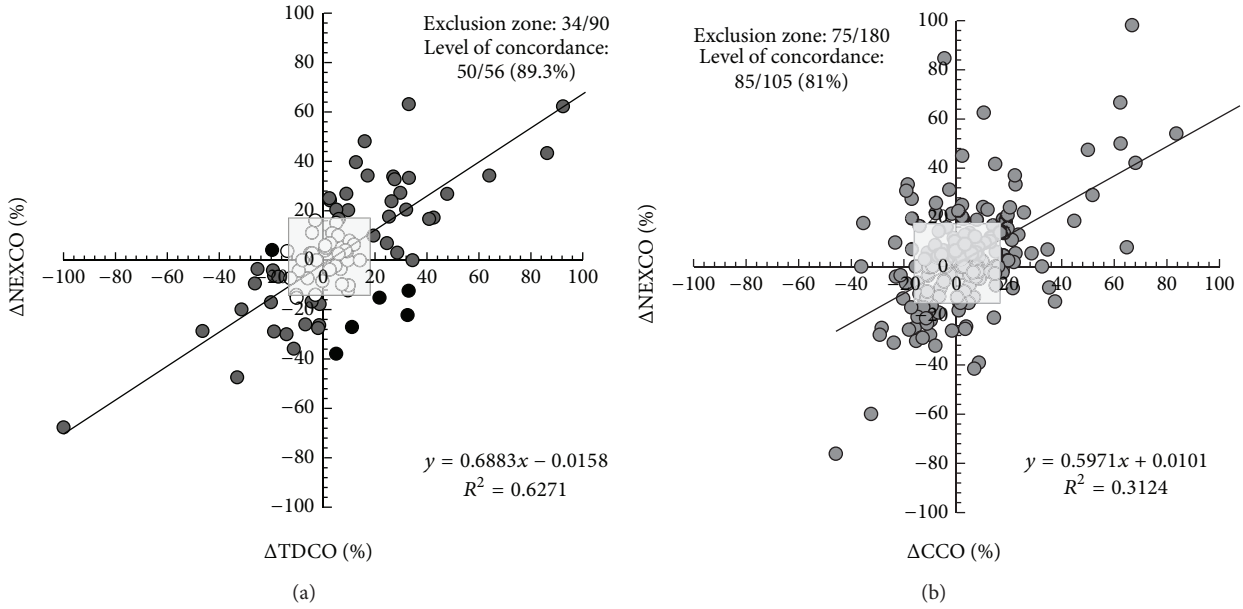

Figure 3: Four quadrants trend plot. (a) Plot for 90 paired measurements of ΔNeXCO and ΔTDCO. From the 90 initial paired measurements, 34 pairs were excluded (exclusion zone is indicated as grey dots within grey-shaded square) because either ΔNexCO or ΔTDCO was ≤ ±15% or because ΔNexCO or ΔTDCO was equal to zero. The calculated level of concordance was 89.3% (50/56) (6 pairs felt within the upper left or lower right quadrant and correspond to poor concordance, black dots). See text for explanation. (b) Plot for 180 paired measurements of ΔNeXCO and ΔCCO. From the 180 initial paired measurements, 75 pairs were excluded (exclusion zone is indicated as grey-shaded square) because either ΔNexCO or ΔCCO was ≤ ±15% change or because ΔNexCO or ΔCCO was equal to zero. The calculated level of concordance was 81% (85/105). See text for explanation.

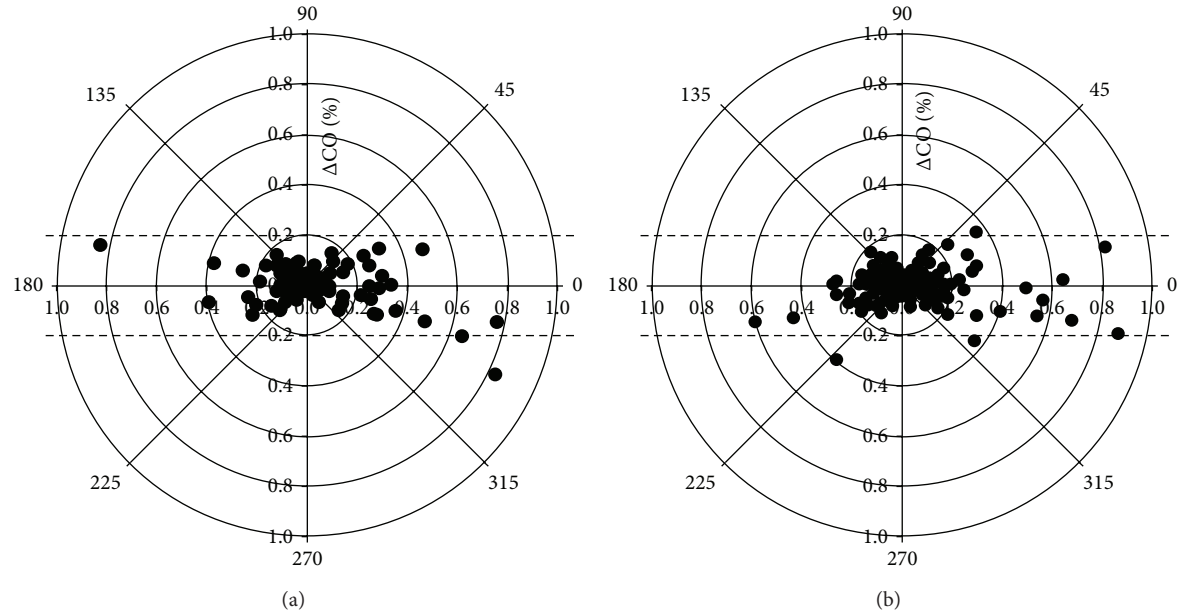

Figure 4: Polar plot. The distance from the center of the plot represents the mean change in cardiac output (ΔCO, expressed as %, with 1,0 referring to 100% change from baseline) and the angle $\boldsymbol{\theta}$ with the horizontal (0-degree radial) axis represents agreement. The less the disagreement between CO measurements, the closer data pairs will lie along the horizontal radial axis. Data with good trending will lie within 10% limits of agreement. However, data with poor trending will be scattered throughout the plot and lie outside the limits of good and acceptable agreement (i.e., 10% and 20%, resp.). See text for explanation. (a) Polar plot for 90 paired measurements of mean ΔCO (%), calculated as absolute value of (ΔNeXCO + ΔTDCO)/2. From the 90 initial data 98.9% of the data points lie within the 20% lines and 89% within the 10% lines, suggesting acceptable trending capabilities. (b) Polar plot for 180 paired measurements of mean ΔCO (%), calculated as absolute value of (ΔNeXCO + ΔCCO)/2. From the 180 initial data 98.3% of the data points lie within the 20% lines and 88.9% within the 10% lines, suggesting acceptable trending capabilities.

that real-time measurement of the hemodynamic effects of ongoing therapeutic interventions may be reliable with the Nexfin device. Since the absolute ΔTDCO/ΔNexCO amplitude did not show sufficient clinical correlation, clinical decision making should be based on hemodynamic trends rather than on absolute values of changes in measured CO. However, ideal concordance should be above 90%, which was not the case when looking at changes in CCO and NexCO during the same time interval (4 values of ΔCCO/ΔNexCO within each 8-hour interval) with a concordance of only 81%. Fourth, analysis with polar plots showed an acceptable trending capability with 89% of the data points lying within the ±1.0 L/min (or ±10%) limits of agreement lines. Our study is the first to use polar plot analysis in this setting. Finally, the short time to first measurement, the limited number of repositions needed to start measuring, and the high scores on the nurse questionnaires illustrate that the device is very easy to use ("plug and play") in the majority of patients. However to play the devil's advocate, one could also state that we were unable to use the device in 2 out of 47 patients (4.3%). Monnet et al. found worse results with the inability to obtain CO values in 15.6% of study patients [23].

Based on these results and review of the literature, we think that the Nexfin device can be applied in ICU or ER patients, potentially also on the regular wards and even out of hospital (if the manufacturer would provide a battery), for an initial quick hemodynamic assessment as a bridge to installation of a more advanced invasive monitoring system. Differentiation of the different types of shock on a clinical basis showed to be a major challenge and often inaccurate even in hands of experienced ICU and ER physicians [18]. Also, Nexfin can be applied when catheter placement is problematic for instance in patients with active catheter infections after removal of the previously infected arterial line.

However, in our opinion there are 5 main reasons why Nexfin cannot always be used as a first choice in the general ICU population with good IV and IA access requiring prolonged advanced hemodynamic monitoring. First, not only is the overall calculated PE too high but we also think that the LA are too broad to be clinically acceptable. If a CO is measured at 8 L/min, the true value can be between 5.7 and 10.3 L/min. Of note; however, is that the obtained correlation coefficients and LA are comparable to previous validation studies with PiCCO against PAC [6–11] and better than results obtained with other noncalibrated, more invasive monitoring devices such as the Vigileo [13, 28], NiCO [13, 29], and PrAM [30]. Also, in a recent meta-analysis, none of the four tested methods achieved satisfactory agreement with bolus thermodilution within the expected 30% PE limits [31]. Therefore, questions are raised on the feasibility of the current validation criteria for uncalibrated CO devices. Second, in our study, Nexfin showed to be less reliable in patients with hypothermia and to be completely unreliable in patients with low TDCO and high SVRI (e.g., cardiogenic, obstructive, and hypovolemic shock). In this subgroup NexCO showed systematic overestimation of CO. This is in line with a previous study conducted in postcardiac surgery ICU patients showing a PE of 50%, mainly driven by inaccuracy in patients with a low CI [32]. This is in contrast however with another study in patients during CABG where half of the patients had a CI < 2.5 L/min/m^2 and good CO correlation coefficients and PE were still found [25]. Third, Nexfin cannot entirely replace (less) invasive monitoring with an arterial line since arterial blood gas analyses and followup of lactate will always be one of the cornerstones of critical care management. Fourth, in some unstable patients and especially those with changing conditions of preload, afterload, or contractility, it may be advisable to calibrate the CO device in relation to the new hemodynamic situation [33]. Finally, we could not obtain any measurements in 4.3% of patients and others found that the Nexfin could not record the arterial curve due to finger hypoperfusion in 15.6% of patients [23].

Some limitations of this study need to be considered. First, this is a validation study of CO by Nexfin against PiCCO. PAC is still considered by some clinicians as a golden standard. Although highly validated and widely used, PiCCO obtained CO shows some error against PAC. Second, the patient sample size and the size of the subgroups are probably too small to allow extensive further subgroup analysis. Third, we did not perform therapeutic intervention to assess the trending capabilities of the Nexfin. Fourth, we need to be aware that these results were obtained in an ICU patient group already receiving a lot of vasopressors and inotropic hemodynamic support thereby possibly not representing the initial hemodynamic pattern. Future studies should be performed to confirm that these results can be extrapolated to ER patients. Finally, the number of patients was determined on a random basis and no power analysis was performed.

5. Conclusions

In conclusion, Nexfin is a totally noninvasive, easy to use blood pressure and CO monitor based on finger arterial blood pressure pulse contour analysis. Nexfin obtained CO showed a moderate to good correlation with CO measured by PiCCO although the PE was too high. The Nexfin can be used for keeping track of changes in CO over time (e.g., to assess the therapeutic effect of a given treatment), although the absolute criteria for full interchangeability were not met in this population of mixed ICU patients.

Key Messages

(i) Nexfin is a totally noninvasive, easy to use blood pressure and cardiac output monitor.

(ii) Nexfin shows a moderate to good cardiac output correlation with transcardiopulmonary thermodilution (TDCO) and continuous pulse contour CO (CCO) obtained by PiCCO in a mixed ICU population although the obtained percentage error was too high to allow full interchangeability.

(iii) Changes in NexCO correlate well with changes in TDCO and CCO although the obtained concordance coefficient was too high to allow full trending interchangeability.

Abbreviations

CCO:	Continuous cardiac output by PiCCO
TDCO:	Thermodilution
NEXCO:	Nexfin obtained cardiac output
CVP:	Central venous pressure
EVLWI:	Extravascular lung water index
GCS:	Glasgow coma scale
GEDVI:	Global end-diastolic volume index
GEF:	Global ejection fraction
IAP:	Intra-abdominal pressure
MAP:	Mean arterial pressure
PPV:	Pulse pressure variation
PE:	Percentage error
SAS:	Sedation and agitation scale
SVRI:	Systemic vascular resistance index
SVV:	Stroke volume variation
SAPS II:	Simplified acute physiology score
SOFA:	Sequential organ failure assessment
APACHE II:	Acute physiology and chronic health evaluation.

Conflict of Interests

Manu Malbrain and Berthold Bein are members of the medical advisory board of Pulsion Medical Systems (Munich, Germany) but have no direct financial relation with the commercial identities mentioned in the paper that might lead to a conflict of interests. The other authors have no competing interests.

Acknowledgments

Part of this paper has been presented previously in abstract and poster form at the 31st International Symposium on Intensive Care and Emergency Medicine (ISICEM) held in Brussels in 2011 [34]. The authors are indebted to Bert Ferdinande, Nelie Desie, and Annelies Gerits for their excellent input and feedback.

References

[1] J. E. Calvin, A. A. Driedger, and W. J. Sibbald, "Does the pulmonary capillary wedge pressure predict left ventricular preload in critically ill patients?" *Critical Care Medicine*, vol. 9, no. 6, pp. 437–443, 1981.

[2] M. Malbrain, P. De Potter, and D. Deeren, "Cost effectiveness of minimally invasive hemodynamic monitoring," in *Yearbook of Intensive Care and Emergency Medicine*, J. L. Vincent, Ed., pp. 603–618, 2005.

[3] F. Michard, "Do we need to know cardiac preload?" in *Yearbook of Intensive Care and Emergency Medicine*, J. L. Vincent, Ed., pp. 694–701, 2004.

[4] A. Oren-Grinberg, "The piCCO monitor," *International Anesthesiology Clinics*, vol. 48, no. 1, pp. 57–85, 2010.

[5] A. Genahr and A. McLuckie, "Transpulmonary thermodilution in the critically ill," *British Journal of Intensive Care*, vol. 14, no. 1, pp. 6–10, 2004.

[6] C. Holm, B. Melcer, F. Hörbrand, G. H. Von Donnersmarck, and W. Mühlbauer, "Arterial thermodilution: an alternative to pulmonary artery catheter for cardiac output assessment in burn patients," *Burns*, vol. 27, no. 2, pp. 161–166, 2001.

[7] M. S. G. Goepfert, D. A. Reuter, D. Akyol, P. Lamm, E. Kilger, and A. E. Goetz, "Goal-directed fluid management reduces vasopressor and catecholamine use in cardiac surgery patients," *Intensive Care Medicine*, vol. 33, no. 1, pp. 96–103, 2007.

[8] F. Mielck, W. Buhre, G. Hanekop, T. Tirilomis, R. Hilgers, and H. Sonntag, "Comparison of continuous cardiac output measurements in patients after cardiac surgery," *Journal of Cardiothoracic and Vascular Anesthesia*, vol. 17, no. 2, pp. 211–216, 2003.

[9] S. Ritter, A. Rudiger, and M. Maggiorini, "Transpulmonary thermodilution-derived cardiac function index identifies cardiac dysfunction in acute heart failure and septic patients: an observational study," *Critical Care*, vol. 13, no. 4, article R133, 2009.

[10] A. J. G. H. Bindels, J. G. van der Hoeven, A. D. Graafland, J. De Koning, and A. E. Meinders, "Relationships between volume and pressure measurements and stroke volume in critically ill patients," *Critical Care*, vol. 4, no. 3, pp. 193–199, 2000.

[11] A. Kortgen, P. Niederprün, and M. Bauer, "Implementation of an evidence-based "standard operating procedure" and outcome in septic shock," *Critical Care Medicine*, vol. 34, no. 4, pp. 939–939, 2006.

[12] B. V. Scheer, A. Perel, and U. J. Pfeiffer, "Clinical review: complications and risk factors of peripheral arterial catheters used for haemodynamic monitoring in anaesthesia and intensive care medicine," *Critical Care*, vol. 6, no. 3, pp. 198–204, 2002.

[13] P. J. Palmers, W. Vidts, K. Ameloot et al., "Assessment of three minimally invasive continuous cardiac output measurement methods in critically ill patients and a review of the literature," *Anaesthesiology Intensive Therapy*, vol. 44, no. 4, pp. 188–199, 2012.

[14] J. F. Stover, R. Stocker, R. Lenherr et al., "Noninvasive cardiac output and blood pressure monitoring cannot replace an invasive monitoring system in critically ill patients," *BMC Anesthesiology*, vol. 9, article 6, 2009.

[15] F. J. Belda, G. Aguilar, J. L. Teboul et al., "Complications related to less-invasive haemodynamic monitoring," *British Journal of Anaesthesia*, vol. 106, no. 4, pp. 482–486, 2011.

[16] K. H. Wesseling, J. R. C. Jansen, J. J. Settels, and J. J. Schreuder, "Computation of aortic flow from pressure in humans using a nonlinear, three-element model," *Journal of Applied Physiology*, vol. 74, no. 5, pp. 2566–2573, 1993.

[17] J. M. Bland and D. G. Altman, "Statistical methods for assessing agreement between two methods of clinical measurement," *The Lancet*, vol. 1, no. 8476, pp. 307–310, 1986.

[18] R. M. Nowak, A. Sen, A. J. Garcia et al., "Noninvasive continuous or intermittent blood pressure and heart rate patient monitoring in the ED," *The American Journal of Emergency Medicine*, vol. 29, no. 7, pp. 782–789, 2011.

[19] L. A. H. Critchley and J. A. J. H. Critchley, "A meta-analysis of studies using bias and precision statistics to compare cardiac output measurement techniques," *Journal of Clinical Monitoring and Computing*, vol. 15, no. 2, pp. 85–91, 1999.

[20] M. Cecconi, A. Rhodes, J. Poloniecki, G. Della Rocca, and R. M. Grounds, "Bench-to-bedside review: the importance of the

precision of the reference technique in method comparison studies: with specific reference to the measurement of cardiac output," *Critical Care*, vol. 13, no. 1, pp. 201–206, 2009.

[21] G. Biancofiore, L. A. H. Critchley, A. Lee et al., "Evaluation of an uncalibrated arterial pulse contour cardiac output monitoring system in cirrhotic patients undergoing liver surgery," *British Journal of Anaesthesia*, vol. 102, no. 1, pp. 47–54, 2009.

[22] L. A. Critchley, A. Lee, and A. M.-H. Ho, "A critical review of the ability of continuous cardiac output monitors to measure trends in cardiac output," *Anesthesia and Analgesia*, vol. 111, no. 5, pp. 1180–1192, 2010.

[23] X. Monnet, F. Picard, E. Lidzborski et al., "The estimation of cardiac output by the Nexfin device is of poor reliability for tracking the effects of a fluid challenge," *Critical Care*, vol. 16, no. 5, article R212, 2012.

[24] G. Chen, L. Meng, B. Alexander, N. P. Tran, Z. N. Kain, and M. Cannesson, "Comparison of noninvasive cardiac output measurements using the Nexfin monitoring device and the esophageal Doppler," *Journal of Clinical Anesthesia*, vol. 24, no. 4, pp. 275–283, 2012.

[25] O. Broch, J. Renner, M. Gruenewald et al., "A comparison of the Nexfin® and transcardiopulmonary thermodilution to estimate cardiac output during coronary artery surgery," *Anaesthesia*, vol. 67, no. 4, pp. 377–383, 2012.

[26] E. Rivers, B. Nguyen, S. Havstad et al., "Early goal-directed therapy in the treatment of severe sepsis and septic shock," *The New England Journal of Medicine*, vol. 345, no. 19, pp. 1368–1377, 2001.

[27] M. L. N. G. Malbrain, A. Perel, and E. Segal, "How to implement the recent Surviving Sepsis Campaign Guidelines at the bedside? A focus on initial fluid resuscitation," *Fluids*, vol. 2, no. 1, pp. 25–29, 2013.

[28] E. Giustiniano, E. Morenghiz, and N. Ruggier, "Flotrac/Vigileo validation trials: are there reliable conclusions?" *Clinical Psychology Review*, vol. 3, no. 6, pp. 62–65, 2011.

[29] B. P. Young and L. L. Low, "Noninvasive monitoring cardiac output using partial CO_2 rebreathing," *Critical Care Clinics*, vol. 26, no. 2, pp. 383–392, 2010.

[30] H. Paarmann, H. V. Groesdonk, B. Sedemund-Adib et al., "Lack of agreement between pulmonary arterial thermodilution cardiac output and the pressure recording analytical method in postoperative cardiac surgery patients," *British Journal of Anaesthesia*, vol. 106, no. 4, pp. 475–481, 2011.

[31] P. J. Peyton and S. W. Chong, "Minimally invasive measurement of cardiac output during surgery and critical care," *Anesthesiology*, vol. 113, pp. 220–235, 2012.

[32] M. O. Fischer, R. Avram, I. Cârjaliu et al., "Non-invasive continuous arterial pressure and cardiac index monitoring with Nexfin after cardiac surgery," *British Journal of Anaesthesia*, vol. 109, no. 4, pp. 514–521, 2012.

[33] M. Cecconi and M. L. Malbrain, "Cardiac output obtained by pulse pressure analysis: to calibrate or not to calibrate may not be the only question when used properly," *Intensive Care Medicine*, vol. 39, no. 4, pp. 787–789, 2013.

[34] K. Van de Vijver, A. Verstraeten, C. Gillebert et al., "Validation of non-invasive hemodynamic monitoring with Nexfin in critically ill patients," *Critical Care*, vol. 15, supplement 1, p. 75, 2011.

Hindawi Publishing Corporation
The Scientific World Journal
Volume 2013, Article ID 182038, 5 pages
http://dx.doi.org/10.1155/2013/182038

Clinical Study

Ocular Surface Disorders in Intensive Care Unit Patients

Tuba Berra Saritas,[1] Banu Bozkurt,[2] Baris Simsek,[1] Zeynep Cakmak,[3] Mehmet Ozdemir,[4] and Alper Yosunkaya[1]

[1] *Anesthesiology and Reanimation Department, Meram Medical Faculty, Necmettin Erbakan University, 42080 Konya, Turkey*
[2] *Ophthalmology Department, Faculty of Medicine, Selcuk University, 42130 Konya, Turkey*
[3] *Ophthalmology Department, Bitlis Government Hospital, 13000 Bitlis, Turkey*
[4] *Microbiology Department, Meram Medical Faculty, Necmettin Erbakan University, 42080 Konya, Turkey*

Correspondence should be addressed to Tuba Berra Saritas; tsaritas@konya.edu.tr

Received 19 July 2013; Accepted 17 September 2013

Academic Editors: D. Karakitsos, A. E. Papalois, and A. Shiloh

Patients in intensive care units (ICU) are at increased risk of corneal abrasions and infectious keratitis due to poor eyelid closure, decreased blink reflex, and increased exposure to pathogenic microorganisms. The aim of this retrospective study was to evaluate the ocular surface problems in patients who stayed in ICU more than 7 days and were consulted by an ophthalmologist. There were 26 men and 14 women with a mean age of 40.1 ± 18.15 years (range 17–74 years). Conjunctiva hyperemia, mucopurulent or purulent secretion, corneal staining, and corneal filaments were observed in 56.25%, 36.25%, 15%, and 5% of the eyes, respectively. Keratitis was observed in 4 patients (10%) who were treated successfully with topical antibiotics. Mean Schirmers test results were 7.6 ± 5.7 mm/5 min (median 6.5 mm/5 min) in the right, and 7.9 ± 6.3 mm/5 min (median 7 mm/5 min) in the left eyes. Schirmers test results were <5 mm/5 min in 40% of the subjects. The parameters did not show statistically significant difference according to mechanical ventilation, sedation, and use of inotropes. As ICU patients are more susceptible to develop dry eye, keratopathy, and ocular infections, they should be consulted by an ophthalmologist for early diagnosis of ocular surface disorders.

1. Introduction

Patients in intensive care units (ICU) are at increased risk of corneal abrasions and infectious keratitis due to impaired ocular defence mechanisms such as poor eyelid closure, inhibition of Bell's phenomenon, decreased blink reflex, reduced tear production, and increased exposure to pathogenic microorganisms [1–7].

ICU medical and nursing staff are primarily concerned with life threatening conditions; therefore the ocular signs and symptoms may be missed leading to serious ocular complications including corneal ulceration and infectious keratitis [1, 2]. Ocular complications lead to corneal opacities and even perforation which will seriously impair visual acuity and quality of life. For these reasons, meticulous eye care with regular cleaning of the eyes, installation of lubricating drops and ointments, and consultation from an ophthalmologist in case of a suspected infection [8–11] are recommended.

The aim of this retrospective study was to evaluate the prevalence of ocular surface disorders in patients who stayed in ICU more than 7 days and were consulted by an ophthalmologist.

2. Materials and Methods

The study was approved by the Local Ethics Committee of Meram Medical Faculty. Our ICU is an eleven-bed general unit, which accepts average of 300 patients per year. The study included patients older than 17 years, who were hospitalized in the ICU more than 7 days, with no facial or eye injuries. The medical records of 272 ICU patients who were hospitalized between February 2010 and February 2011 were reviewed.

In routine clinical practice, ICU staff examined the eyes for the presence of lagophthalmus, redness, secretion, and pupillary reflex. Ophthalmic consultation was required if patients' ICU stay exceeded 7 days or if the ICU staff suspected any eye problems. Ophthalmologists evaluated the patients for the presence of lagophthalmus, Bell phenomenon, and pupil reflex. Anterior segment examination was

done with a hand-held biomicroscopic device for the presence of punctate keratopathy, corneal erosions, infectious conjunctivitis, and keratitis. Punctate keratopathy or corneal erosion was diagnosed when corneal epithelium was stained with fluorescein under cobalt blue filter. Conjunctivitis was diagnosed when purulent or mucopurulent exudate, chemosis and redness were apparent in the conjunctiva. Keratitis was diagnosed in case of an infiltration or ulcer. Schirmers I test was performed to determine the rate of tear production by inserting a Schirmers test strip into the inferior fornix, at the junction of middle and lateral third of the lower eyelid margin, for 5 minutes without topical anesthesia. After 5 minutes, the strip was carefully withdrawn and the length of wet strip was measured with a millimeter (mm) ruler. Conjunctival and/or corneal cultures were obtained by using a sterile cotton swab. The swab was directly inoculated to serum bouillon and transferred to microbiology laboratory and cultured on blood eosin methylene blue agars. These agars were incubated at 37°C for 18–24 hours. In case of positivity, an antibiotic therapy was started according to the susceptibility tests.

Routine eye care included ocular lubrication with artificial tear drops every 6 hours and ointments twice a day. Ophthalmologists altered the treatment regimen according to the status of the subjects by increasing the artificial tears in case of dry eye, corneal erosions, or lagophthalmus or adding antibiotics in case of eye infections. In case of lagophthalmus, the eyelids are closed gently by taping or tarsorhaphy.

Acute Physiology and Chronic Health Evaluation II (APACHE II) is one of several ICU scoring systems. It is applied within 24 hours of admission of a patient to ICU; a score between 0 to 71 is computed based on several measurements; higher scores correspond to a more severe disease and a higher risk of death. Simplified Acute Physiology Score II (SAPS II) is also a scoring system that measures the severity of the disease. Its score is between 0 and 163 and it predicts mortality between 0% and 100%. It describes the morbidity of a patient when comparing the outcome with other patients. These scores were routinely calculated and noted for every patient in the ICU.

The age, gender, hospitalization period, APHACE II scores, SAPS II scores, the presence of mechanical ventilation, inotropes, muscle relaxants, sedatives, eye findingsm, and trachea culture results were recorded.

3. Statistical Analysis

The prevalence of conjunctival hyperemia, conjunctival secretion, corneal staining, and culture positivity were compared in patients with and without mechanical ventilation, sedation and inotropes using Chi-Square test and Schirmers test results were compared with Student's t-test. A P value less than 0.05 was accepted as statistically significant.

4. Results

The medical records of 40 patients who had a detailed ophthalmic examination during ICU hospitalization was included in the study. There were 26 men and 14 women with a mean age of 40.1 ± 18.15 years (range 17–74 years). The hospitalization periods ranged between 2 and 20 weeks (median 3 weeks). Mean APACHE II score was 24.05 ± 6.67 (range 12–40) and mean SAPS II score was 36.9 ± 22.17 (range 9–77). Twenty-two subjects (55%) had mechanical ventilation, 16 (40%) had sedation, 10 (25%), had inotropes and 3 (7.5%), had muscle relaxants. Blink reflex was negative in 12 subjects (30%), Bell phenomenon was absent in 30 subjects (75%), and pupillary reflex was negative in 2 subjects (5%). Inadequate lid closure was detected in 16 subjects (40%).

Out of 80 eyes, conjunctiva hyperemia was noted in 45 eyes (56.25%), mucopurulent or purulent secretion in 29 eyes (36.25%), corneal staining in 12 eyes (15%), and corneal filaments in 4 eyes (5%). Keratitis was observed in 4 patients (10%) and treated successfully with topical antibiotics. The rates of conjunctival hyperemia, secretion and corneal staining were similar between subjects with and without mechanical ventilation, with and without sedation, and with and without inotropes ($P > 0.05$) (Table 1).

Mean Schirmers test results were 7.6 ± 5.7 mm/5 min (median 6.5 mm/5 min) in the right eyes and 7.9 ± 6.3 mm/5 min (median 7 mm/5 min) in the left eyes. In right eyes, Schirmers test results were ≤5 mm in 18 eyes (45%), 6–10 mm in 13 eyes (32.5%), and ≥11 mm in 9 eyes (22.5%). In left eyes, Schirmers test results were ≤5 mm in 17 eyes (42.5%), 6–10 mm in 12 eyes (30%), and ≥11 mm in 11 eyes (27.5%). No significant differences were found in mean Schirmers test results between subjects with and without mechanical ventilation ($P > 0.05$), with and without sedation ($P > 0.05$), and with and without inotropes ($P > 0.05$) (Table 1). Right Schirmers test results were ≤5 mm in 45% of patients with mechanical ventilation, and 44.4% of patients without ($P = 1$), left Schirmers test results were ≤5 mm in 45.5% of patients with mechanical ventilation, and 38.9% of patients without ($P = 0.75$). Right Schirmers test results were ≤5 mm in 50% of patients with sedation and 41.7% of patients without ($P = 0.75$) and left Schirmers test results were ≤5 mm in 50% of patients with sedation and 37.5% of patients without ($P = 0.52$). Right Schirmers test results were ≤5 mm in 30% of patients with inotropes and 50% of patients without ($P = 0.46$), left Schirmers test results were ≤5 mm in 40% of patients with inotropes and 43.3% of patients without ($P = 1$).

Out of a total of 40 cultures from the conjunctiva, 17 (42.5%) were positive for bacteria: 10 *Staphylococcus epidermidis*, 2 *Pseudomonas aeruginosa*, 2 *Acinetobacter baumannii*, 1 *Staphylococcus haemolyticus*, 1 *Klebsiella*, and 1 *Proteus mirabilis*. Conjunctiva culture positivity did not differ between subjects with and without mechanical ventilation, with and without sedation and with and without inotropes ($P > 0.05$, all) (Table 1). Corneal and conjunctival culture was positive for *Pseudomonas aeruginosa* and *Acinobacter baumannii* in 2 of the patients with keratitis and both of the subjects had tracheal culture positivity. Blood culture was positive in only one subject without mechanical ventilation and trachea culture was positive in 4 subjects, 2 with mechanical ventilation and 2 without.

Table 1: The rates of conjunctival hyperemia, conjunctival secretion, corneal staining, conjunctival culture positivity, and Schirmers test values (MD ± SD) in ICU patients.

	Conjunctival hyperemia % OD/OS	Conjunctival secretion % OD/OS	Corneal staining % OD/OS	Schirmers values mm/5 min OD/OS	Culture positivity %
Mechanical ventilation					
Yes	63.6/59.1	50/45.5	18.2/18.2	6.7 ± 4.4; 7.1 ± 5.6	45.5
No	50/50	22.2/22.2	11.1/11.1	8.7 ± 6.9; 8.9 ± 7	38.9
P values	0.52; 0.75	0.1; 0.19	0.67; 0.67	0.27; 0.36	0.75
Sedation					
Yes	68.8/68.8	50/43.8	18.8/18.8	6.1 ± 4.3; 6 ± 4.2	31.2
No	50/45.8	29.2/29.2	12.5/12.5	8.6 ± 6.4; 9.2 ± 7.1	50
P values	0.33/0.2	0.21/0.50	0.67/0.67	0.18; 0.11	0.33
Inotropes					
Yes	70/70	40/40	30/30	7.1 ± 4.7; 6.8 ± 4.5	40
No	53.3/50	36.7/33.3	10/10	7.8 ± 6.0; 8.3 ± 6.8	43.3
P values	0.47/0.46	1/0.72	0.15/0.15	0.74; 0.52	1

5. Discussion

Ocular surface disorders have been reported to occur in up to 60% of critically ill patients [1, 2]. Patients in ICU often have impaired ocular defence mechanisms as a result of multiorgan dysfunction, metabolic disturbances, mechanical ventilation, and unconsciousness [1, 2].

The eyelids are important physical barriers to trauma and infections preventing the adherence of microorganisms to the ocular surface. The sedatives and neuromuscular blockers inhibit contraction of the orbicularis oculi muscle, resulting in incomplete eyelid closure, which has been reported to occur in 20% to 75% of sedated patients in ICUs [1–4, 7]. Sedation interferes with random eye movements and inhibits Bell's phenomenon, making the eye more susceptible to nocturnal lagophthalmos [1, 2, 7, 12]. Neuromuscular blockers also abolish the blink reflex, which is one of the major ocular protective mechanisms [1, 2, 7, 10–12]. Orbital haemorrhage, lid trauma, conjunctival chemosis due to positive pressure ventilation, and facial nerve paralysis may also lead to inadequate lid closure [1, 2]. Incomplete lid closure leads to drying of the ocular surface, desiccation of the cornea epithelial cells, and corneal ulceration, with an increased risk of microbial keratitis. Lesions range from punctuate epithelial keratopathy to macroepithelial erosions, and if untreated, to corneal thinning and perforation. The reported incidence rates for superficial keratopathy and corneal abrasions are between 3–60% in the ICU patients [5–7]. In the study of Hernandez and Mannis [5], superficial keratopathy was detected in 40% of randomly selected ICU patients and 90% of those were intubated. The prevalence of corneal abnormalities was higher in patients staying in ICU for 1 week or longer. In the study of Imanaka et al. [6] ocular surface disorder was found in 28 of the 143 patients (20%) whose ICU stay exceeded 7 days, which increased with continuous sedation and neuromuscular blockade. Out of 15 patients who had sedatives or muscle relaxants administered continuously for more than 48 hours in the ICU, nine patients (60%) developed corneal erosion [6]. In the study of Mercieca et al. [7], 42% of ICU patients had some degree of keratopathy, which was detected in the majority in the first week of their stay. The presence of ocular surface disease was closely correlated with the degree of lagophthalmos, which in turn was closely related to the depth of sedation or paralysis. In this study, the rates of conjunctival hyperemia, remarkable corneal staining, and corneal filaments were 56.25%, 15%, and 5%, respectively. We could not find any significant differences in conjunctival hyperemia, secretion, and corneal staining according to mechanical ventilation, sedation, and use of inotropes.

Tears lubricate the ocular surface and wash away debris and organisms. They contain antimicrobial substances including secretory immunoglobulin A, lysozyme, lactoferrin, ceruloplasmin, and complement components. In this study, decreased tear production (less than 10 mm/5 min) was found in 70% of the subjects and in 40% of the subjects; the Schirmers test results were less than 5 mm/5 min. Paralyzing and sedating agents, atropine, antihistamines, and tricyclic antidepressants were shown to decrease tear fluid production [1, 2, 10–12]. In this study, we could not find a difference in Schirmers test results according to mechanical ventilation, sedation, and use of inotropes ($P > 0.05$). As the number of subjects treated with muscle relaxants was small (3 patients), a statistical comparison could not be done.

Patients in ICU are more exposed to pathogenic microorganisms with significant antimicrobial resistance resulting from the widespread use of multiple antibiotics, which also increases the risk of conjunctivitis and keratitis [3, 4]. Conjunctivitis is a common complication within the ICU setting and without the necessary care; this condition can spread rapidly among the patients [1, 2, 6, 13, 14]. In the study of King et al. [13], *Pseudomonas aeruginosa* was recovered from the conjunctiva of 30 patients in a university-affiliated pediatric hospital and 70% of cases occurred in pediatric ICU (PICU) patients. In the study of Brito et al. [14], out of 1443 patients in

neonatal ICU, 52 developed conjunctivitis (17.7%). Mechanical ventilation, total parenteral nutrition, orogastric tube, previous antibiotic therapy, use of CVC, and birth weight of 751–1,000 g appeared to be associated with a significantly higher risk of nosocomial infections ($P < 0.05$). Coagulase-negative Staphylococcus (36.5%) and Staphylococcus aureus (23.6%) were the most common etiologic agents isolated from cultures. In this study, the rate of mucopurulent or purulent secretion was 36.25%, respectively, and conjunctival culture positivity was 42.5%. Most of the specimens were positive for *Staphylococcus epidermidis*. The other isolated microorganisms were *Pseudomonas aeruginosa*, *Acinobacter baumannii*, *Staphylococcus haemolyticus*, *Klebsiella*, and *Proteus mirabilis*. In the study of Mela et al. [3], 54 (77%) patients were colonised by at least one bacterial species other than normal flora within seven to 42 days and their isolation was closely associated with the time period of hospitalisation. Early identification of ocular surface bacteria colonisation and the administration of topical antibiotics for prophylaxis prohibited corneal infection in these patients. In our clinical practice, antibiotic drops and ointments are used routinely in ICU patients with conjunctival hyperemia and mucopurulent/purulent secretion without waiting for the culture results.

In this study, keratitis was diagnosed in 4 patients and in 2 of them, both trachea and conjunctiva/cornea cultures were positive for *Pseudomonas aeruginosa*, and *Acinobacter baumannii*. In the literature, *Pseudomonas aeruginosa, Acinetobacter spp., Staphylococcus aureus, Staphylococcus epidermidis, Haemophilus influenzae, and Streptococcus species* were shown to cause microbial keratitis [3, 4, 15, 16]. Among these microorganisms, the most common one is *Pseudomonas aeruginosa*, which is highly virulent and causes a rapid onset devastating infection [4, 15–17]. Kirwan et al. [4] reported 3 cases of microbial keratitis in ICU. *Pseudomonas aeruginosa* was isolated in 2 cases and *Acinetobacter calcoaceticus* in one patient. In 2 of the subjects, the microorganisms were also isolated from the respiratory tract. Hilton et al. [15] reported that 10 nosocomial eye infections occurred in three ICU during an 18-month period. Nine patients were intubated, all were obtunded, and all had copious sputum production. The bacteria isolated from the patients' sputum samples and from the eyes were identical in nine patients. *Pseudomonas aeruginosa* was the cause in six of the subjects with complications (three corneal ulcers, two hypopyon, one opaque cornea, and two corneal rupture).

Eye care is a very important part of nursing care in sedated and ventilated patients in the ICU. Our standard eye care in ICU patients include ocular lubrication with artificial tear drops and ointments, and topical antibiotics when needed. Ophthalmic consultations are routinely done in ICU subjects who are hospitalized for more than one week or if ICU staff suspects any eye problems. In case of lagophthalmos, monitoring of eyelid closure needs to be carefully performed as incomplete closure which may be unrecognized under the eye patches. Incomplete eye closure might lead to drying of the ocular surface, corneal epithelium abrasion, infectious keratitis, melting of the cornea, and even perforation, which might lead to loss of vision. Closure of the eyelid is most effectively done by taping. However, tarsoraphy might be needed in some cases. Prophylactic use of antibiotic ointment might be helpful in avoiding ocular surface drying and preventing secondary infection. With our standard eye care, the rate of keratitis was only 10% in high risk patients, and all of the subjects had been treated successfully with topical antibiotics. However, there is still no standard nursing eye care in ICUs and the practice varies greatly in terms of the frequency and method of eye care.

The main limitations of this study are the retrospective design and the small sample size. In this study, the prevalence of dry eye with Schirmers test results less than 5 mm was around 40% in ICU patients and ocular signs were found at least in half of the subjects. However, we only included 40 patients out of 272 who stayed in ICU more than 7 days, consulted by an ophthalmologist for a suspected ocular problem and had a detailed ophthalmological examination, which might cause a bias giving higher rates of ocular complications. We also did not evaluate the improved outcomes or quality of life with regular ophthalmology consultations, which also necessitates a further investigation.

6. Conclusion

As ICU patients are more susceptible to develop dry eye, keratopathy, and ocular infections, they should be consulted by an ophthalmologist for early diagnosis of ocular surface disorders.

Conflict of Interests

The authors declared no conflict of interests.

References

[1] A. Grixti, M. Sadri, J. Edgar, and A. V. Datta, "Common ocular surface disorders in patients in intensive care units," *The Ocular Surface*, vol. 10, pp. 26–42, 2012.

[2] N. Joyce, "Eye care for the intensive care patient," A Systematic Review 21, The Joanna Briggs Institute for Evidence Based Nursing and Midwifery, Adelaide, Australia, 2002.

[3] E. K. Mela, E. G. Drimtzias, M. K. Christofidou, K. S. Filos, E. D. Anastassiou, and S. P. Gartaganis, "Ocular surface bacterial colonisation in sedated intensive care unit patients," *Anaesthesia and Intensive Care*, vol. 38, no. 1, pp. 190–193, 2010.

[4] J. F. Kirwan, T. Potamitis, H. El-Kasaby, M. W. Hope-Ross, and G. A. Sutton, "Lesson of the week: microbial keratitis in intensive care," *British Medical Journal*, vol. 314, no. 7078, pp. 433–434, 1997.

[5] E. V. Hernandez and M. J. Mannis, "Superficial keratopathy in intensive care unit patients," *American Journal of Ophthalmology*, vol. 124, no. 2, pp. 212–216, 1997.

[6] H. Imanaka, N. Taenaka, J. Nakamura, K. Aoyama, and H. Hosotani, "Ocular surface disorders in the critically ill," *Anesthesia and Analgesia*, vol. 85, no. 2, pp. 343–347, 1997.

[7] F. Mercieca, P. Suresh, A. Morton, and A. Tullo, "Ocular surface disease in intensive care unit patients," *Eye*, vol. 13, no. 2, pp. 231–236, 1999.

[8] J. McHugh, P. Alexander, A. Kalhoro, and A. Ionides, "Screening for ocular surface disease in the intensive care unit," *Eye*, vol. 22, no. 12, pp. 1465–1468, 2008.

[9] M. Farrell and F. Wray, "Eye care for ventilated patients," *Intensive and Critical Care Nursing*, vol. 9, no. 2, pp. 137–141, 1993.

[10] N. Koroloff, R. Boots, J. Lipman, P. Thomas, C. Rickard, and F. Coyer, "A randomised controlled study of the efficacy of hypromellose and Lacri-Lube combination versus polyethylene/Cling wrap to prevent corneal epithelial breakdown in the semiconscious intensive care patient," *Intensive Care Medicine*, vol. 30, no. 6, pp. 1122–1126, 2004.

[11] S. B. Lenart and J. A. Garrity, "Eye care for patients receiving neuromuscular blocking agents or propofol during mechanical ventilation," *American Journal of Critical Care*, vol. 9, no. 3, pp. 188–191, 2000.

[12] P. Suresh, F. Mercieca, A. Morton, and A. B. Tullo, "Eye care for the critically ill," *Intensive Care Medicine*, vol. 26, no. 2, pp. 162–166, 2000.

[13] S. King, S. P. Devi, C. Mindorff, M. L. Patrick, R. Gold, and E. L. Ford-Jones, "Nosocomial *Pseudomonas aeruginosa* conjunctivitis in a pediatric hospital.," *Infection Control and Hospital Epidemiology*, vol. 9, no. 2, pp. 77–80, 1988.

[14] D. V. Brito, C. S. de Brito, D. S. Resende, J. Ó. do Moreira, V. O. S. Abdallah, and P. P. G. Filho, "Nosocomial infections in a Brazilian neonatal intensive care unit: a 4-year surveillance study," *Revista da Sociedade Brasileira de Medicina Tropical*, vol. 43, no. 6, pp. 633–637, 2010.

[15] E. Hilton, A. Uliss, S. Samuels, A. A. Adams, M. L. Lesser, and F. D. Lowy, "Nosocomial bacterial eye infections in intensive-care units," *The Lancet*, vol. 1, no. 8337, pp. 1318–1320, 1983.

[16] D. Ommeslag, F. Colardyn, and J.-J. de Laey, "Eye infections caused by respiratory pathogens in mechanically ventilated patients," *Critical Care Medicine*, vol. 15, no. 1, pp. 80–81, 1987.

[17] B. Parkin, A. Turner, E. Moore, and S. Cook, "Bacterial keratitis in the critically ill," *British Journal of Ophthalmology*, vol. 81, no. 12, pp. 1060–1063, 1997.